Identification and characterization of Abelson Interactor 1, as a novel substrate of Protein Kinase D2

Dissertation
zur Erlangung des akademischen Grades
doctor rerum naturalium
(Dr. rer. nat.)

vorgelegt der
Naturwissenschaftlichen Fakultät I
Biowissenschaften
der Martin-Luther-Universität Halle-Wittenberg

von **Herr Subbaiah Chary Nimmagadda**
geboren am 30. Juni 1983
in Hyderabad, Indien

Gutachter:
1. Prof. Dr. Thomas Seufferlein, Universitätsklinikum Halle, Deutschland.
2. Prof. Dr. Sven-Erik Behrens, Martin-Luther-Universität Halle-Wittenberg, Deutschland
3. Prof. Michael Seckl, Imperial College London, London.

Tag der mündlichen Prüfung: 27.06.2013, Halle (Saale).

Identification and characterization of Abelson Interactor 1, as a novel substrate of Protein Kinase D2

Subbaiah Chary Nimmagadda

AG Seufferlein, Klinik für Innere Medizin 1,

Universitätsklinikum Halle,

Halle (Saale), Deutschland

August, 2012

Dedication

To my parents, Nimmagadda Anasuya and Jalaiah; for all the endless love, support and encouragement you have been offering me over years. Love you Mom and Dad. This one is for you.

Subbaiah Chary Nimmagadda

CONTENTS

I. Index of Figures

II. Index of Tables

1. Abbreviations

Ab	Antibody
ABI1	Abelson Interactor 1
Abl	Abelson tyrosine-protein kinase
AC	Acidic domain
Ala	Alanine (three letter code)
Amp	Ampicillin
APS	Ammonium persulfate
ATCC	American Type Culture Collection
ATP	Adenosine triphosphate
bp	base pairs
BSA	Bovine serum albumin
°C	degree Celsius
C1a	First cysteine rich domain
C1b	Second cysteine rich domain
CAMK	Ca2+/Calmodulin-depenent protein kinase
cAMP	Cyclic adenosine monophosphate
CRD	Cysteine rich domain
CSF-1	Colony stimulating factor-1
DAG	Diacylglycerol
DMEM	Dulbecco's Modified Eagles medium
DMSO	Dimethylsulfoxide
DNA	Deoxyribo nucleic acid
dNTP	deoxy ATP/ CTP/ GTP/ TTP
DTT	Dithiothreitol
ECL	Enhanced chemiluminescence
ECM	Extra cellular matrix
EDTA	Ethylendiamine-N, N, N´, N´- tetra-acetate
EGFP	Enhanced green fluorescent protein
EGTA	Ethylene glycolbis(aminoethylether)-tetra-acetic acid
FA	Focal adhesions
FAK	Focal adhesion kinase
FCS	Fetal calf serum
FN	Fibronectin
g	Gram
Gαq	G-protein-subunit αq
GFP	Green fluorescent protein
GPCR	G-protein coupled receptor
GST	Glutathione S Transferase
HDAC	Histone deacetylase
HRP	Horseradish peroxidase
IB	Immunoblot
IF	Immunofluorescence

IP	Immunoprecipitation
IP3	Inositol triphosphate
IVK	Invitro kinase assay
kb	kilo base pairs
Kidins 220	Kinase D-interacting substrate-220 kD
kD	kilo Dalton
l	Liter
LMB	Leptomycin B
LSM	Laser scanning microscope
Lys	Lysine (three letter code)
M	Molar
MAPK	Mitogen activated protein kinase
MEF	Myocyte enhancing factor
MnSOD	Manganese dependent superoxide dismutase
mg	Milligram
min	Minute
ml	Milliliter
mM	Millimolar
Nap1	Nck-associated protein 1
NFAT	Nuclear factor of activated T cells
NFκB	Nuclear factor κ B
µg	Microgram
µl	Microliter
nM	Nanomolar
PAK	P21- activated kinase
PBS	Phosphate buffered saline
PCR	Polymerase chain reaction
PDGF	Platelet derived growth factor
PFA	para-formaldehyde
PEI	Poly Ethylen imine
PE	Phorbol ester
pH	negative logarithm of hydrogen concentration
PH	Pleckstrin homology domain
PIP2	Phosphatidylinositol 4,5-bisphosphate
PKC	Protein Kinase C
PKD	Protein Kinase D
PLC	Phospholipase C
PMA	Phorbol 12-myristate 13-acetate
PVDF	Polyvinylidene Fluoride
RNA	Ribonucleic Acid
ROS	Reactive oxygen species
RPM	Revolutions per minute
RT	Room temperature
S	Serine (one letter code)

SDM	Site directed mutagenesis
SDS-PAGE	Sodium dodecyl sulfate - polyacrylamide gel electrophoresis
Ser	Serine (three letter code)
siRNA	small interfering RNA
STAT	Signal transducers and activators of transcription
TAE	Tris-Acetate EDTA
TGN	Trans golgi network
TGFβ	Transforming growth factor β
Thr	Threonine (three letter code)
Tris	Tris(hydroxymethyl) aminomethane
TNF	Tumour necrosis factor
U	Enzyme unit
uPA	Urokinase-like plasminogen-activator
WT	Wild type
WAVE2	Wiskott-Aldrich syndrome protein family member *2*
WASp	Wiskott-Aldrich syndrome protein

2. Introduction

2.1 Kinase/s and their importance

A kinase is an enzyme that transfers phosphate group from a high energy donor molecule like ATP, to a specific substrate (Manning et al., 2002). Kinases are extensively involved in the signal transduction and control of complex processes including metabolism, transcription, cell cycle progression, cytoskeletal rearrangement, apoptosis, and differentiation. Since the discovery of glycogen phosphorylase 50 years ago, there has been intense interest in the role of protein phosphorylation in protein function (Manning et al., 2002). The protein kinase D (PKD) family is a recent addition to the calcium/calmodulin-dependent protein kinase group of serine/threonine kinases, within the protein kinase complement of the mammalian genome (Johannes et al., 1994; Valverde et al., 1994; Van Lint et al., 1995).

2.2 Protein kinase D family

The Protein Kinase D (PKD) family of proteins comprises the three isoforms PKD1, 2 and 3 (Rykx et al., 2003). Although originally grouped under the protein kinase C (PKC) family, the PKD family is now recognized as a subfamily of the Calcium/calmodulin dependent kinase (CaMK) superfamily (Manning et al., 2002; Wang, 2006). Downstream of PLC-DAG-PKC signaling cascade PKD's have been implicated in various physiological and pathophysiological conditions.

2.2.1 Structural organization of PKD's

Members of the PKD family share a similar architecture with regulatory sub-domains that play specific roles in the activation, translocation and function of the enzymes at the amino terminus and a catalytic domain (KD) at the carboxy terminus. The catalytic domain of PKD's is highly homologus to Ca2+/Calmodulin-dependent kinases, thus their classification as a subfamily of CaMK superfamily (Manning et al., 2002). Regulatory regions of PKD's contain a cysteine rich domain (CRD), a short acidic region (AC) followed by pleckstrin homology domain. CRD in turn contains individual functionally dissimilar cysteine rich motifs, referred to as C1a and C1b. While C1a has a specific inhibitory effect on the catalytic activity only in PKD1, C1b

binds to phorbol dibutyrate (PDBu) with a high affinity and is responsible for PDBu dependent translocation of PKD's (Iglesias et al., 1998a; Iglesias and Rozengurt, 1999). Deletion of C1a, C1b or the entire cysteine rich domain results in a constitutively active form of the PKD's (Iglesias and Rozengurt, 1999).This region is followed by a acidic region (AC). Interposed between the AC and the catalytic (KD) domain, is a pleckstrin homology (PH) domain. PH domains bind to membrane lipids (Cozier et al., 2004) and have an auto-regulatory role in some protein kinases, including PKD. Deletion of the entire PH domain markedly increased the basal activity of the enzyme. Partial deletions or single amino acid substitutions (e.g. R447C and W538A) within PH domain also increased basal kinase activity (Iglesias and Rozengurt, 1998; Waldron et al., 1999), indicating that the PH domain, like the CRD, helps to maintain PKD in an inactive state. In addition to these domains, the amino terminus of PKD1 and PKD2 (but not PKD3) starts with an apolar region, rich in alanine and/or proline residues (Rykx et al., 2003).

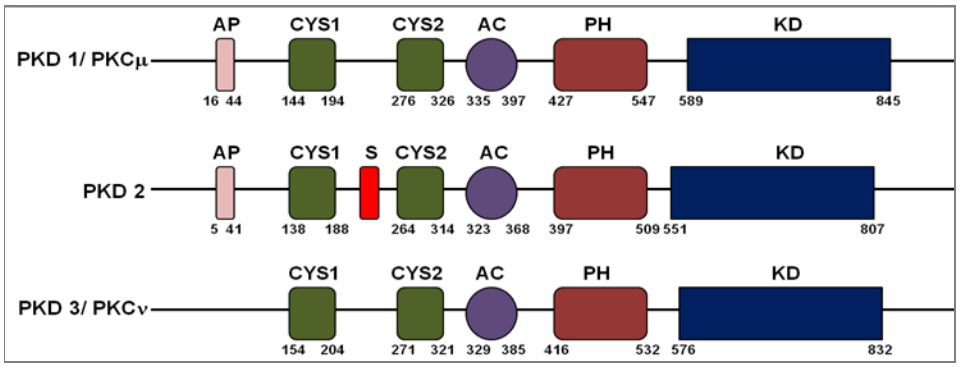

Figure 1: **Molecular architecture of PKD enzymes.** ***AP-*** *alanine and proline-rich domain;* ***S-*** *serine rich domain;* ***CYS-*** *cysteine rich Zn finger domain;* ***AC-*** *acidic domain;* ***PH-*** *pleckstrin homology domain;* ***KD****- kinase catalytic domain. Image based on original figure from (Rykx et al., 2003).*

2.2.2 Activation of PKD's

PKD's are generally activated via a phosphorylation-dependent mechanism involving the canonical PKC/PKD pathway (Rozengurt et al., 2005; Zugaza et al., 1996). Diacylglycerol responsive PKD isoforms, predominantly the novel PKC's (δ, ε, η, and θ) phosphorylate the two conservative serine residues in the activation loop relieving PKD's from repression by its PH domain and leading to a full activation of

the kinase (Waldron and Rozengurt, 2003; Zugaza et al., 1996; Zugaza et al., 1997). The PKC/PKD pathway was shown to be activated in response to a wide variety of stimuli including GPCR agonists such as mitogenic neuropeptrides (Bombesin, vasopressin, endothelin, bradykinin, and platelet-derived growth factor etc) (Paolucci and Rozengurt, 1999; Zugaza et al., 1997), Angiotensin II (Tan et al., 2004), lysophosphatidic acid (Paolucci et al., 2000), thrombin (Tan et al., 2003), vascular endothelial growth factor (Wong and Jin, 2005), oxidative stress (Storz et al., 2004; Waldron and Rozengurt, 2000) and phorbol esters (Van Lint et al., 1995). While activation of PKC/PKD pathway by growth factors and GPCR agonists is mediated by phospho lipase C, activation by oxidative stress requires additionally the tyrosine kinases Src and Abl. PKD1, 2 and 3 were reported to be trans-phosphorylated at ser 744 and 748 (Iglesias et al., 1998b), 706 and 710 (Sturany et al., 2001), 731 and 735 (Rey et al., 2003a) respectively. Following trans-phosphorylation the three isoforms PKD1, 2 and 3 were reported to undergo auto phosphorylation at the c-terminus at serine 916 (Matthews et al., 1999), 876 (Sturany et al., 2001) and 888 (Rey et al., 2003b) respectively. The interaction of PH domain with Gβγ subunits of heterotrimeric G proteins (Jamora et al., 1999) or caspase-3 mediated cleavage of PKD1 at two distinct sites (between AC and PH domains) during the induction of apoptosis by genotoxic drugs also leads to activation of PKD1 (Vantus et al., 2004). An additional phosphorylation site (Ser244) within the zinc-finger domain of PKD2, is crucial for blocking nuclear export of active PKD2 by preventing its interaction with the Crm-1 export machinery (von Blume et al., 2007).

Therefore, a thorough knowledge of PKD-mediated signaling at the Golgi, mitochondrial and plasma membranes and in the nucleus would expand our understanding of localized, organelle-specific PKD regulation and functions in normal and disease derived cells.

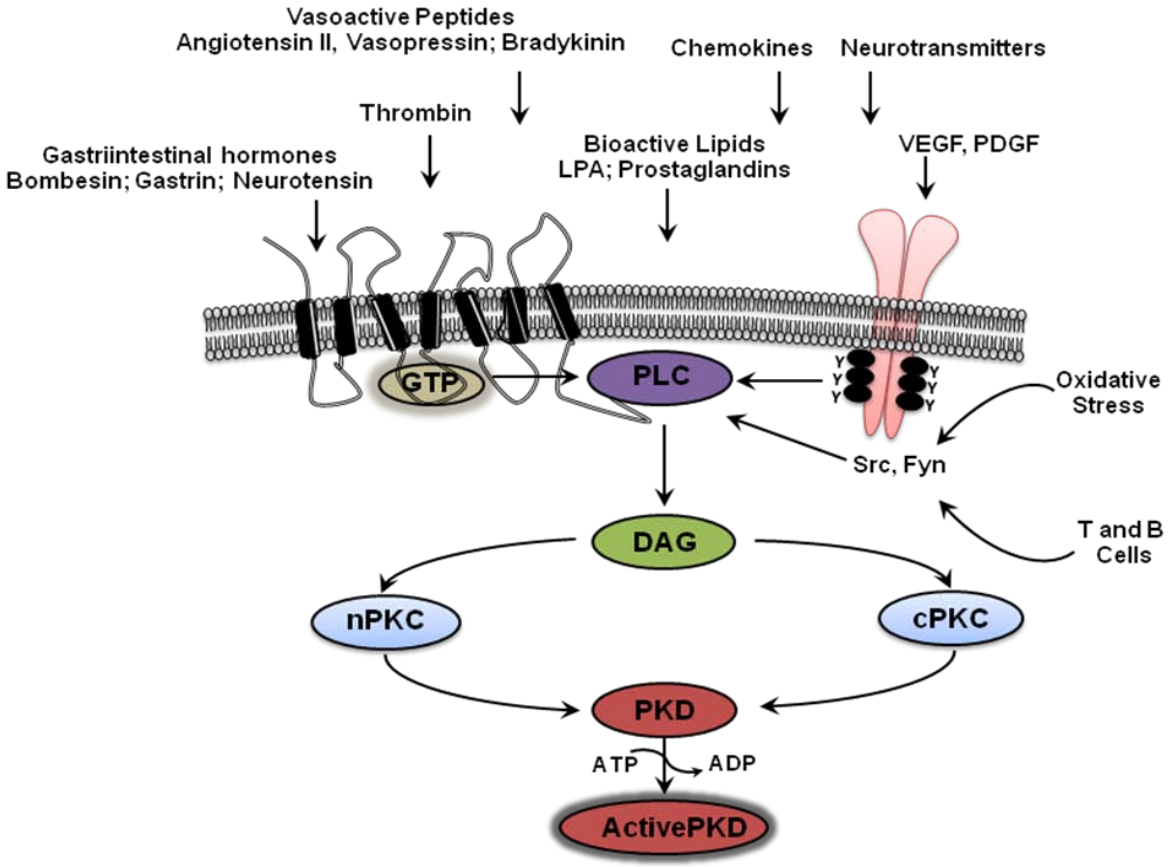

Figure 2: Multiple signals leading to PKD activation. *Hormones, growth factors, neurotransmitters, chemokines, bioactive lipids, proteases, and oxidative stress induce PLC-mediated hydrolysis of phosphatidylinositol 4, 5-biphosphate (PIP2) to produce DAG at the plasma membrane. Inactive PKD translocates from the cytosol to the plasma membrane in response to DAG produced via PLC-mediated hydrolysis of phosphatidylinositol 4, 5-bisphosphate. DAG also recruits to the plasma membrane and simultaneously activates novel PKCs, which then mediate the transphosphorylation and activation of PKD. Image based on original figure from (Rozengurt, 2011).*

2.2.3 Localization of PKDs

PKDs localize in cytosol and several intracellular compartments including nucleus, Golgi apparatus, plasma membrane and mitochondria. In quiescent cells, PKD's largely reside in the cytosol, a smaller fraction localizes to the Trans-Golgi (Prestle et al., 1996). PKDs also localize to the mitochondria in some specialized cells (Storz et al., 2000) and to secretory granules (Matthews et al., 2000). The differential subcellular localization of PKD's is largely dependent on the two Zn-fingers of PKD1 which have different lipid binding specificities (Iglesias and

Rozengurt, 1999). Stimulation of cells with PDBu or mitogenic agonist's results in a second cysteine rich domain (C1b) mediated translocation of PKD from the cytosol to the plasma membrane, followed by a rapid redistribution to the cytosol, which requires phosphorylation of the PKD activation loop (Iglesias et al., 2000; Rey et al., 2004). PKD1 is a nucleo-cytoplasmic shuttling protein. Accumulation in the nucleus is dependent on the C1b domain, while Crm-1 dependent nuclear export is mediated by the PH domain of PKD (Rey et al., 2001). PKD's localization at the trans-Golgi network is mediated by the C1a (Maeda et al., 2001) and C1b (Pusapati et al., 2010) domains and is dependent on local DAG production (Baron and Malhotra, 2002). Depending on the nature of stimuli and the site of localization, PKDs interact with substrates or binding molecules and regulate a variety of cellular processes.

2.2.4 Substrates of PKDs

PKDs phosphorylate and control distinct substrates (Doppler et al., 2005; Iglesias et al., 2000; Nishikawa et al., 1997). Given the multitude of signaling pathways and biological effects regulated by the PKD family of proteins, it is obvious that the whole PKD signaling network is still incompletely understood and a large number of physiological substrates are yet to be identified. Activated PKDs associate with the plasma membrane, Golgi, mitochondria and the nucleus, thereby engaging in a range of diffusible and anchored substrates (Fu and Rubin, 2011). PKD's are known to phosphorylate substrates that contain the substrate motif -LXRXXpS/pT-, (L, R, pS, pT and X are leucine, arginine, phosphorylated serine, phosphorylated threonine and any other amino acid residue, respectively; (Nishikawa et al., 1997). Table 1 summarizes a list of known PKD substrates, their cellular role and the functional consequences of their phosphorylation. Advances in the generation of phosphorylation site specific antibodies led to the identification of novel substrate of PKD's, for example: Human heat shock protein (Hsp27), Rin1 and HDAC5 (Doppler et al., 2005). This antibody was directed against the optimum phosphorylation consensus motif of PKD.

PKD Substrate	Cellular role	Functional Consequence	Reference
Troponin I	Inhibitor of actin myosin interaction	Increased inhibition	(Haworth et al., 2004)
Kiddins	Integral membrane protein	Regulation of Kidins220 membrane localization in PC12 cells and NT hormone secretion in BON cells	(Iglesias et al., 2000)
Vanilloid receptor 1	Non-selective cation channel	Increased response to low pH and capsaicin	(Wang et al., 2004)
HDAC5	Repression of fetal gene expression in heart	Nuclear export of HDAC5	(Vega et al., 2004)
E-cadherin	Cell-cell adhesion and cell-cell contact associated signaling	Increased cellular adhesion. Decreased cellular motility (prostate cancer)	(Jaggi et al., 2005)
PI4K IIIβ	Lipid kinase activity and enhanced vesicular transport to plasma membrane	Activation; PI4P synthesis	(Hausser et al., 2005)
HDAC7	Repression of Nur77 expression in thymocytes	Nuclear export of HDAC7, followed by de-repression of Nur 77expression	(Dequiedt et al., 2005; Matthews et al., 2006)
CREB	Transcriptional regulation of CREB-responsive genes via recruitment of co-activators CBP/p300	Stimulation of CREB mediated transcription	(Johannessen et al., 2007)
CERT	Transport of ceramide	Decreased affinity for PI4P and Golgi membrane dissociation	(Fugmann et al., 2007)
RIN1	Ras interactor that prevents Ras-Raf interaction	Inhibit F-actin remodeling	(Wang et al., 2008)
EVL-I	Splice variant of EVL (Ena/VASP like protein)	Phosphorylated EVL-1 can support filopodia	(Janssens et al., 2009)
Cortactin	Actin binding protein	Inhibit F-actin remodeling	(De Kimpe et al., 2009)
SSH1L	Phosphatases	Inactivation	(Eiseler et al., 2009b)

SNAIL	Epithelial to mesenchymal transition.	Transcription de-repression, 14-3-3 binding	(Du et al., 2010)
PAK4	Links Rho GTPases to cytoskeleton reorganization	Increased activity of PAK4 and LMK and increased levels of phospho-cofilin.	(Spratley et al., 2011)
Hsp27	Chaperone	Unknown	(Doppler et al., 2005)
C-jun	Transcription factor	Unknown	(Hurd et al., 2002)
Centaurin α1	Regulator of sub-cellular trafficking of macro molecular signaling complexes	Unknown	(Zemlickova et al., 2003)
p53	Integration of cellular stress detection and response signals	Unknown	(Uhle et al., 2003)

Table 1: PKD substrates and consequences of phosphorylation/s. *Kidins220- Kinase D interacting substrate of 220 kDa; HDAC5- Histone deacetylase* 5; HDAC7- *Histone deacetylase* 7; *PI4KIII-β- phosphatidylinositol 4-kinase IIIβ; CREB- cAMP-response element-binding protein; CERT- ceramide transfer protein; EVL1- Ena/VASP like protein 1; SSH1L- Slingshot 1L protein phosphatase; RIN1- Ras and Rab interactor 1; PAK4- p21 activated kinase, Hsp27- Heat shock protein 27.*

2.2.5 Biological functions of PKDs

PKD1, PKD2 and PKD3 are expressed in a large variety range of cells and the plethora of proteins with which PKD's interact indicate a multifaceted function and regulation (Van Lint et al., 2002). Important for this study is the observation that PKD's have recently drawn a lot of attention for its potential role in monocyte (Tan et al., 2009) and cancer cell migration, the latter via phosphorylating SSH1L (Eiseler et al., 2009b), cortactin (Eiseler et al., 2010), E-Cadherin (Jaggi et al., 2005), SNAIL (Du et al., 2010), RIN1 (Ziegler et al., 2011) or by controlling MMP expression (Eiseler et al., 2009a). PKDs also participate in a variety of other processes, such as the transcriptional response to mitochondrial oxidative stress (Storz, 2007), regulation of Golgi vesicle fission and transport (Bard and Malhotra, 2006; Preisinger and Barr,

2005; Pusapati et al., 2010), regulation of cardiac gene expression and contractility (Avkiran et al., 2008), regulation of tumor cell-endothelial cell communication in cancer (Azoitei et al., 2010), cardiac valve formation in zebra fish by regulating histone deacetylase 5 activity (Just et al., 2011), endothelial cell proliferation and angiogenesis (Hao et al., 2009). Some of the biological processes regulated by PKD are described in detail in the following sections.

2.2.5.1 Golgi vesicle fission and transport

PKDs associated with the cytoplasmic surface of Golgi membranes regulate the fission of vesicles that carry protein and lipid cargo from the trans-Golgi network (TGN) to the plasma membrane (Bard and Malhotra, 2006). The Golgi apparatus is a key component of the secretory pathway involved in protein sorting. PKD binds to diacylglycerol (DAG) and this binding was necessary for its recruitment to the TGN via DAG (Baron and Malhotra, 2002). The interaction of PKD with DAG at the TGN is mediated via its CRD1 domain (Baron and Malhotra, 2002; Maeda et al., 2001; Prestle et al., 1996). Upon activation of PKDs at the TGN through their interaction with Gβγ subunits of G-proteins (Jamora et al., 1999) they phosphorylate and activate the Golgi enzyme PI4KIIIβ (Hausser et al., 2005). Subsequent binding of 14-3-3 proteins to PI4KIIIβ inhibits its dephosphorylation, thereby stabilizing enzymatic activity (Hausser et al., 2006). A p21 GTP-binding protein, ARF1, regulates PI4KIIIβ activation by PKD (Graham and Burd, 2011). ARF1 activates phospholipase D (PLD), thereby triggering DAG synthesis at the Golgi membranes. In addition, binding of both ARF1 and DAG to PKD2 selectively target it to the TGN which was specifically mediated by Pro-275 in second cysteine rich domain (Pusapati et al., 2010). Thus, ARF1 ensures an efficient PI4P synthesis by coordinating DAG production with recruitment of PKC, PKD and PI4KIIIβ to the TGN.

2.2.5.2 Cell proliferation and differentiation

PKD1 can be activated by multiple growth promoting GPCR agonists, suggesting that PKD functions in mediating mitogenic signaling (Rozengurt et al., 2005). Over expression of either PKD1or PKD2 potentiated DNA synthesis and cell proliferation in swiss 3T3 fibroblasts (Sinnett-Smith et al., 2004; Sinnett-Smith et al., 2007; Sinnett-Smith et al., 2009; Zhukova et al., 2001). The potentiating effect of

PKD on GPCR induced cell proliferation has been coupled to its ability to increase the duration of the MEK/ERK/RSK pathway leading to the accumulation of immediate gene products like c-Fos that stimulates cell cycle progression (Sinnett-Smith et al., 2004, Sinnett-Smith et al., 2009). PKD is prominently expressed in proliferating primary keratinocytes and down regulated during differentiation of these cells, suggesting that PKD plays a pro-mitogenic and/or anti-differentiation role in these cells (Ernest Dodd et al., 2005). It was also shown that there is a correlation between PKD1 expression and keratinocyte proliferation since PKD1 was highly expressed in basal dividing cells, while differentiating cells exhibited a low expression level (Rennecke et al., 1999). In another report, PKD2 was shown to be an essential regulator of murine myoblast differentiation (Kleger et al., 2011). This regulation is mediated by active PKD2 induced transcriptional activation of myocyte enhancer factor 2D and repressed Pax3 transcriptional activity. Depletion of PKD2 impaired regulation of muscle development associated genes without affecting the proliferative capacity.

2.2.5.3 Transcription

Class-IIa histone deacetylases (HDAC4, HDAC5, HDAC7 and HDAC9), are recruited to gene promoters by transcription factors, such as MEF2, RUNX and CAMTA2 and coordinately repress genes that co-regulate cell type specific functions. When neonatal rat ventricular myocytes are persistently stimulated by α-adrenergic agonist or endothelin 1 (ET1), PKD1 phosphorylates HDAC5. Phospho-HDAC5 dissociates from MEF2 and binds to 14-3-3 adaptor proteins, which promote export of HDACs from nucleus to cytoplasm (Vega et al., 2004). MEF2 then recruits co-activators and drives transcription of fetal genes encoding proteins involved in contraction, Ca^{2+} handling and energy metabolism. Phosphorylation by PKD1 also elicits the dissociation of HDAC5 from CAMTA2, a co-activator that cooperates with the Nkx2-5 transcription factor (Song et al., 2006). An activated CAMTA2-Nkx2-5 complex drives cardiac gene transcription, promoting hypertrophy along with MEF2. In skeletal muscle, PKD1 elicits expression of slow-twitch contractile proteins that mediate muscle endurance, through HDAC5 phosphorylation and MEF2 activation (Kim et al., 2008). VEGF induced exit of HDAC7 from the nucleus through PKD mediated phosphorylation resulted in activation of VEGF-responsive genes in

endothelial cells (Ha et al., 2008; Wang et al., 2008). RUNX, a regulator of osteoblast gene transcription is repressed by HDAC7 binding, and bone morphogenetic proteins induce PKD1-catalysed phosphorylation of HDAC7 (Jensen et al., 2009). Thus PKDs have a central role in stimulating gene expression in various cells and tissues including cardiac and skeletal muscle and endothelial cells.

2.2.5.4 Apoptosis and cell survival

Reactive oxygen species (ROS) trigger phospho lipase D1 (PLD1) and phosphatidic acid phosphatase catalyzed DAG synthesis with concomitant recruitment of PKD1 and PKCδ at the outer mitochondrial membrane (Cowell et al., 2009). Src phosphorylates Tyr 93, creating a binding site for the PKCδ. Tethered PKCδ phosphorylates and activates PKD1, which in turn activates a cytoplasmic IKKα-IKKβ-Nemo complex, eliciting Iκb degradation and nuclear translocation of NF-κB (Storz et al., 2005). NF-κB further induces expression of mitochondrial super oxide dismutase (MnSOD), which removes toxic ROS. In another report, treatment of cells with ROS leads to the activation of PKD1 in a coordinated two step process. First, Abl phosphorylates Tyr463 in the PH domain of PKD1 promoting a second phosphorylation step where by PKCδ phosphorylates the activation loop of PKD resulting in a synergistic PKD1 activation and subsequent NFκB induction. The PKD-mediated induction of NFκB then induces protective genes and leads to cell survival (Storz et al., 2003; Storz et al., 2004). Thus, Src-mediated phosphorylation of PKD is essential to elicit signaling that leads to NF-κB-mediated transcription of pro-survival genes.

2.2.5.5 Cell motility

Several studies indicated a role for PKD in the organization of cytoskeleton, cell shape modulation and adhesion. PKD1 forms a complex in the lamellipodia with SSH1L and F-actin (Eiseler *et al*, 2009b) where it phosphorylates SSH1L, disrupting its association with F-actin and creating a binding site for 14-3-3 adaptor proteins (Eiseler et al., 2009b; Peterburs et al., 2009). As a result, the pSer-3 cofilin concentration increases, barbed-end formation is blocked and cell migration ceases, thus regulating directed cell movement. PKD1 also reduces leading edge F-actin polymerization by phosphorylating cortactin, enabling 14-3-3 protein binding and

stabilization of a complex containing WAVE-2, ARP2/3, F-actin and phospho-cortactin (Eiseler et al., 2010). PKD1 also inhibits F-actin remodeling and cell motility by phosphorylating the Ras effector RIN1. Phosphorylated RIN interacts and activates c-Abl. Further the RIN1-c-Abl complex phosphorylates and alters the conformation and affinity of CRK (also known as p38), an adapter protein that recruits F-actin remodeling proteins (Hu et al., 2005; Ziegler et al., 2011). As a result, there is a diminished actin remodeling, leading-edge protrusion and a reduction in cell motility. Activated PKD1 phosphorylates the cytoplasmic tail of E-Cad, thereby stabilizing its association with β-catenin and the F-actin cytoskeleton (Jaggi et al., 2005). This leads to a strengthening of adherens junctions and inhibition of motility. It was also suggested that PKD1 is essential for maintaining E-Cadherin gene transcription and repressing mesenchymal protein expression (Du et al., 2010). PKD1 phosphorylates SNAIL. As a result, SNAIL target genes are de-repressed and E-Cadherin and other proteins that mediate adherens-junction formation and immobility are produced. In accordance with this, ectopic expression of PKD1 inhibits mesenchymal gene transcription and decreases tumor development by 70% in a xenograft model (Du et al., 2010). Human breast cancer tissue arrays revealed a decrease in expression of PKD1 by approximately 60% in invasive and metastatic ductal carcinomas (Eiseler et al., 2009a), indicating a possible loss of PKD1 in metastasis.

2.3 Cell Migration

2.3.1 Introduction

Cell migration plays an essential role in embryogenesis, wound healing and inflammatory responses. A deregulation of cell movement can cause pathological states such as developmental defects, chronic inflammation, invasion and metastasis. Actin cytoskeleton is regarded as the essential engine that drives cell protrusion (Betz et al., 2006; Hofman et al., 1999). The continuous creation of new actin network at the leading edge is considered to be essential for pushing the cell forward (Kaverina et al., 2002).

2.3.2 Integration of signals

A cell begins to move in response to a variety of physical, chemical, diffusible or non-diffusible signals detected by receptor proteins located at the cell membrane (Bruce Alberts, 2002). Acting through receptors and multiple signal transduction pathways, the stimuli transmitted by the Rho family GTPases, Rac and Cdc42 (Machesky and Gould, 1999; Machesky and Insall, 1999) converge on WASp/Scar proteins and Arp2/3 complex which then stimulates actin filament nucleation by Arp2/3 complex. As a consequence, the cortical actin filament network is assembled (Figure 3).

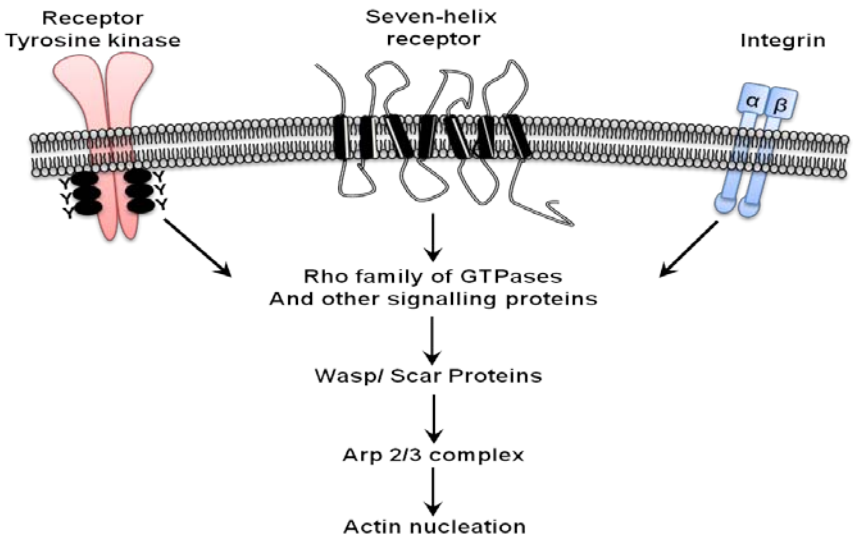

Figure 3: Signaling pathways through WASp/Scar to Arp2/3 complex. *Acting through receptor tyrosine kinase/ seven helix receptors and integrins, a variety of stimuli regulates cellular actin polymerization. Image based on original figure from (Pollard et al., 2000).*

2.3.3 Dynamic regulation of the Actin cytoskeleton

Extension of the leading edge through actin polymerization drives cancer cell migration (Tilney et al., 1981; Tilney et al., 1983; Zigmond, 1993; Pollard et al., 2000). Activating proteins like WAVE and WASp enable nucleator proteins (e.g. arp2/3 complex) to initiate the polymerization and assembly of new actin filaments. Actin depolymerization promoting proteins (e.g. cofilin) also aid network growth (Bi and Zigmond, 1999). Cofilin (also known as Actin Depolymerizing Factor or ADF) severs actin filaments and creates new plus ends for the growth of new actin filaments (Bamburg et al., 1999; Carlier et al., 1999). Actin binding proteins (e.g. profilin) maintain a steady actin monomer pool for polymerization. Capping proteins (e.g. CapZ) control filament length by attaching to actin filament ends and stopping further polymerization, while severing and fragmenting proteins (e.g. gelsolin, severin) cut actin filaments and networks (Schafer et al., 1996). All these proteins work together to coordinate actin network formation and bring about leading edge motility (Pollard et al., 2000). The individual steps are illustrated in the figure 4.

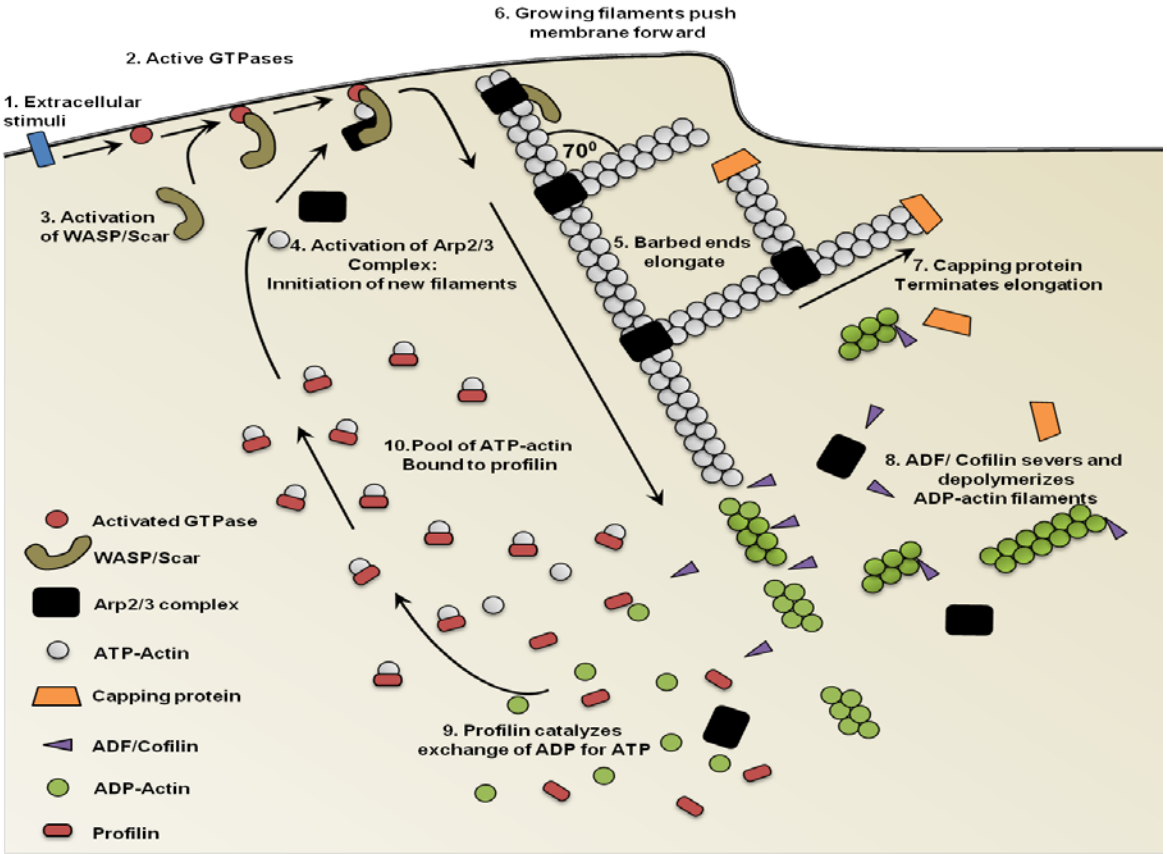

Figure 4: Dendritic nucleation hypothesis for the assembly of actin networks at the leading edge of motile cells. *(1 and 2) External cues activate of GTPases. (3 and 4) Activated Wiskot Aldrich syndrome family of proteins (WAVEs/ WASP) and related proteins in turn activate Arp2/3 complex leading to initiation of a new filament as a branch on the side of an existing filament. (5 and 6) Supported by a high concentration of profilin-bound actin stored in the cytoplasm each new filament grows rapidly, and this pushes the plasma membrane forward. (7) Capping protein binds to the growing ends, terminating elongation. (8 and 9) Actin-depolymerizing factor (ADF)/ cofilin then sever and depolymerizes the ADP filaments. Profilin re-enters the cycle at this point, promoting dissociation of ADP and binding of ATP to dissociated subunits. (10) ATP bound actin binds to profilin, refilling the pool of subunits available for a new assembly. Image based on original figure from (Mullins et al., 1998; Pollard et al., 2000).*

2.3.4 Initiation of cell movement

The process of cell movement can be divided into three stages (Abercrombie, 1980). First, a cell propels the membrane forward by orienting and reorganizing (growing) the actin network at its leading edge. Second, it adheres to the substrate at the leading edge and de-adheres (releases) at the cell body and rear of the cell. Cellular adhesions link intracellular F-actin with the extracellular substratum and function as traction sites and mechanosensors. Finally, the interaction of myosin motors and actin filaments generates the traction force necessary for the cells to move forward (Chhabra and Higgs, 2007; Rogers et al., 2003). As the extending edge moves forward, the cell constantly monitors the signal direction and tailors its direction of motion (Figure 5).

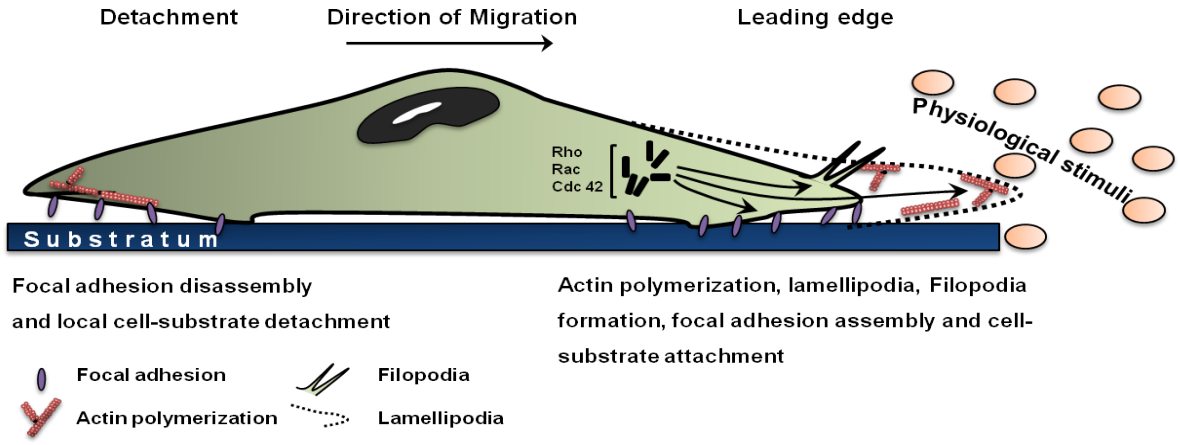

Figure 5: Overview of cell migration. *Directed cell migration in response to a variety of stimuli is dependent on a cycle of events involving a dynamic sequence of cell-substrate attachment at the leading edge of the cell coordinated with cell-substrate detachment at the rear. Wasp/ Scar proteins interact with a variety of cell signaling molecules known to influence cytoskeletal dynamics, bridging surface receptor stimulation to actin polymerization, lamellipodia, filopodia formation, and focal adhesion assembly at the leading edge of the cell initiating the process of cell migration. Image based on original figure from (Frame et al., 2002)*

2.4 Abelson Interactor 1

2.4.1 Identification

Abelson Interactor (ABI) family of proteins 1 and 2 were identified as substrates and binding partners of the c-Abl tyrosine kinase, a proto-oncogene product of the Abelson murine leukemia virus oncogene, v-abl (Dai and Pendergast, 1995; Goff et al., 1980; Shi et al., 1995). Later on a third member of Abelson interactor family of proteins, NESH was reported (Miyazaki et al., 2000). Although NESH was initially identified as a novel protein containing SH3 domain, it was later included in ABI family of proteins based on its amino acid sequence similarity with ABI1 and 2.

2.4.2 Structural organization

Amino acid sequence analysis of ABI family of proteins across the species revealed a highly variable central region and highly conserved amino and carboxy terminal regions (Echarri et al., 2004). ABI1 contain proline rich and SH3 domains in the carboxy terminus and the WAVE binding (Macoska et al.), SNARE and homeo domain homology region in the amino terminus (Ring et al., 2011; Stradal et al., 2001). Structural organization of ABI1 (isoform B- 481a.a) used in this investigation is shown here under (Figure 6).

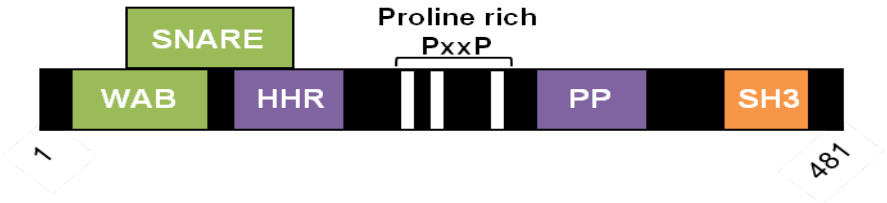

Figure 6: Structural organization of Abelson Interactor 1- WAB; *WAVE binding domain,* ***SNARE;*** *Region homologous to coiled-coil domain of SNARE (**S**oluble **N**-ethylmaleimide-sensitive fusion protein **a**ttachment protein **re**ceptor),* ***HHR;*** *Homeodomain homology region,* ***PP;*** *Proline rich and* ***SH3;*** *Src Homology domain.*

2.4.3 Localization

Endogenous ABI1 is a nucleo-cytoplasmic protein under resting conditions (Leng et al., 2005; Proepper et al., 2007). However ABI1 was reported to localize to actin based membrane protrusions, such as membrane ruffles, lamellipodia and filopodia, after growth factor or integrin-mediated cell stimulation (Stradal et al., 2001). The translocation of ABI1 from cytosol to the highly dynamic peripheral region in a motile cell is mediated exclusively by the first 145 residues of the N terminus, containing a region of the coiled-coil domain of t-SNARE and a portion of the HHR region (Stradal et al., 2001).

2.4.4 Expression

ABI1 is widely expressed in human and mouse tissues (Biesova et al., 1997; Shi et al., 1995). The highest expression levels of ABI1 are observed in brain, testis, bone marrow, and spleen. Highly invasive breast cancer cell lines (MDA-MB-231, MDA-MB-157, BT549, and Hs578T) also express high levels of ABI1 (Wang et al., 2007). Expression array analyses suggest that high ABI1 expression is associated with liver metastasis in small cell lung cancer and paclitaxel resistance in ovarian cancer (Duan et al., 2005; Kakiuchi et al., 2003).

2.4.5 Molecular interactions

ABI1 could undergo multiple protein-protein interactions given its several domains (Figure 6), and its localization to distinct subcellular compartments. ABI1 was initially identified as the substrate and binding partner for Src homologous 3 (SH3) domain of the c-Abl tyrosine kinase (Shi et al., 1995) and was later shown to interact with several other proteins such as guanine nucleotide exchange factors, Sos1 and Sos2. ABI1 can inhibit mitogenesis activated by both growth factors and v-Abl (Fan and Goff, 2000). ABI1 interacts directly with the WAVE homology (WHD) domain of WAVE2, increases WAVE2 actin polymerization activity and mediates the assembly of a multi protein complex, WAVE2-ABI1-Nap1-PIR121 (Innocenti et al., 2004). On the other hand, ABI1 interacts with WAVE2 via its coiled coil domain and promotes membrane localization upon fibronectin stimulation (Gautreau et al., 2004; Innocenti et al., 2004). ABI1 also couples WAVE2 to Abl and mediates tyrosine phosphorylation and activation of WAVE2 (Leng et al., 2005). Interaction of ABI1 with

Neural Wiskott-Aldrich syndrome protein (N-WASP) potently induces N-WASP activity *in vitro* (Innocenti et al., 2005).

ABI-1 forms an epidermal growth factor inducible complex with Cbl ubiquitin ligase and regulates internalization of EGFR (Tanos and Pendergast, 2007). Interaction of ABI1 with p21-activated Kinase 2 (PAK-2) is essential for the regulation of PDGF induced membrane ruffles (Machuy et al., 2007). A variety of other molecules, including those involved in the signal transductions of small GTP-binding protein Rac and PI3 also interact with ABI1 (Innocenti et al., 2002; Innocenti et al., 2003; Scita et al., 1999). A recent investigation identified an interaction between ABI1 and α4 integrin, important for cell spreading. In addition, ABI1 or α4 integrin knockout mice exhibit mid-gestational lethality with abnormalities in the placental and cardiovascular development, thus revealing a direct link between the α4 integrin and actin polymerization and uncover a role for ABI1 in the regulation of morphogenesis *in vivo* (Ring et al., 2011).

2.4.6 Functions of ABI1

ABI1 participates in the transduction of signals from Ras to Rac (Scita et al., 1999), in the regulation of proliferation, migration, invasion (Wang et al., 2007) and invadopodia formation of breast cancer cells and MMP-9 expression (Sun et al., 2009). The protein localizes to the leading edge of lamellipodia and filopodia (Stradal et al., 2001), promotes lamellipodia formation (Steffen et al., 2004), actin cytoskeleton reorganization through the regulation of Rho family members (Stovold et al., 2005; Stradal and Scita, 2006) and formation and activation of the WAVE2 signaling complex (Innocenti et al., 2004). ABI1 is required for the integrity and the stability of the WAVE2 complex (Dubielecka et al., 2011).

2.4.6.1 Cell proliferation

Analysis of ABI1 expression levels in nine breast cancer cell lines with varying degrees of invasiveness indicated that it is weakly expressed in lowly invasive (MCF-7, T47D, MDA-MB-468, SKBR3, and CAMA1) compared to highly invasive breast cancer cells (MDA-MB-231, MDA-MB-157, BT549, and Hs578T). Knockdown of ABI1 in highly invasive breast cancer cells, MDA-MB 231 negatively regulated cell proliferation. Such cells were characterized by an overall increase in doubling time

(from 29.8 to 41.4 hours) and a growth arrest in G_0-G_1 phase and delayed entry into G_2-M phase (Sun et al., 2009; Wang et al., 2007). A recent tissue-array-based investigation in 988 patients with invasive breast carcinoma demonstrated a significant association between ABI1 and its downstream effector phospho-Akt (p-Akt) expression. ABI1 expression also showed significant positive correlation with older age at diagnosis and the Ki67 index and most importantly, it was demonstrated to be an independent predictor of both disease free survival (DFS) and overall survival (Fazioli et al., 1993; Wang et al., 2011).

2.4.6.2 Migration, Invasion and Metastasis

Actin polymerization and lamellipodia formation play critical roles in cell migration and metastasis (Ridley, 2001). ABI1 is an adaptor protein involved in actin reorganization, lamellipodia formation, cell spreading and migration via WASP family verprolin-homologous proteins 2 (WAVE2) (Innocenti et al., 2004; Leng et al., 2005; Steffen et al., 2004). Loss of ABI1 resulted in the down regulation of WAVE2, nucleosome assembly protein 1 (Nap1), and PIR121 protein levels (Innocenti et al., 2004). It was also reported that the ABI1 based macromolecular complex (Hspc300/WAVE2/ABI1/Nap1/PIR121 and/or Abl/ABI-1/WAVE2) mediates signaling transduction between Rho family proteins and the actin cytoskeleton by activating Arp2/3 (Innocenti et al., 2004; Leng et al., 2005). RNA interference indicated that ABI1 is required for the formation of platelet derived growth factor induced membrane ruffles, Rac dependent actin remodeling, cell spreading, and migration (Chen et al., 2010; Eto et al., 2007; Kheir et al., 2005; Leng et al., 2005; Ring et al., 2011; Wang et al., 2007; Yu et al., 2008).

Many metastatic cancer cell lines contain a specialized adhesive/ invasive structure, called an invadopodium (Gimona et al., 2008; Kelly et al., 1994) and can be distinguished by their ability to degrade extracellular matrix (ECM) via matrix metalloproteinase's (MMPs), the enzymes for ECM degradation. A report from (Sun et al., 2009; Wang et al., 2007) identified a function for ABI1 in regulation of invadopodia formation and the Src-inhibitor of differentiation protein 1 (Id1)-matrix metalloproteinase (MMP-9) pathway in human breast cancer cells, MDA-MB-231. Epigenetic silencing of the ABI1 in these cells impaired the formation of invadopodia

and resulted in down regulation of Src activation, Id1/MMP-9 expression and reduced the ability of these cells to degrade extracellular matrix.

Another study (Chen et al., 2010) indicated that in ovarian cancer cell lines, lysophosphatidic acid (LPA, a growth factor like phospholipid)-induced Rac activation, facilitated by SOS1/EPS8/ABI1 trimeric complex is a prerequisite for ovarian cancer metastasis. Their study also implied that the integrity of this tri-complex is essential for LPA stimulated metastases and at least one member of the tricomplex is missing in non-metastatic cancer cells. However, reports from other groups have suggested that ABI1 might function as an invasion suppressor, notably in prostate and gastric cancers (Cui et al., 2010; Macoska et al., 2001).

3. Aims and Objective

Aim of the investigation

PKD's are implicated in numerous biological processes, which play a role in the development or the progression of cancer. To establish the signaling context of PKDs and in particular downstream mediators for PKD-controlled tumor cell motility we aimed to identify and characterize novel PKD substrates**.**

Abelson Interactor 1 (ABI1), one of the potential substrates identified, does play a role in cell migration. In addition, both PKD's and ABI1 localize to the leading edge structures, plasma membrane, lamellipodia and filopodia. This prompted us to further investigate a potential role of ABI1 as substrate of PKDs.

This investigation was divided into following sections;

i. ProtoArray® Human Protein Microarray based identification of novel substrates.

ii. *In silico* prediction and validation of potential phosphorylation sites.

iii. Basic biochemistry between PKD2 and ABI1

iv. Impact of phosphorylation on localization and interaction with WAVE2, a known constitutive binding partner of ABI1.

v. Examination of the functional consequences of ABI1 phosphorylation on tumor cell motility.

4. Materials and Methods

4.1 Chemicals and Biochemicals

Chemical	Company
ATP	Sigma-Aldrich, Deisenhofen
dNTP Set (100mM)	Invitrogen, Karlsruhe
BSA	Sigma-Aldrich, Deisenhofen
Glycine	Roth, Karlsruhe
Methanol	Sigma-Aldrich, Deisenhofen
Isopropanol	Roth, Karlsruhe
ECL substrate	Thermoscientific
Glycerol	Roth, Karlsruhe
Ethidium bromide	Roche Diagnostics, Basel, Switzerland
Fluoromount® G	Biozol, Eching
Acrylamide, Rotophorese Gel30	Roth, Karlsruhe
Ammoniumpersulfate	Roth, Karlsruhe
Bio-RAD protein assay solution, 5x	Bio-RAD Laboratories, München
Complete protease inhibitor cocktail (EDTA free)	Roche Diagnostics, Basel, Switzerland
Phenylmethylsulfonylfluoride (PMSF)	Sigma-Aldrich, Deisenhofen
SDS	Roth, Karlsruhe
TEMED	Sigma-Aldrich, Deisenhofen
PageRuler™ prestained prot. Ladder	MBI Fermentas, St. Leon-Roth
Tween20	Sigma-Aldrich, Deisenhofen
Triton X100	Sigma-Aldrich, Deisenhofen
Dry milk powder	Roth, Karlsruhe
Sodium fluoride (NaF)	Sigma-Aldrich, Deisenhofen
Sodium orthovanadate	Sigma-Aldrich, Deisenhofen
DTT	Sigma-Aldrich, Deisenhofen
EDTA	Roth, Karlsruhe
EGTA	Roth, Karlsruhe
Tryptone	Roth, Karlsruhe
Yeast extract	Roth, Karlsruhe
Agar-agar	Roth, Karlsruhe
FCS (foetal calf serum)	PAA, Austria
Ampicillin	Roth, Karlsruhe
Kanamycin	Roth, Karlsruhe

Dimethysulfoxide (DMSO)	Roth, Karlsruhe
OptiMEM®I	Invitrogen/Gibco, Karlsruhe
FCS (fetal calf serum)	PAA Laboratories, Linz, Austria
Penicillin/ Streptomycin	Sigma-Aldrich, Deisenhofen
DMEM	Invitrogen/Gibco, Karlsruhe
RPMI 1640	Invitrogen/Gibco, Karlsruhe
32P γATP (5000Ci/mmol; 37 GBq= 1mCi)	Perkin Elmer (Germany)

Table2: Chemicals/ biochemicals and source

4.2 Buffers and Solutions

Buffers	Composition
Acrylamide running gel buffer	10%/12,5% (v/v) acrylamide, 375 mM Tris, 0.1% SDS, pH 8.8
Acrylamide stacking gel buffer	4% (v/v) acrylamide, 125 mM Tris, 0.1% SDS, pH 6.8
TGS buffer for SDS-PAGE	192 mM glycine, 25 mM Tris-HCl, 0.1 % (w/v) SDS, pH 7.4
TBS buffer	20mM Tris, 136 mM NaCl, pH 7.6
TBS/Tween	TBS buffer + 0.05% (v/v) Tween20
SDS sample buffer (5x)	250 mM Tris-HCl, 25% (v/v) Beta-mercaptoethanol, 25% (v/v) glycerol, 10% (w/v) SDS, 0.05% (w/v) bromophenol blue, pH 6.8
PBS (phosphate buffered saline)	140 mM NaCl, 2.7 mM KCl, 8 mM Na2HPO4, 1.5 mM KH2PO4, pH 7.2
Cell lysis buffer	20 mM Tris, 1% (v/v) TritionX100, 5 mM MgCl2,150 mM NaCl, pH 7.4
Sodium orthovanadate	1 M in ddH2O
PMSF solution	100 mM in isopropanol
TBE (10x)	900 mM Tris-borate, 20 mM EDTA (5.5% (w/v) boric acid)
DNA sample buffer (6x)	250 pg/ml xylene cyanol, 250 pg/ml bromophenol blue, 50 mM EDTA, 80% (v/v) glycerol
LB medium	10 g/l tryptone, 5 g/l yeast extract, 10 g/l NaCl, pH 7.0

Table 3: Different buffers and their compositions

4.3 Antibodies

Species	Specificity	Supplier	Dilution
Mouse	Flag M2	Sigma	1 in 1000
Mouse	GFP	Roche	1 in 1000
Mouse	ABI1	MDL	1 in 1000
Mouse		Abcam	1 in 1000
Rabbit	pMOTIF	Dr. Peter Storz, Mayo Clinic, Jacksonville, USA.	1 in 1000
Rabbit	PKD1	Bethyl	1 in 1000
Rabbit	PKD2	Orbigen	1 in 1000
Rabbit	PKD2	Bethyl	1 in 1000
Rabbit	PKD3	Bethyl	1 in 1000
Rabbit	PKD(P-Ser744/748)	Cell Signaling	1 in 1000
Rabbit	WAVE2	Cell Signaling	1 in 1000
Rabbit	PIR121/Sra-1	Millipore	1 in 1000
Rabbit	HSPC 300	Abcam	1 in 1000
Rabbit	NCKAP1	Abcam	1 in 1000
Mouse	β-Actin	Sigma	1 in 1000
Mouse	Anti-Mouse IgG (peroxidase-conjugated)	Amersham, Pharmacia	1 in 5000
Rabbit	Anti-Rabbit IgG (peroxidase-conjugated)	BioRad	1 in 5000

Table 4: Different antibodies used for western blotting

4.4 Enzymes

Enzyme	Supplier
Restriction endonucleases	New England BioLabs
DNA ligase	New England BioLabs
Taq polymerase	Invitrogen
PfuTurbo DNA polymerase	Stratagene

Table 5: Enzymes used in site-directed mutagenesis and cloning procedures.

4.5 Ready to use kits

Application	Kit	Supplier
DNA preperation	Purelink HiPure Plasmid DNA purification Kit	Invitrogen
	High pure plasmid isolation kit	Roche
DNA gel extraction	QIAquick Gel extraction kit	Qiagen
Site directed mutagenesis	QuickChange XL Kit	Stratagene
Transfection	Lipofectamine 2000 kit	Invitrogen
	Lipofectamine LTX	Invitrogen
	Fugene HD	Roche
	Hiperfect	Qiagen
F-actin turn over	Actin polymerization kit	Cytoskeleton
Affinity purification	α-FLAG M2-Agarose (A2220)	Sigma

Table 6: Ready to use kits for molecular biology

4.6 Plasmid purification

The host *E. coli* XL-1 blue (genotype: recA1, endA1, gyrA96, thi-1, hsdR17, supE44, relA1, lac, [F'proAB, lac ZΔM15Tn10 (tet^r)], (Bullock et al, 1987) was used for the plasmid propagation. Plasmid DNA was purified from the transformed bacteria according to the manufacturer's instructions using anion-exchange chromatography based PureLink™ HiPure Plasmid Purification Kits (Invitrogen).

4.7 Plasmids

For the plasmid propagation the host E. coli XL-1 blue (genotypes: recA1, endA1, gyrA96, thi-1, hsdR17, supE44, relA1, lac, [F'proAB, lacqZΔM15Tn10 (tetr)], was used.

Plasmid	Size (kb)	Resistance	Supplier
pEGFP-C2	4.7	Kanamycin	Clontech
pCMV-Tag 3b	4.3	Kanamycin	Stratagene
Flag-pcDNA3	4.7	Ampicillin	Osswald F., Ulm
pGEX-4T-3	4.9	Ampicillin	Amersham

Table 7: Vectors used for cloning

4.8 Primer pairs used for sub-cloning

Construct	Primer	Sequence
pEGFP N1 ABI1	-	Provided by Dr. Johan Van lint, Belgium
pCMV-Tag3b ABI1	Forward	Gatgaattcagtatggcagagctgcagatg
	Reverse	Agtctcgagagtttaatcagtatagtgcatgattga
ABI1ΔT-Snare	Forward	Ttgttgtcaaaataccaatctctcttgtctgtagcctgtatgt
	Reverse	Atacaggctacagacaagagagagattggtattttgacaacaaa
ABI1Δ Proline	Forward	Cctcctcatcttcataatccacagcaatagaaattgaattttga
	Reverse	Tcaaaattcaatttctattgctgtggattatgaagatgaggagg
ABI1Δ SH3	Forward	Agtggtaccagtctacttgggggcccaagc
ABI1Δ NT	Forward	Acgtctcgagtcgagattggtattttgacaacaaa
pGEX 4T3-ABI1	Forward	Aaccgaattccgcagagctgcagatgttactagaggaggagat
	Reverse	Ggagaggcggccgctttaatcagtatagtgcatgattgattc
ABI1 S88A	Forward	Ctcagcttcggagaatggaggcttccatcaatcatatctcacag
	Reverse	Ctgtgagatatgattgatggaagcctccattctccgaagctgag
ABI1 S88E	Forward	Ctcagcttcggagaatggaggagtccatcaatcatatctcacag
	Reverse	Ctgtgagatatgattgatggactcctccattctccgaagctgag
ABI1 S296A	Forward	Cagatatctcgacacaacgcgactacttcttcgacatct
	Reverse	Agatgtcgaagaagtagtcgcgttgtgtcgagatatctg
ABI1 S296E	Forward	Cagatatctcgacacaacgagactacttcttcgacatct
	Reverse	Agatgtcgaagaagtagtctcgttgtgtcgagatatctg

Table 8: Primers used for ABI1 cloning

4.9 Polymerase chain reaction (PCR)

The polymerase chain reaction was used for the amplification of DNA segments with two defined (sense and antisense) primers for analytical (using *Taq* DNA polymerase, Fermentas) or preparative (using *Pfu* Turbo DNA polymerase, Stratagene) applications. A typical PCR reaction mixture for *Taq*- and *Pfu* polymerase (table 8) as well as a PCR program profile (table 9) is listed below.

Substance	Concentration
10 x buffer	1X
Pfu / Taq polymerase	2.5U/ 1.2U
Primers	100 pM
dNTPs	.6 mM
MgCl2	2mM
Template	100ng

Table 9: PCR mixture

PCR-conditions	Temperature	Time
1 Cycle	94	2 min
35 cycles	94	30 sec
	59	1 min
	72	1kb/ min of the construct
	72	Final extension

Table 10: PCR conditions

4.10 Site directed mutagenesis (SDM)

The QuickChange site-directed mutagenesis kit (Stratagene) was used to insert point mutations. Briefly, *PfuTurbo* DNA polymerase replicates both plasmid strands without displacing the mutant oligonucleotide primers. The oligonucleotide primers, each complementary to opposite strands of the vector, are extended during temperature cycling by *PfuTurbo* DNA polymerase. Incorporation of the oligonucleotide primers generates a mutated plasmid containing staggered nicks. Following temperature cycling, the product is treated with *Dpn* I. The *Dpn* I is an endonuclease (target sequence: 5´-Gm6ATC-3´) specific for methylated and hemi-methylated DNA and was used to digest the parental DNA template and to select for mutation-containing synthesized DNA. The nicked DNA-vector containing the desired mutations is then transformed into XL1-Blue super competent cells. The small amount of starting DNA template required for performing this method, the high fidelity of the *PfuTurbo* DNA polymerase, and the low number of thermal cycles all contributes to the high mutation efficiency and decreased potential for generating random mutations during the reaction.

4.11 Cell biology: Cell lines and growing conditions

HEK293, HeLa, Panc 1 and MiaPaCa were cultured in Dulbecco's Modified Eagle's Medium (GIBCO) and MCF 7 and MDA MB231 were cultured in RPMI medium (GIBCO). The medium were supplemented with 10% (v/v) fetal bovine serum (Biochrom), penicillin (100U/ml), and 100 µg/ml streptomycin at 37°C in a humidified atmosphere containing 5% CO2.

Cell type	Tissue	Species
HEK 293	Embryonic kidney	*Homo sapiens/ ATCC*
HeLa	Cervical carcinoma	*Homo sapiens/ ATCC*
Panc 1	Pancreatic carcinoma	*Homo sapiens/ ATCC*
MiaPaCa	Pancreatic cancer cells	*Homo sapiens/ ATCC*
MCF 7	Breast cancer cell line	*Homo sapiens/ ATCC*
MDAMB 231	Breast cancer cell line	*Homo sapiens/ ATCC*

Table 11: Different Cell lines used in the investigation

4.12 Transient transfection: Various reagents

Poly Ethylen Imine (PEI)

Transfection of HEK293T was performed with Polyethyleneimine (PEI, linear, MW ~ 25000, Polysciences Inc., Warrington, Pennsylvania, stock concentration of 1 mg/ml) with a ratio of 1:7,5 (µg DNA : µl PEI) (Zhang et al., 2004). Other transfections were performed according to manufacturer's instructions.

Cell Type	Application	Method	Company
HEK 293T	Biochemical detection of proteins	PEI	Polyscience Inc.
HEK 293T	Biochemical detection of phosphorylation events	PEI	Polyscience Inc.
MiaPaCa	Biochemical detection of proteins	Lipofectamine 2000	Invitrogen
HeLa	Random migration assay	FugeneHD	Roche
Panc1	Transwell migration assay	Lipofectamine LTX	Invitrogen

Table 12: Transient transfection methods applied in different assays.

4.13 Stimulation/ treatment of cells

i. Activation of PKD2 in HEK 293T

Over expressed PKD2 in HEK293 cells (Flag-PKD2-WT/-CA/-DA transfected) or endogenous PKDs in MiaPaCa cells (Scrambled Si RNA or PKD1/ 2 /3 specific Si RNA treated), were subjected to 400nM phorbol 12-myristate 13-acetate (Calbiochem) stimulation for 10 minutes. Control cells received an equivalent amount of solvent (DMSO).

ii. Heregulin stimulation of MCF7 cells

For Heregulin stimulation MCF 7 cells transfected with the constructs indicated were serum-starved for at least 3-4 hours and then stimulated with 100ng/ml human Heregulin1 (PeproTech, NJ) for 10 minutes.

iii. siRNA treatment of cells

Functionally validated Stealth RNAi directed against PKD1, 2 and 3 were from Qiagen. Cells were transfected with siRNA using Lipofectamine 2000 according to the manufacturer's instructions in a 6 well plate format at a final concentration of 30nM (Invitrogen, CA). Corresponding fluorescently labeled stealth RNAi purchased from Invitrogen (Invitrogen, CA) was used as negative control. Twenty-four hours after the first transfection, cells were re-transfected with 30nM siRNA. Cells were then lysed and analyzed by western blotting.

4.14 Preparation of cell extracts

Cells at a confluency of 90% (6 well- ≈1X10^6 ; 10 cm dish- ≈9X10^6) were washed twice with PBS, scraped in regular lysis buffer (50 mM Tris pH 7.4, 1% Triton-X-100, 1 mM DTT, 2 mM EDTA, 2 mM EGTA, 50 mM NaF, 1 mM Na-orthovanadate, EDTA-free protease inhibitors) and centrifuged at 15 000 x g for 20 min. Protein concentration in the lysates was estimated (Bradford Biorad Protein Assay; Biorad), mixed with SDS- sample buffer (30% (w/v) glycerol, 4% (w/v) SDS, 50 mM TrisHCl pH 6.8, 5% (w/v) DTT, 0.005% (w/v) bromphenolblue) and denatured at 95°C for 5 minutes.

4.15 Immunoprecipitations

MiaPaCa/ MDAMB-231/ transiently transfected HEK293T cells expressing the indicated constructs were lysed at 4 °C in 1 ml lysis buffer (20 mM Tris/HCl,pH 7.4, 1% Triton X-100, 150 mM NaCl, 5 mM MgCl2, 10 mM sodium fluoride, 20 mM glycerophosphate) containing protease and phosphatase inhibitors . After 45 minutes the samples were centrifuged (14,000 rpm for 20 min at 4 °C), the supernatant was collected and equal amounts of total protein (2.5 mg), as described in the individual figures, were subjected to immunoprecipitations (IP's) with specific antibodies, ABI1 (1.25µl/ mg), PKD2 (1µl/ 1mg), WAVE2 (1µl/ 1.5mg), GFP (1µl/ 1mg) and FLAG M2

(1µl/ 1mg). After incubation for 1.5 hours at 4°C on a roller incubator 30 µl of Protein G-Sepharose (Amersham Bioscience, Freiburg) was added and the mixture was incubated for an additional hour at 4°C. Subsequently the sepharose pellet was washed three times in lysis buffer, then 4x SDS sample buffer was added and pellets were heated to 95°C for 5 min to release the precipitated proteins. Samples were then subjected to western blot analysis to detect precipitated proteins.

4.16 Western blot analyses

Western blots were performed according to standard procedures to detect proteins from whole cell lysates and immunoprecipitations. Briefly the protein samples for western blot analysis were fractionated by 8% or 10% SDS-PAGE and transferred on to an activated PVDF membrane. Membranes were blocked with 5% milk (GFP, FLAG, ABI1, HSPC 300, NCKAP1, PIR121/Sra1, PKD2 and 3 antibodies), 5%BSA (PKD1, Phospho-PKCμ and WAVE2 antibodies), 2% BSA (pMOTIF Antibody) in TBS-T (0.2 % Tween 20) for 1hour, followed by incubation with appropriate primary antibodies in PBST (dilutions are listed in table 1) for 1 hour at RT or at 4°C over night with gentle agitation. After washing the membrane (3 times for 15 minutes each with TBS-T) and incubating with alkaline phosphatase conjugated anti–mouse IgG or anti–rabbit IgG secondary antibodies (1:5000) for an additional 1 hour, HRP-linked secondary antibodies were detected by chemiluminescence (Pierce or Amersham).

4.17 Expression and purification of GST-tagged proteins in bacteria

GST fusion proteins of ABI1were purified from *Escherichia coli* BL21 extracts using Glutathione Sepharose 4B beads according to the instructions of the manufacturer (Amersham, Buckinghamshire, England). The system is based on inducible expression of genes or gene fragments as fusions with *Schistosoma japonicum* GST. NEB Iq Express Competent E.coli were used as a host for GST-proteins expression. The host bacteria were grown in Luria Bertani medium (Goff et al., 1980) at 37°C to achieve exponential growth (approximately 3.5 hours with 5% overnight culture used as seeding material; OD 600: ~0.75). Expression of GST-tagged proteins was stimulated by adding IPTG (Isopropyl-thiogalactopyaranosid, PeqLab) to a final concentration of 0.5mM and the cultures were grown at lower

temperature for the next 12 hours, to decrease metabolism and avoid formation of the inclusion bodies. The cells were harvested by centrifugation at 6000 rpm (Suprafuge 22, Heraeus) for 20 minutes and the pellet was resuspended in the lysis buffer (500 mM NaCl, 50 mM Tris pH 7.5, 10 mM $MgCl_2$ and 5% glycerol (w/v), complete protease inhibitor mix (Roche)). After addition of lysozyme (25 µg/ml, Fluka) the cells were sonicated (3 X 10 seconds, constant pulse; B-15 Sonicator, Sartorius Biotech GmbH). The cell lysate was precleared by centrifugation (10,000 rpm, 30 minutes, at 4°C, Heraeus). GST fusion proteins were then purified from clear bacterial lysates by affinity chromatography using immobilized glutathione for overnight on a rotating wheel. Fusion proteins were eluted under mild, non-denaturing conditions using reduced 50 mM glutathione (Sigma) and the eluted fractions were stored at -80 for further use.

4.18 Kinase substrate identification assay

The assay was performed by Invitrogen. Briefly the methodology involves the following steps. The protein microarrays (containing approximately 3000 GST tagged full-length human proteins), were blocked for 2 hours with blocking buffer (1% BSA in 1X PBS). A kinase reaction mixture (120 µl) containing kinase buffer (1% BSA, 1% NP-40, 100 mM MOPS pH 7.2, 100 mM NaCl, 5 mM MgCl2, 5 mM MnCl2), recombinant protein kinase, PKD2 (30 nM), and [γ-32P] ATP (~33 nM, 1 mCi/ml) was added to the surface of the microarrays. Microarrays were covered with glass cover slips and incubated at 30°C in an incubator for 60 min. After incubation, arrays were washed twice with 0.5% SDS for 15 min at room temperature followed by two washes with distilled water for 15 min and allowed to dry. The dried microarrays were exposed to a phosphorimager screen (50 µm resolution) overnight and images were acquired with a Packard Cyclone Phosphor imager. The images were processed with Adobe Photoshop software, and data were acquired using GenePix Pro software (Molecular Devices) and analyzed using ProtoArray Prospector software (Invitrogen).

4.19 In vitro kinase assay

To examine *in vitro* GST-ABI1 or histone phosphorylation by PKD2 and its mutants, PKD2 was enriched by immunoprecipitation as described above. Immune complexes were washed once with lysis buffer I (50 mM Tris pH 7.6, 1% Triton-X-

100, 1mM DTT, 2 mM EDTA, 2 mM EGTA, complete EDTA-free protease inhibitor mix (Roche), phosphatase inhibitor mix (Phospho-Stop Roche)), twice with lysis buffer II (buffer I without triton X-100) and thrice with kinase buffer (30 mM Tris-HCl, pH 7.4, 10 mM $MgCl_2$, 1 mM DTT) and then resuspended in 20 µl of kinase buffer in the presence of 0.5 mg/ml histone H1 or 4 µg GST-ABI1-WT/ -S88A/ -S296A/ -S88 296A and 100 µM [γ32 P] ATP. Reactions were incubated at 30°C for 15 minutes. Reaction was terminated by adding an equal amount of the 5xSDS-PAGE sample buffer. Finally, the kinase activity is observed after performing SDS-PAGE and exposing the gel to x-ray or Fujifilm's phosphor Imaging Plate. Phosphor Imaging Plate is a high-sensitive, two-dimensional sensor for the detection of radioisotopes. The AIDA Image Analyzer software was used for the evaluation and annotation of images that were obtained with a luminography scanner (Fuji Film BAS).

4.20 Purification of WAVE2 from 293T lysates: FLAG-M2 affinity purification

HEK 293T cells seeded at a density 4 x 10^6 cells/ 10 cm dish were transfected with FLAG-WAVE2 using PEI (8 µg DNA and 20 µl PEI in 400µl serum-free DMEM). After 48 hours cells were harvested, washed once with PBS and then lysed in lysis buffer supplemented with EDTA-free protease and phosphatase inhibitors. Whole cell lysates were spun at 14,000 RPM at 4^0C for 20 minutes and the cleared lysates were incubated with 400 µl of activated FLAG M2-Agarose (A2220, Sigma-Aldrich) for 2 hours at 4°C on a rocker. Activation of FLAG M2-Agarose was done according to the manufacturer's descriptions. FLAG M2-Immunoprecipitates were subsequently loaded onto a column (Bio Rad, Munich) equilibrated with lysis buffer. The packed column was washed three times with ice-cold lysis buffer followed by three times PBS. Elution of the bound FLAG-WAVE2 was done for 3 times with 200 µl of elution buffer (100mM glycine pH 2.3) in reaction tubes containing 20 µl 1,5M Tris pH 8.8 to buffer the eluate. Eluted proteins were stabilized by the addition of sterile glycerol to a final concentration of 10 % (v/v) and stored at -80°C. FLAG-WAVE2 concentrations as well as purity were subsequently assayed by Coomassie- stained bands to a BSA standard dilution series.

4.21 In vitro pyrene-actin polymerization assays

Pyrene-actin polymerization assays were performed as described earlier (Eiseler et al., 2010). Briefly, Pyrene-labeled rabbit muscle G-actin (Cytoskeleton Inc.) was diluted at 3µM in G-buffer (5mM Tris-HCL pH8, 0.2mM CaCl2 and 0.2mM fresh ATP). The polymerization assays were performed in black 96 well plates (Greiner Bio-one) in a volume of 100 µl containing G-actin, WAVE2, Arp 2/3 complex, GST alone, GST-ABI1 Wt and GST-ABI1 SE at a final concentration of 3 µM, 80 nM, 40 nM, and 300 nM, respectively. Polymerization reactions were initiated by adding 10 µl 10X F-buffer (Cytoskeleton Inc.) and increase in Pyrene fluorescence following polymerization was measured with a Tecan M200 plate reader: Excitation: 360 nm, Emission: 407 nm every 15 seconds. Three independent experiments in triplets were performed. To quantify changes in polymerization rate, curves were fitted with Boltzmann sigmoidal equations (GraphPad, Prism) and half-maxima of saturated polymerization values (T½Max [s]) were calculated from RAW data.

4.22 Lamellipodia extension assay

MCF7 cells were transfected with GFP-ABI1-WT/ -$S^{88/296}$A/ -$S^{88/296}$E and WAVE2-WT constructs. 16 hours later, cells were serum starved for 4 hours and stimulated with 100ng/ml Heregulin (PeproTech) for 10 minutes. Samples were processed as described in confocal microscopy section. Representative images under each condition were obtained using a confocal laser scanning microscope (TCS SP5, Leica). For quantification, images were acquired using a BZ-8000 Keyence epifluorescence microscope with 40x oil immersion objective. A minimum of 125 cells per condition (both GFP- and WAVE2-positive cells) were examined and categorized into three groups of lamellipodial extension as described earlier (Steffen et al., 2004): Lamellipodia present (large continuous sheet of extension), lamellipodia ambiguous (extension as occasional patches) and lamellipodia absent (no extension at all). Cell numbers were then calculated as percentage of entire cell population visualized.

4.23 Immunofluorescence studies

HeLa and MCF7 cells were plated onto glass cover slips a day before and transfected with GFP-ABI1-WT and mutant constructs as indicated. The following

day cells were washed with phosphate buffered saline (PBS) and fixed with 3.7% formaldehyde in PBS for 10 minutes. Subsequently cells were neutralized, permeabilized with 0.1% Triton X-100 and incubated with specific antibodies (ABI1/ PKD2/ WAVE2) overnight followed by secondary antibody treatment for 1hour at room temperature. F-Actin was stained using Rhodamine-Phalloidine (Alexa fluor 567 1:400, Invitrogen) for 20 min at room temperature. Nuclei were stained using DAPI (Invitrogen). Slides were then analyzed for localization/ co-localization/ change in co-localization of proteins via fluorescence microscope (BZ-8000 Keyence Fluorescence Microscope) and confocal microscope (Confocal Laser scanning Microscope Leica). Image analysis was performed using the public domain software ImageJ (v1.36b) and Leica confocal software lite V2.61.

4.24 Migration assays

i. Random migration assay

HeLa cells transfected with different ABI1constructs were allowed to spread for 30 minutes in 1% FBS DMEM on glass bottom culture dishes (MakTek Corporation) coated with fibronectin (50 µg/ ml). Imaging of living cells expressing EGFP-tagged ABI1constructs was performed with a BZ-8000 Keyence Fluorescence Microscope. An image was captured every 10 min for at least 10 hours and motion pictures (AVI format) were created from time-lapse images using BZ-Analyzer software (Keyence Corporation). During the entire experiment, cells were kept at 37°C in a humidified atmosphere containing 5% CO2 using a Keyence incubation chamber. Movement of cells was analyzed using tracking routines implemented in ImageJ. At least 75 cells from three independent experiments were monitored for each condition.

ii. Transwell migration assay

Migration assays with Panc1 cells were performed using 24 well Transwell filter inserts with a pore size of 8.0µm (Corning, New York, USA). Briefly, 30,000 Panc1 cells transfected with the constructs indicated were serum starved for at least 4 hours and seeded at a density of 30,000 cells/ insert in a medium containing 1% FCS. Migration was induced by an FCS gradient of 1% - 10% FCS (top of insert/ well) for 30 hours. Cells on the filter were washed twice with PBS and the interior of

the Transwell insert was wiped with a cotton swab to remove cells, which had not migrated and washed again two times with PBS. Cells were then fixed in 4% paraformaldehyde and stained with DAPI (20 min at room temperature), to quantify migration of cells on the filter (RT). Filters were then documented using a wide field fluorescence microscope (BZ-8000 Keyence Fluorescence Microscope) equipped with a CCD camera, and a monochromatic light source under 20X magnification. At least 6 visual fields per filter were photographed. Results were calculated as mean number of migrated cells/ visual field. Statistics were done on the data obtained from three independent experiments.

4.25 Softwares

Generunner 3.05, Expasy (Gasteiger et al., 2003) were used for primer designing and sequence analysis of nucleotides and peptides. Web based analysis of nucleotides and amino acids was done via Basic Local Alignment Tool (BLAST, (Altschul et al., 1990)). Protein domains or residues that are likely to be phosphorylated by a specific protein kinase were identified by Scansite 2.0 (Obenauer et al., 2003). Leica confocal software V2.61 and lite V2.61 were used in confocal studies. Image J (Manual tracking plug-in) was used to monitor cell migration velocity (Abramoff, 2004; Rasband, 1997). Statistical significances were analyzed by unpaired; two-tailed Students t-test calculated using the Graph Pad Prism software. Differences were considered significant at * $p < 0.05$, ** $p < 0.001$ and *** $p < 0.0001$.

5. Results

5.1 Identification of ABI1 as a potential substrate of PKD2

Using the ProtoArray Human Protein Microarray v4.0 (Invitrogen) we performed a substrate screen to identify novel PKD substrates that could play a role in the regulation of cell migration. The protoarrays contain approximately 3000 GST tagged full-length human proteins, including fiduciary kinases that serve as orientation landmarks spotted in duplicate onto microscope slides. Protein arrays (n=3 per experimental group) were incubated with recombinant, active PKD2 or assay buffer only. Signal intensity of proteins between control arrays and arrays incubated with kinase were observed. Protein spots phosphorylated only by PKD2 but absent in controls were characterized as putative substrates. Similar arrays have been used to identify novel substrates for a variety of different protein kinases, including Cdk5 (Schnack et al., 2008), and the *Arabidopsis thaliana* MAPKs, Mkp3 and Mkp6 (Feilner et al., 2005). ABI1 was one of the potential substrates that were identified.

Although kinase substrate screen identified potential novel kinase substrates, we needed to confirm that ABI1 was a PKD2 phosphoacceptor in solution. This is an important consideration as not every protein identified from protein microarrays recapitulates in solution. To confirm that ABI1 was a substrate of PKD2, ABI1 was sub-cloned into a suitable expression vector followed by expression and purification of the ABI1 protein from bacteria. This protein was then analyzed for a potential phosphorylation by PKD2 in an *in vitro* kinase assay. As shown in Fig. 7A, PKD2 induced phosphorylation of GST-ABI1-WT or histone as a control substrate. Phosphorylation of GST-ABI1-WT or histone was more pronounced when PKD2 activity was stimulated by phorbol-12-myristate-13-acetate (Sturany et al., 2001) or when constitutively active PKD2 (PKD2-CA-$S^{244/706/710}$E) was employed (von Blume et al., 2007). In contrast, catalytically inactive PKD2 (PKD2-DA=D^{695}A) (Auer et al., 2005) failed to induce GST-ABI1-WT phosphorylation.

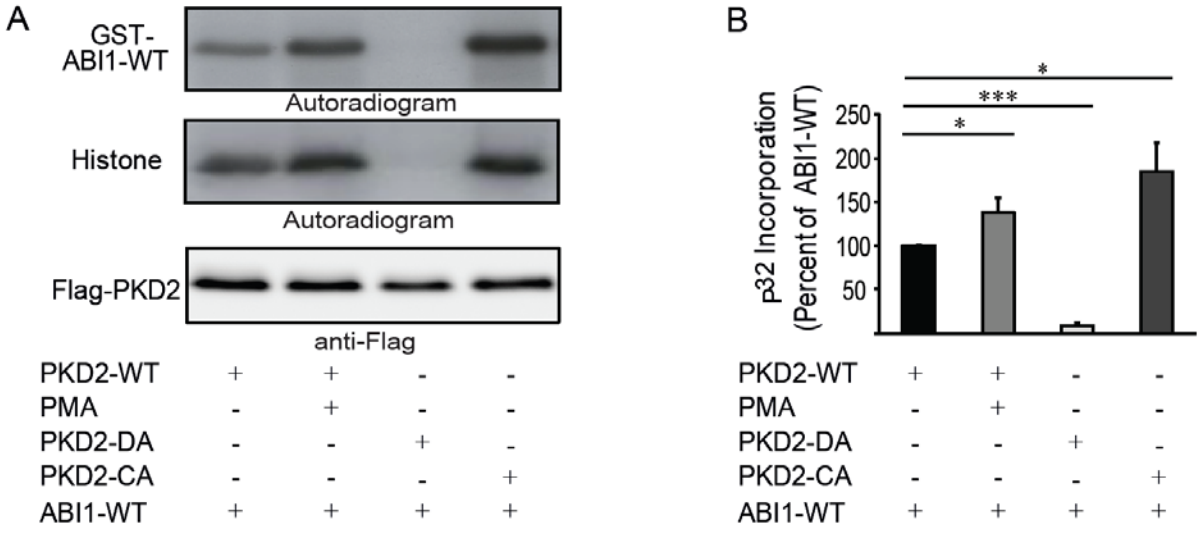

Figure 7: PKD2 phosphorylates ABI1. (A) *Substrate phosphorylation: 4 µg each of recombinant GST-ABI1-WT alone (upper autoradiogram) or histone (middle autoradiogram) and Flag-PKD2-WT (with or without PMA), -CA ($S^{244/706/710}E$) and -DA ($D^{695}A$) immunoprecipitates were incubated as indicated, in the presence of kinase buffer and [γ- ^{32}P] ATP at 30^0C for 10 minutes. Phosphorylated proteins were resolved by SDS–PAGE and detected by autoradiography. Expression levels of the PKD2 constructs used were verified by immunoblotting using an anti-Flag antibody (A, lower blot).* ***(B)*** *^{32}P incorporation in ABI1: Densitometric analysis of autoradiograms of four independent experiments, plotted as percentage of ^{32}P incorporation in ABI1 by PKD2 against the conditions indicated. * $p < 0.05$, and *** $p < 0.001$.*

5.2 PKD2 phosphorylates ABI1 at Serine 88 and 296

Having identified ABI1 as an *in vitro* substrate of PKD2, we next aimed to map the phosphorylation residue(s). To identify potential PKD2 phosphorylation site(s) in ABI1, we at first performed an *in silico* analysis using Scansite, a web-based domain to identify motifs within proteins that are likely to be phosphorylated by specific protein kinases (Obenauer et al., 2003). PKDs are known to phosphorylate substrates that contain the substrate motif -[L/V/I]-XRXX-[S/T]-, (L, R, S, T and X are leucine, arginine, serine, threonine and any other amino acid residue, respectively; (Nishikawa et al.,

1997). The Scansite search yielded 12 potential phosphorylation sites in ABI1. Two of these sites closely resembled the typical PKD substrate phosphorylation motif: S88 (-SQ*L*R*R*ME*S**SI-) and S296 (-RQ*IS*R*H*N*S**TT-), respectively. The amino acid motif around S88 contains an arginine and leucine at positions -3 and -5, respectively. The amino acid sequence around S296 contains an arginine at the -3 positions and isoleucine at the -5 position (Figure 8). These sites were also described as being accessible by the kinase.

A

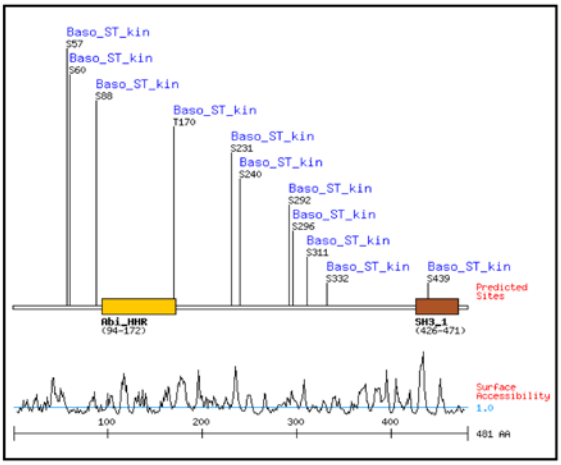

B

S.No	Kinase	Gene card	Site	Score	Sequence
1	PKC epsilon	PRKCE	S57	.4378	TKAYTTQ**S**LASVAYQ
2	Protein Kinase A	PRKACG	S311	.4457	GGYRRTP**S**VTAQFSA
3	Akt Kinase	AKT1	S240	.4462	NQRPRTH**S**GSSGGSG
4	PKC epsilon	PRKCE	S50	.4541	YTTQSLA**S**VAYQINA
5	PKC epsilon	PRKCE	S439	.4541	KDKDDEL**S**FMEGAII
6	Calmodulin dependent Kinase 2	CAMK2G	S332	.4793	GPLYSQN**S**ISIAPPP
7	Akt Kinase	AKT1	T170	.5015	NQPARTG**T**LSRTNPP
8	Akt Kinase	AKT1	S311	.5375	GGYRRTP**S**VTAQFSA
9	Akt Kinase	AKT1	S231	.5707	HSPGRTA**S**LNQRPRT
10	AMP Kinase	PRKAA1	S88	.5732	SQLRRME**S**SINHISQ
11	Clk2 Kinase	CLK2	S296	.6909	RQISRHN**S**TTSSTSS
12	AMP Kinase	PRKAA1	S292	.6038	GTMTRQI**S**RHNSTTS

C

Consensus motif	**X**	**L**	**X**	**R**	**(Q/K/E/M)**	**(M/L/K/E/Q/A)**		**S***	
ABI-1 S 88	**Q**	**L**	**R**	**R**	**M**		**E**	**S**	**S**
ABI-1 S 296	**Q**	**I**	**S**	**R**	**H**		**N**	**S**	**T**

Figure 8: Prediction of potential phosphorylation sites in ABI1. (A and B) *Motif Scan Graphic result (http://scansite.mit.edu/motifscan_seq.phtml). Possible phosphorylation sites within ABI1 were predicted using the Scansite 2.0, an algorithm that identifies short protein sequence motifs likely to bind to specific protein domains or to be phosphorylated by specific protein kinase. The ABI1 Scansite motif scan proposed 12 potential phosphorylation sites.* ***(C)****Two sites S88 and 296 with a high homology to the typical PKD phosphorylation motif were chosen for further investigation.*

To examine whether and which of these two predicted phosphorylation sites in ABI1 were actually phosphorylated by PKD2, we generated GST-ABI1-S^{88}A, GST-ABI1-S^{296}A and GST-ABI1-$S^{88/296}$A mutant proteins. Changing either S88 or S296 to alanine resulted in a marked reduction of GST-ABI1 phosphorylation in *vitro* kinase assays using catalytically active PKD2. Substituting both serine residues to alanine abolished phosphorylation of GST-ABI1 by constitutively active Flag-PKD2-CA *in vitro* (Figure 9A). Densitometric quantification of the autoradiograms revealed that S296 is a more prominent phosphorylation site compared to S88 (Figure 9B).

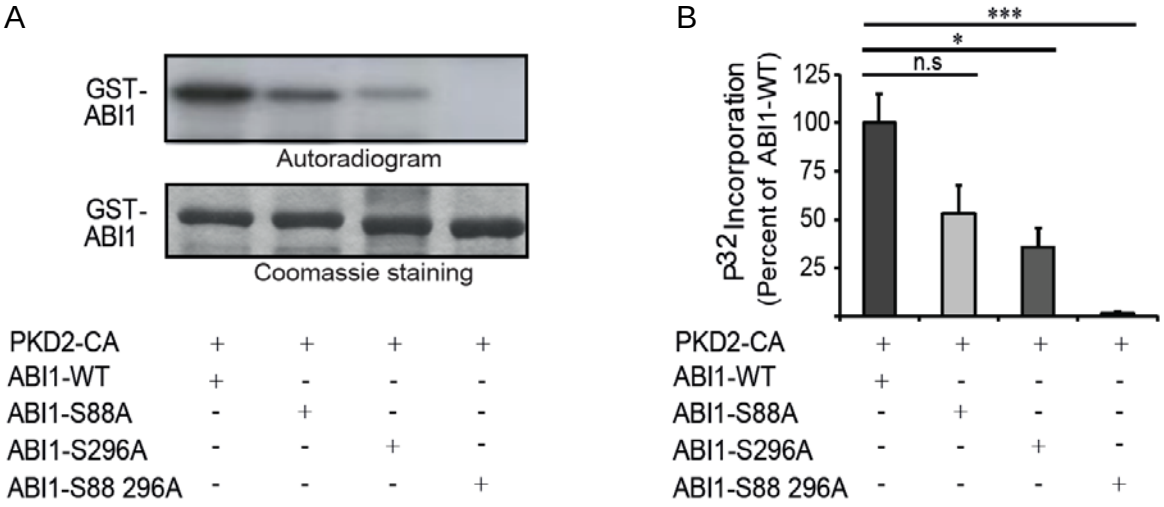

Figure 9: PKD2 phosphorylates ABI1 at Ser 88 and 296. (A) *4 µg each of GST-ABI1-WT/ -S^{88}A/ -S^{296}A/ -$S^{88/296}$A mutants and Flag-PKD2-WT (with or without PMA), -CA ($S^{244/706/710}$E) and -DA (D^{695}A) immunoprecipitates were incubated in the presence of kinase buffer and [γ−32P] ATP at 30^0C for 10 minutes. Phosphorylated proteins were resolved by SDS–PAGE and*

detected by autoradiography. Coomassie staining of GST-ABI1-WT/ -$S^{88}A$/ -$S^{296}A$ and -$S^{88/296}A$ confirmed equal amount of proteins (A, lower panel). ***(B)*** *P^{32} incorporation in ABI1: Densitometric analysis of autoradiogram from four independent experiments, plotted as percentage of P^{32} incorporation in ABI1 by PKD2 against the conditions indicated. * $p < 0.05$, and *** $p < 0.001$.*

5.3 PKD2 phosphorylates ABI1 in intact cells

To investigate whether the ABI1 phosphorylation sites, Ser 88 and Ser 296 were also phosphorylated in intact cells and may therefore be of physiological relevance we used an antibody that detects the optimal phosphorylation motif of PKDs (pMOTIF antibody, (Doppler et al., 2005; Nishikawa et al., 1997). HEK-293T cells were co-transfected with GFP-ABI1-WT or GFP-ABI1-$S^{88/296}$A, together with Flag-PKD2-WT, constitutively active Flag-PKD2-CA or the catalytically inactive Flag-PKD2-DA (Auer et al., 2005) as indicated (Figure 10). ABI1 immunoprecpitates were subsequently analyzed by immunoblotting using the pMOTIF antibody. Ectopic expression of PKD2, which already results in some degree of kinase activation, induced phosphorylation of GFP-ABI1-WT. ABI1 phosphorylation was further increased by incubation of cells with PMA. Constitutively active Flag-PKD2-CA substantially increased phosphorylation of GFP-ABI1-WT. In contrast, catalytically inactive Flag-PKD2-DA could not induce phosphorylation of GFP-ABI1-WT and even abolished the basal level of GFP-ABI1-WT phosphorylation observed upon expression of PKD2-WT. Vice versa, constitutively active Flag-PKD2-CA failed to induce phosphorylation of an ABI1 mutant protein in which S88 and S296 were changed to alanine. These data show that S88 and S296 are indeed the major PKD2 phosphorylation sites in ABI1 in intact cells.

5.4 PKD2 phosphorylates ABI1 at endogenous levels

Having determined that ectopically expressed ABI1 is a PKD2 substrate *in vitro* and in intact cells, we examined whether endogenous ABI1 was also phosphorylated by PKD2. Cervical (HeLa), pancreatic (Panc 1 and MiaPaCa 2), colorectal (Colo 320 and HCT 116) and breast cancer (MDA-MB 231) cells exhibit high levels of both, ABI1 and

PKD2, as determined by Western blotting (Figure 11A). MCF7 cells expressed PKD2, but only low levels of ABI1. Vice versa cell lines of neuronal origin such as NG108 and PC12 cells expressed high levels of ABI1, but rather low levels of PKD2 (Figure 11A). Since MDA-MB 231 cells have been used as a model cell line to investigate the function of ABI1 by various groups we chose this cell line for further analysis.

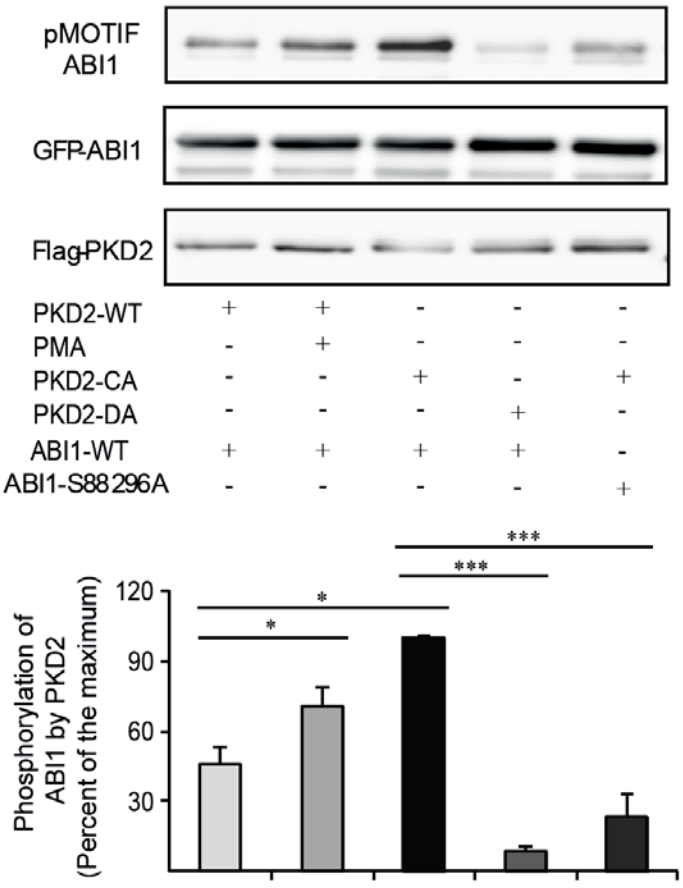

Figure 10: PKD2 phosphorylates ABI1 in intact cells. Upper panel: *Immunoprecipitates from HEK-293T cells co-expressing GFP-ABI1-WT/ -$S^{88/296}$A protein and Flag-PKD2-WT (with or without PMA stimulation) or -CA ($S^{244/706/710}$E) or DA (D^{695}A) constructs as indicated were immunoblotted with pMOTIF antibody (upper blot). Uniform expression of the constructs used was confirmed by immunoblotting with anti-GFP (middle blot) and anti-Flag (lower blot) antibodies.* ***Lower panel:*** *Quantification of phospho-status of ABI1: Immunoblots were analyzed by densitometry and the data represent mean and s.e.m of four independent experiments. ** p <0.001 and *** p <0.0001.*

[50]

Lysates of MDA-MB 231 cells treated with PMA or solvent (DMSO) were evaluated by immunoblotting using the pMOTIF antibody. As shown in Figure 11B phosphorylation of both, ABI1 (left panel) and PKD2 (right panel) was substantially increased upon PMA treatment of MDA-MB 231 cells. To confirm that PMA-induced phosphorylation of ABI1 was PKD-dependent, we depleted all three PKD isoforms by siRNA and again examined phosphorylation of ABI1 in response to PMA treatment using the pMOTIF antibody (Figure 11C, left panel). Depletion of all three PKD isoforms strikingly reduced basal and PMA stimulated ABI1 phosphorylation. Additionally, single knockdown of PKD 1, 2 and 3 indicated that ABI1 is a substrate of all three kinases. However ABI1 appears to be a preferential substrate of PKD2 and 3 (Figure 11D, right panel). The efficacy of the siRNA knockdown was confirmed by Western blotting using specific anti-PKD1,-2 and -3 antibodies, respectively (Figure 11C and 11D, right panels). This indicates that PKDs are indeed the major kinases to phosphorylate ABI1 at these sites.

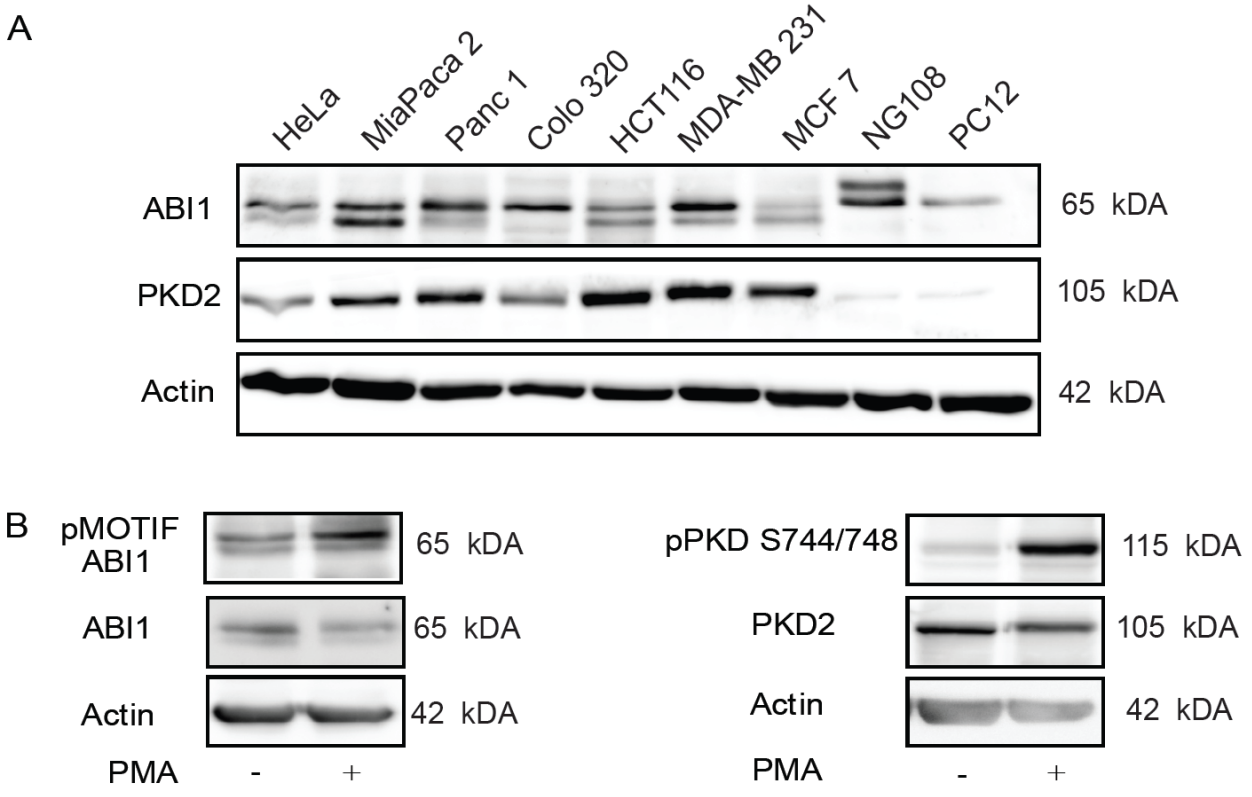

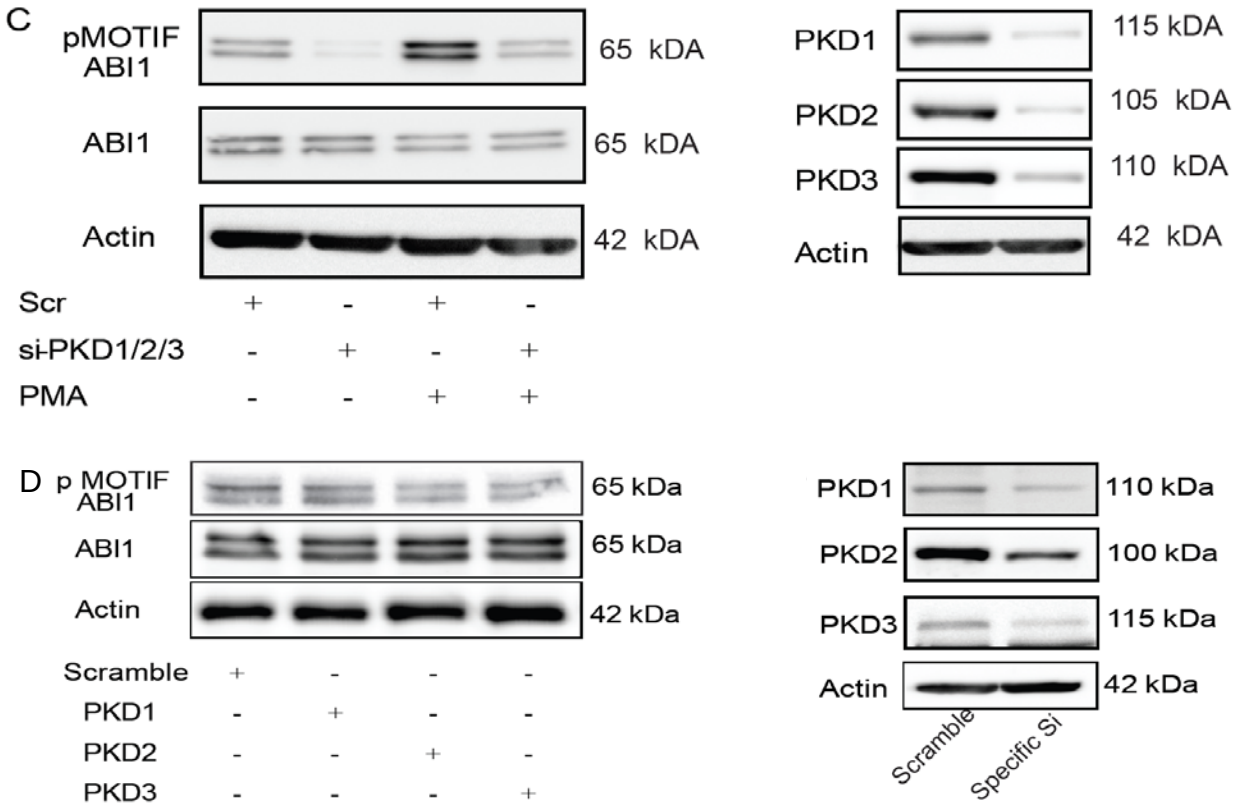

Figure 11: Endogenous PKD2 phosphorylates ABI1. (A) *Whole cell lysates from different cancer cell lines as indicated were immunoblotted using ABI1- (upper blot), PKD2- (middle blot) and actin-specific antibodies (lower blot).* ***(B)*** *Endogenous PKD2 phosphorylates ABI1. Cell lysates from MDA-MB 231 cells treated with 400 mM PMA or solvent for 10 minutes were immunoblotted with anti-pMOTIF (left panel, upper blot) or anti-phospho PKD (right panel, upper blot) antibodies. Membranes were reprobed with anti-ABI1 (left panel, middle blot) and anti-PKD2 (right panel, middle blot) antibodies to confirm equal amounts of proteins.* ***(C)*** *Simultaneous knockdown of PKD1, -2 and -3 abolishes phosphorylation on ABI1. Lysates from MDA-MB 231 cells transfected with specific siRNAs targeting PKD1, -2 and -3 and treated with or without PMA for 10 minutes were immunoblotted with anti-pMOTIF (left panel, upper blot) or anti-ABI1 (left panel, middle blot) antibody respectively.* ***(D)*** *Single knockdown of PKD 1, -2 and -3 does not strikingly influence ABI1 phosphorylation. MDA-MB 231 cells transfected with specific siRNAs targeting PKD1, -2 and -3 were immunoblotted with anti-pMOTIF (left panel, upper blot) or anti-ABI1 (left panel, middle blot) antibody respectively. Actin was used as an internal loading control. Immunoblotting with PKD1, -2 and -3 antibodies (right panel of 11C and D- upper, middle and lower blots, respectively) indicated >80% knockdown efficiency.*

[52]

5.5 ABI1 interacts with PKD2 in vitro and in vivo

Having confirmed that PKD2 phosphorylates ABI1, we next investigated, whether the two proteins would interact. Lysates of HEK-293T cells transfected with GFP-ABI1-WT, Flag-PKD2-WT, or the respective empty vectors (Figure 12A) were subjected to immunoprecipitations using anti-GFP or anti-Flag antibodies, respectively. GFP-ABI1-WT could be detected in Flag-PKD2-WT immunoprecpitates. Vice versa, Flag-PKD2-WT was detectable in GFP-ABI1-WT immunoprecpitates by Western blotting. Thus, PKD2 and ABI1 physically interact with each other. In addition, colocalization studies were performed in MCF7 cells expressing Flag-PKD2-WT and GFP-ABI1-WT. Confocal images presented in Figure 12B revealed an apparent colocalization of ABI1 with PKD2 at the plasma membrane in leading edge structures. To determine whether the direct interaction of ABI1 and PKD2 also occurred between endogenously expressed proteins, PKD2 and ABI1 were immunoprecipitated from MDA-MB 231 cell lysates using anti-PKD2 and ABI1 antibodies. Control immunoprecipitations were performed using preimmune IgG antibodies (Figure 12C). PKD2 was detected in anti-ABI1 immunoprecipitates. Vice versa, ABI1 was detected in PKD2 immunoprecipitates, indicating that the constitutive interaction between ABI1 and PKD2 also occurs at the level of the endogenous proteins.

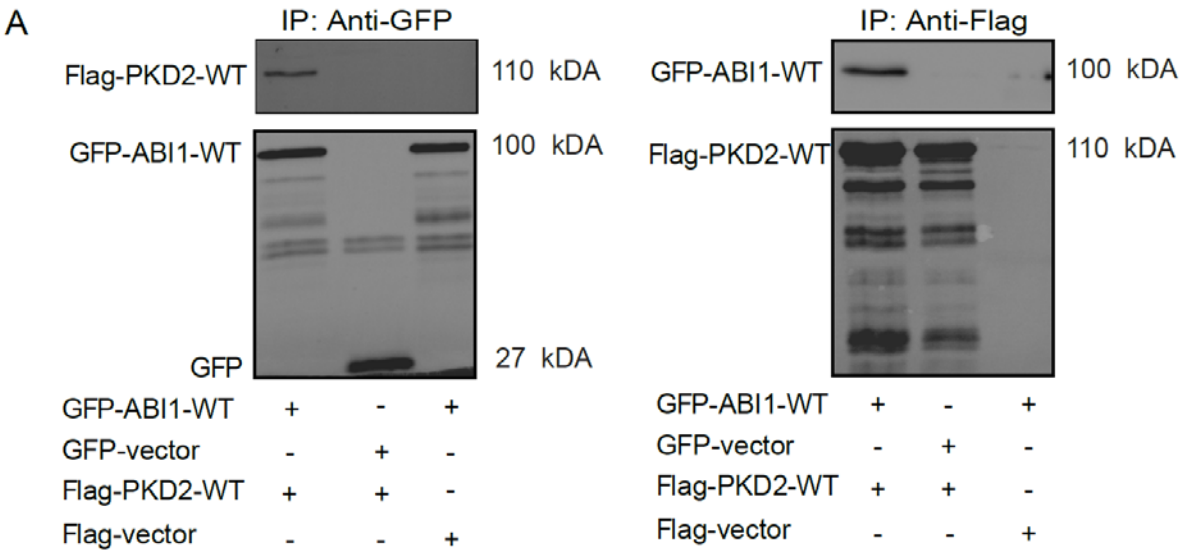

[53]

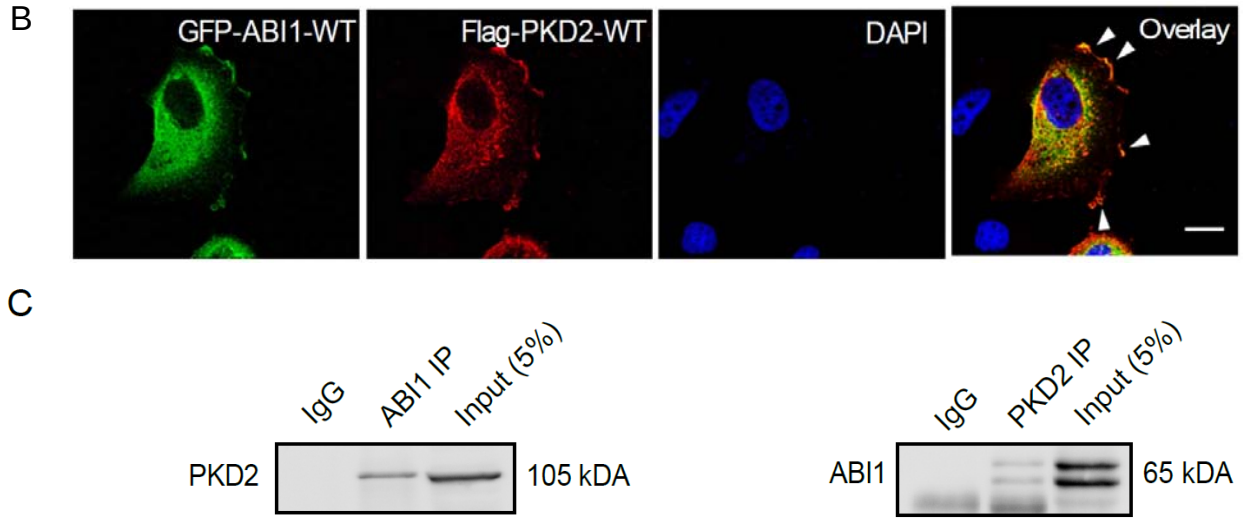

Figure 12: PKD2 and ABI1 interact. (A) *Lysates of HEK-293T cells co-expressing GFP-ABI1-WT or GFP vector together with Flag-PKD2-WT or Flag vector as indicated were immunoprecipitated with anti-GFP (ABI1 IP, left panel) or anti-Flag (PKD2 IP, right panel), respectively, and the precipitated proteins were immunoblotted as indicated. Immunoblots (lower) in either panel suggest uniform expression levels of the constructs used.* ***(B)*** *PKD2 co-localizes with ABI1 at the leading edge of the cell. MCF7 cells co-expressing GFP-ABI1-WT and Flag-PKD2-WT were fixed, immunostained with anti-PKD2/ Alexa 647 antibodies and DAPI (blue). Co-localization areas are indicated by arrowheads. Scale bar 15 µm.* ***(C)*** *Endogenous ABI1 and PKD2 interact. Lysates from MDA-MB 231 cells were immunoprecipitated with anti-ABI1 (left panel) and anti-PKD2 (right panel) antibodies and the precipitated proteins were immunoblotted as indicated. Immunoblotting of the lysates confirmed presence of ABI1 and PKD2 proteins (right panel).*

5.6 Characterization of the ABI1 interaction domain in PKD2

Having identified the constitutive interaction between ABI1 and PKD2 we next aimed at determining the domain/s of PKD2 responsible for this interaction. PKD2 contains several domains including two cysteine rich domains (CRD=C1a+C1b), an acidic domain (AC), a pleckstrin homology domain and a catalytic domain (KD) (Sturany et al., 2001). The N-terminus of both, PKD1 and PKD2, starts with a hydrophobic region, rich in alanine and/or proline residues, which is missing in PKD3 (Figure 13A).

To identify the ABI1 interaction site(s) within PKD2, we co-expressed various Flag-tagged deletion mutants of PKD2 shown in Fig. 5A (Auer et al., 2005) with GFP-ABI1-WT in HEK-293T cells. Lysates were immunoprecipitated with anti-Flag (Fig. 13B, left panel) or anti-GFP (Figure 13B, right panel) antibodies, respectively. ABI1-WT was found to interact with PKD2 mutants lacking the kinase domain and the pleckstrin homology domain, but not with a PKD2 mutant lacking the entire zinc finger domain. A more detailed analysis of this region revealed that the interaction between PKD2-WT and ABI1-WT was mediated by the second cysteine rich domain (C1b). In contrast, the mutant lacking only the first cysteine rich domain (C1a) still interacted with ABI1 (Figure 13B). Deletion of Acidic domain (AC) had no effect on this interaction. These findings suggest that PKD2 interacts with ABI1 exclusively via its second cysteine rich domain (C1b).

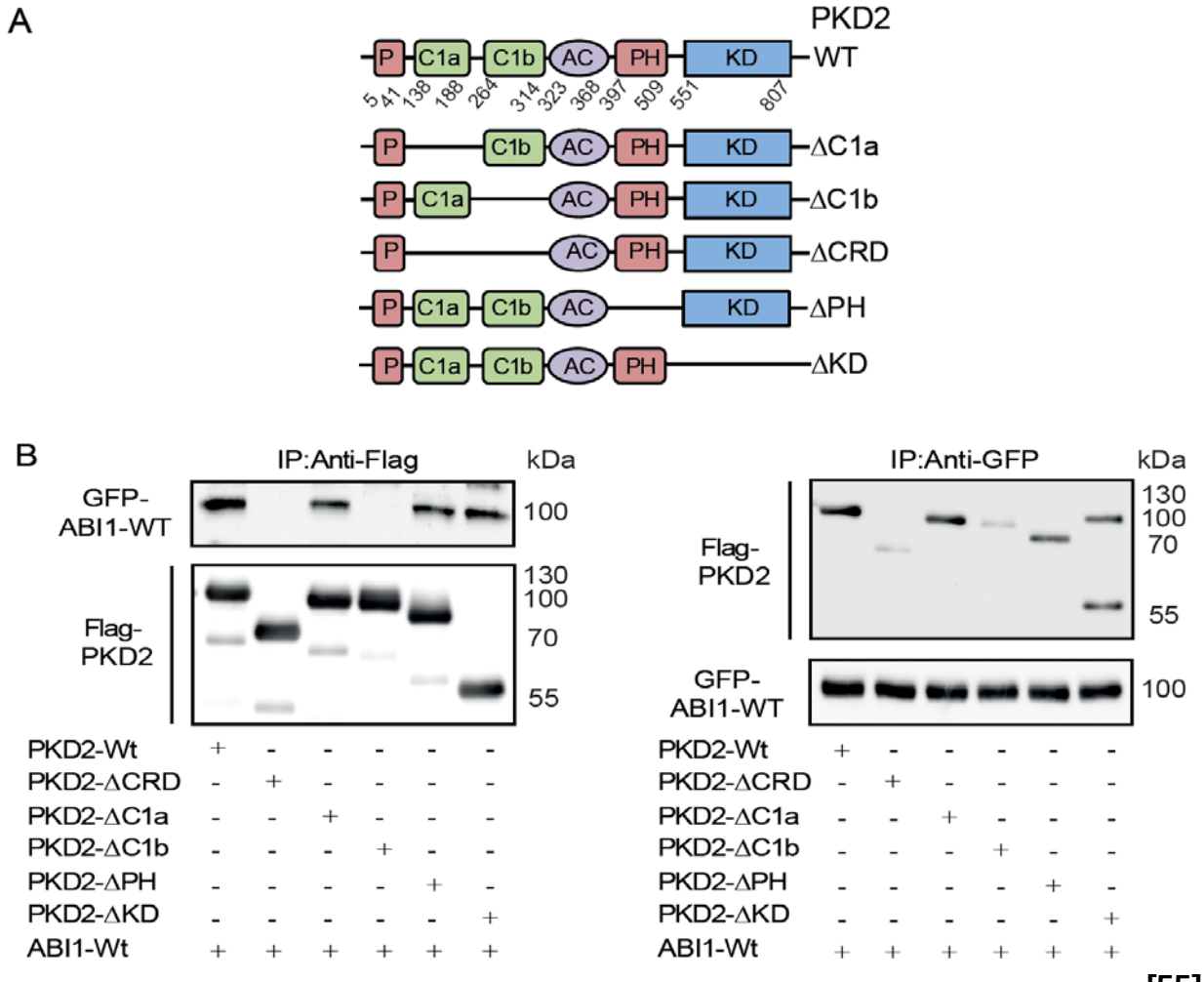

[55]

Figure 13: Interaction of ABI1-PKD2 is mediated exclusively by C1b domain of PKD2 and is lost upon phosphorylation. (A) *Schematic representation of the PKD2 constructs used. Wild type (-WT), Cysteine rich (-∆CRD), first cysteine rich (-∆C1a), second cysteine rich (-∆C1b), pleckstrin homology (-∆PH) and kinase (-∆KD) domain.* ***(B)*** *Identification of the ABI1 interacting region in PKD2 protein. Lysates from HEK-293T cells co-expressing GFP-ABI1-WT and Flag-PKD2-WT and deletion constructs as indicated were immunoprecipitated with anti-Flag (PKD2 IP, left panel) and anti-GFP (ABI1 IP, right panel) antibodies and the precipitated proteins were immunoblotted as indicated.*

5.7 ABI1 phosphorylation affects its interaction with PKD2 and changes its subcellular localization

Kinases often bind their substrates only transiently, and phosphorylation of the substrate terminates the interaction. To investigate if PKD2-induced phosphorylation of ABI1 affects its interaction with the kinase, HEK-293T cells were co-transfected with GFP-ABI1-WT and Flag-PKD2-WT, constitutively active PKD2-CA or catalytically inactive PKD2-DA as indicated (Figure 14A). Cell lysates were then immunoprecipitated with anti-Flag or anti-GFP antibodies, respectively, and immunoblotted with anti-GFP and anti-Flag antibodies. Both PKD2-DA and PKD2-WT interacted with ABI1-WT. In contrast, the interaction of ABI1-WT with PKD2-WT was substantially reduced in the presence of PMA. Likewise, constitutively active PKD2 and ABI1 did not show an appreciable interaction in the co-immunoprecipitation assay. Thus, the constitutive interaction between PKD2 and ABI1 is released upon activation of PKD2 and phosphorylation of ABI1. To examine whether disruption of the ABI1-PKD2 interaction upon phosphorylation would affect the subcellular localization of ABI1, we examined the localization of GFP-ABI1-WT, its phosphomimetic mutant, ABI1-$S^{88/296}$E, and its non-phosphorylatable mutant, ABI1 $S^{88/296}$A. MCF7 cells transfected with the constrcts indicated were fixed, stained and observed for any changes in localization of ABI1. As shown in Figure 14B, ABI1-$S^{88/296}$E was predominantly detectable in the cytoplasm and the perinuclear area of MCF7 cells. In contrast, ABI1-$S^{88/296}$A localized to the plasma membrane in leading edge structures of the cells.

[56]

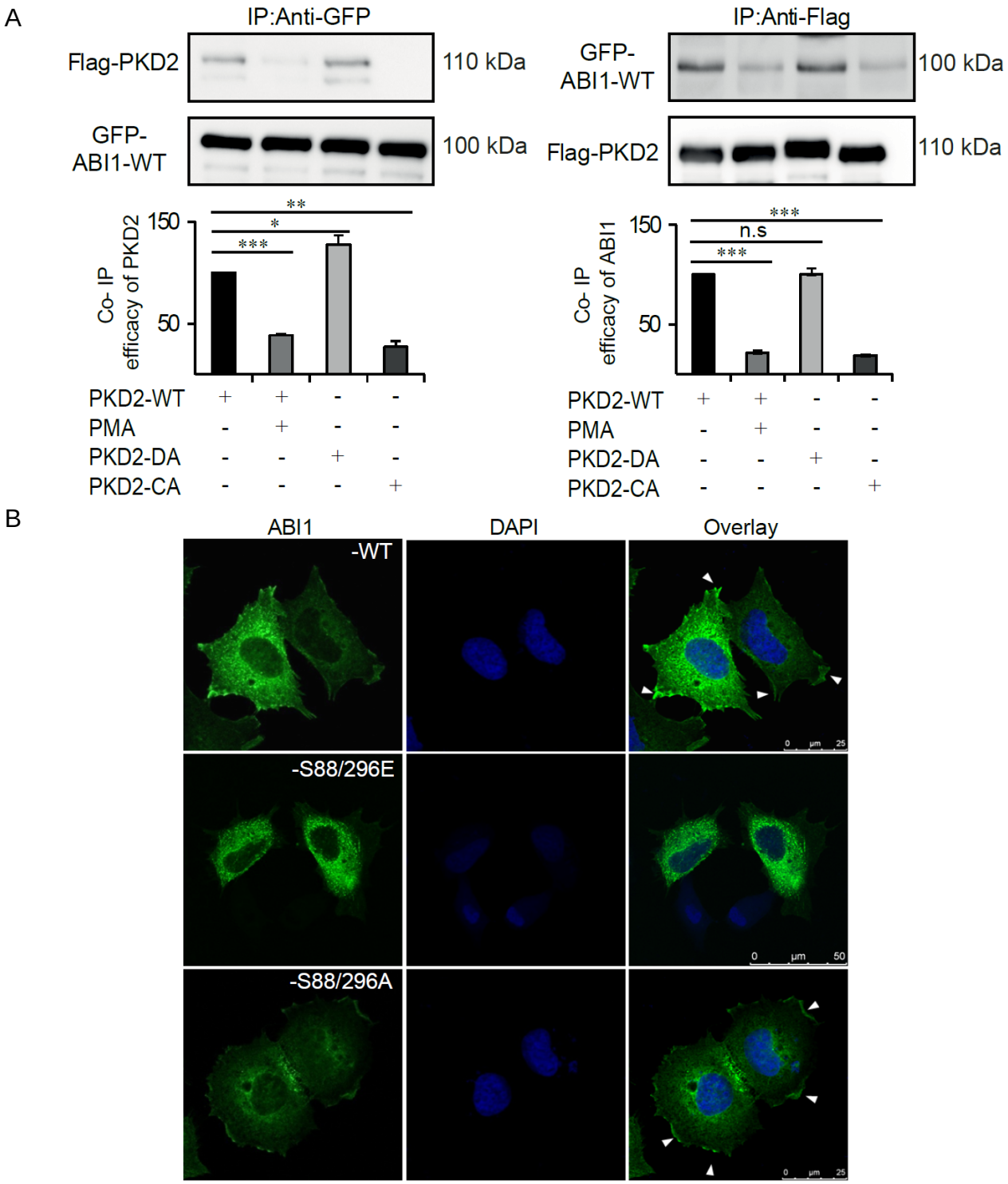
A
IP:Anti-GFP
Flag-PKD2
110 kDa
GFP-ABI1-WT
100 kDa
Co- IP efficacy of PKD2
150
50
**
*
***
PKD2-WT + + - -
PMA - + - -
PKD2-DA - - + -
PKD2-CA - - - +
IP:Anti-Flag
GFP-ABI1-WT
100 kDa
Flag-PKD2
110 kDa
Co- IP efficacy of ABI1
150
50
***
n.s
***
PKD2-WT + + - -
PMA - + - -
PKD2-DA - - + -
PKD2-CA - - - +
B
ABI1
DAPI
Overlay
-WT
-S88/296E
-S88/296A

Figure 14: PKD2 induced phosphorylation on ABI1 shifts localization from cell periphery to the cytosol. (A) *Interaction of ABI1-PKD2 at the plasma membrane is lost upon phosphorylation. Lysates from HEK293T cells co-expressing GFP-ABI1-WT and Flag-PKD2-WT (with or without PMA), -CA ($S^{244/706/710}E$) and -DA ($D^{695}A$) constructs were immunoprecipitated with anti-GFP (ABI1 IP, right panel) or anti-Flag (PKD2 IP, left panel) antibodies and the precipitated proteins were immunoblotted as indicated. Data represent means and S.E.M of co-immunoprecipitation efficacies for PKD2 and ABI1 of four independent experiments. * p < 0.05, ** p <0.001 and *** p <0.0001.* ***(B)*** *The effect of PKD2 mediated phosphorylation of ABI1 on localization. MCF7 cells expressing GFP-ABI1-WT (upper panel)/ -$S^{88/296}E$ (middle panel)/ -$S^{88/296}A$ (lower panel) were fixed and stained with DAPI. Membrane localized areas are indicated by arrow heads.*

5.8 PKD2-mediated phosphorylation of ABI1 destabilizes the ABI1-WAVE2 sub-complex

ABI1 is an adaptor protein involved in actin reorganization and lamellipodia formation. ABI1 interacts with WAVE2 (Innocenti et al., 2004; Leng et al., 2005; Steffen et al., 2004) via its wave homology domain (WHD). This interaction facilitates the formation and activation of a WAVE2-ABI1-Nap1-PIR121 complex. This ABI1-WAVE2 sub-complex can also promote actin polymerization (Innocenti et al., 2004). Our previous data prompted us to investigate whether PKD2-mediated phosphorylation of ABI1-WT would alter the stability of the ABI1-WAVE2 sub-complex and thereby affect the nucleation promoting factor activity of WAVE2.

HEK-293T cells ectopically coexpressing GFP-ABI1-WT, -$S^{88/296}E$ or -$S^{88/296}A$ and Flag-WAVE2-WT were subjected to immunoprecipitations using either anti-Flag or anti-GFP antibodies. As shown in Figure 15A the interaction between WAVE2-WT and the non-phosphorylatable ABI1 mutant (ABI1-$S^{88/296}A$) increased by 50%-60% compared to ABI1-WT or the phosphomimetic ABI1-$S^{88/296}E$ mutant. These results were confirmed at the endogenous level in MDA-MB 231 cells. In the presence of PMA (400 nM) the co-immunoprecipitation efficacy of ABI1 and WAVE2 decreased by 35% and 26%, respectively (data not shown). Thus, phosphorylation of ABI1 by PKD2 also

decreases its interaction with WAVE2. In addition, localization studies performed in MCF7 cells coexpressing GFP-ABI1-WT, -$S^{88/296}$E or -$S^{88/296}$A together with Flag-WAVE2-WT revealed an increase in plasma membrane localization of the non-phosphorylatable ABI1 mutant (GFP-ABI1-$S^{88/296}$A). WAVE2 also exhibited marked plasma membrane localization in cells expressing GFP-ABI1-$S^{88/296}$A. In contrast, the phosphomimetic ABI1-$S^{88/296}$E exhibited a predominantly perinuclear/cytoplasmic localization and in these cells WAVE2-WT was also predominantly localized in the cytoplasm around the nucleus (Figure 15B). Quantification of the co-localization data from the various conditions indicated that cells coexpressing ABI1 $S^{88/296}$A and WAVE2 showed predominant membrane localization. These results suggest that ABI1 can direct the subcellular localization of WAVE2 and that this process is regulatable via PKD2-mediated ABI1 phosphorylation.

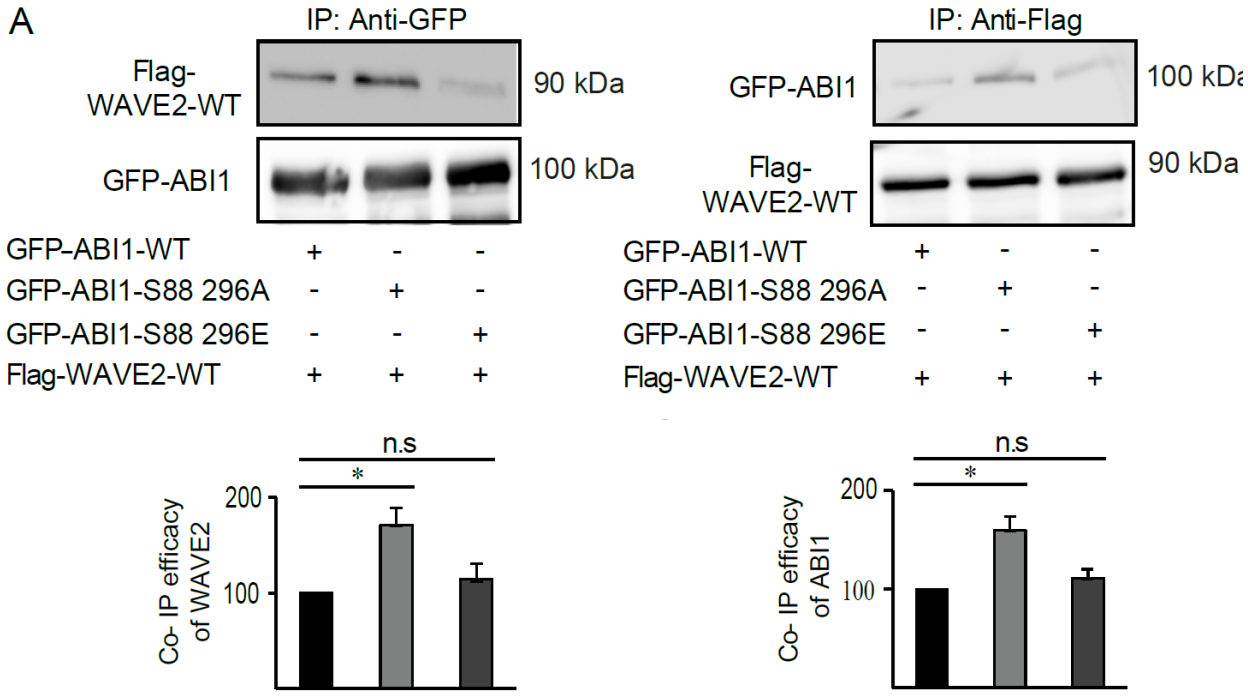

Figure 15: PKD2 mediated phosphorylation of ABI1 destabilizes the ABI1/WAVE2 interaction. (A) *Lysates from HEK-293T cells co-expressing GFP-ABI1-WT/ -$S^{88/296}$A / -$S^{88/296}$E and Flag-WAVE2-WT constructs were immunoprecipitated with anti-GFP (ABI IP, left panel)and*

B

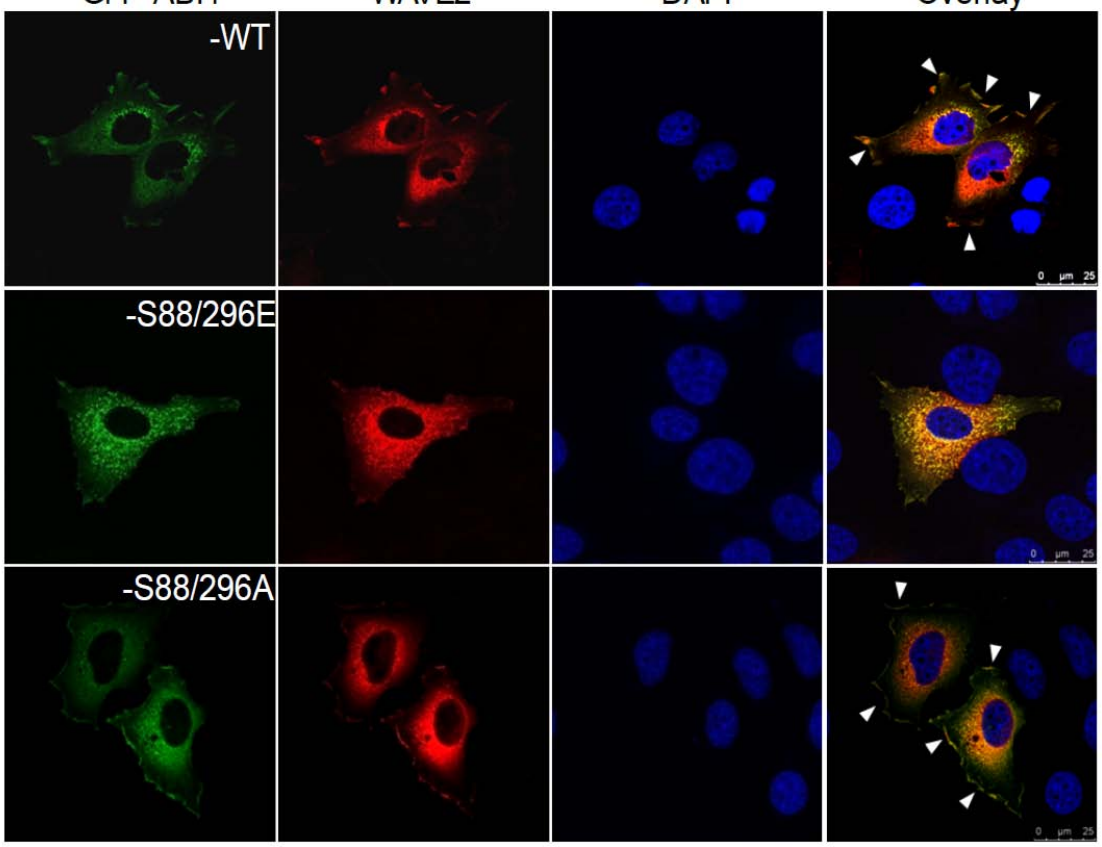
GFP-ABI1
WAVE2
DAPI
Overlay
-WT
-S88/296E
-S88/296A

C

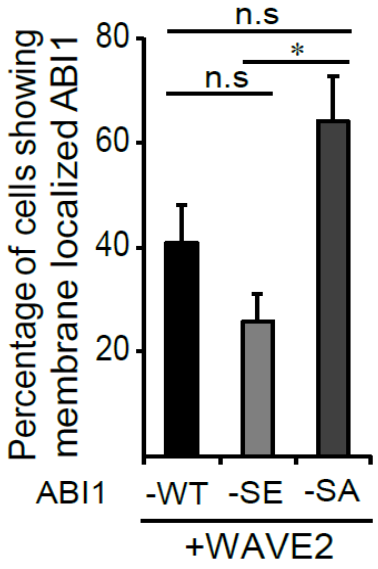
Percentage of cells showing membrane localized ABI1
80
60
40
20
n.s
*
n.s
ABI1
-WT
-SE
-SA
+WAVE2

*anti-Flag (WAVE2 IP, right panel) antibodies and the precipitated proteins were immunoblotted as indicated. Depicted are means and SEM of co-immunoprecipitation efficacies for WAVE2 and ABI1 of four independent experiments. * p < 0.05.* ***(B)*** *Phosphorylation of ABI1 induces a shift in ABI1 and WAVE2 localization from leading edge to perinuclear region. MCF7 cells co-expressing GFP-ABI1-WT/ -$S^{88/296}$E / -$S^{88/296}$A and Flag-WAVE2-WT were fixed, immunostained with anti-WAVE2/ Alexa 647 antibodies and DAPI (blue) and assessed for co-localization (indicated by inserts) using fluorescence microscopy. Scale bar 20 µm.* ***(C)*** *Quantification of membrane localized ABI1.*

5.9 Effect of PKD2-induced ABI1 phosphorylation on WAVE2-mediated actin polymerization

Our earlier experiments indicated that PKD2 mediated phosphorylation of ABI1 destabilizes the ABI1-WAVE2 interaction and changes the subcellular localization of WAVE2. Therefore we examined whether this destabilization would also affect the WAVE2-mediated F-actin turnover. To examine this hypothesis we performed *in vitro* actin polymerization assays using pyrene-labeled G-actin, Arp 2/3 complex and purified proteins. GST alone, GST-ABI1-WT and -$S^{88/296}$E proteins were purified from bacteria. WAVE2-WT was purified from HEK-293T cells ectopically expressing Flag-WAVE2-WT. The polymerization kinetics was determined by the increase in pyrene fluorescence (Figures 16A and B). The half-maxima of the saturated polymerization values ($T½_{max}$ value [s]) calculated from Boltzmann sigmoidal curve fits for the G-actin/Arp reaction was 443.5s±5.7s. In the presence of the nucleation promoting factor-WAVE2, the polymerization rate was enhanced to a $T½_{max}$ value of 396.6±6.4 seconds. ABI1 can synergistically accelerate WAVE2 driven actin polymerization *in vitro* (Innocenti et al., 2004). The $T½_{max}$ values for GST alone and GST-ABI1-WT were 399.4s±4.5s and 329.7s±4.8s, respectively, in accordance with previous data. The $T½_{max}$ value for the combination of G-actin, Arp, WAVE2 and GST-ABI1-$S^{88/296}$E was 381.9s±10.0s and closely resembled the condition when GST alone was used. These results indicate that Arp-complex-driven actin polymerization was more efficient in the presence of ABI1-WT

as compared to the phospho-mimetic ABI1-mutant. There was also a significant difference in the polymerization rates between WAVE2 and ABI1-WT compared to WAVE2 and ABI1-$S^{88/296}E$ when the amount of polymerized F-actin was plotted as percentage of saturation of individual reactions and was analyzed at four time points during the growth phase of the polymerization reaction (T330s, 450s, 555s and 630s) (Figure 17C). The phosphomimetic mutant of ABI1 was the least efficient with respect to actin polymerization with nearly identical polymerization rates throughout. Conversely, the non-modified ABI1 protein strongly enhanced F-actin turn over by 57% (at 330s, in the growth phase) and 33.20% (at 630s, near steady state).

The WAVE Regulatory Complex (WRC) transmits information from the Rac GTPase to the actin nucleator, Arp2/3 complex. However this complex is inactive toward Arp2/3 complex, but can be activated by Rac in nucleotide dependent fashion (Chen et al., 2010, Ismail et al., 2009, Lebensohn et al., 2009). These observations prompted us to test if our findings are a result of ABI1 $S^{88/296}E$ mutation, inhibiting the active ABI1-WAVE2 complex. To test this, an equivalent amount of WAVE2 protein used in the actin polymerization assay was assessed by comassie staining and western blotting. Results confirmed the presence of all the components of WAVE2 complex, ABI1/WAVE2/HSPC300/NAP1/Sra1 (Figure 17D). Therefore, the results presented indicate an affect of ABI1-WT and -$S^{88/296}E$ mutations on the entire auto-inhibited complex. Further, to rule out the possibility of any changes in dimerisation between GST fusion proteins, if any as a result of the mutations induced, we have performed an immunoprecipitation using GFP and Myc-ABI1 WT and $S^{88/296}E$ proteins (Figure 17E). Our results suggest a positive interaction between the conditions presented. However, as a result of $S^{88/296}E$ mutations no significant changes in the extent of interaction were observed.

Taken together, our data suggest that phosphorylation of ABI1 by PKD2 not only affects the stability of the ABI1-WAVE2 sub-complex, but also leads to a decrease in F-actin turnover by inhibiting nucleation promoting factor activity of WAVE2.

A

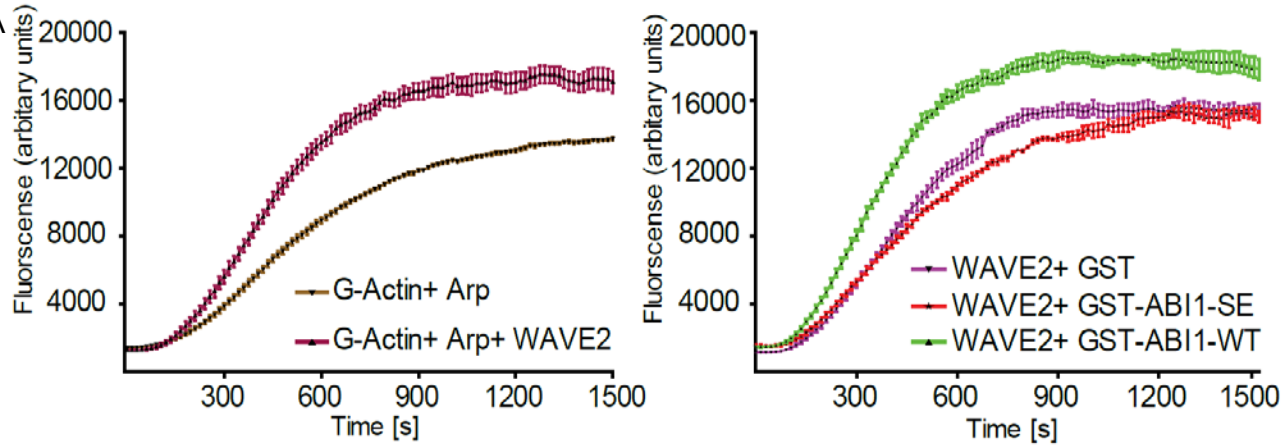

B

Condition	T1/2 Max (sec)
G-actin + Arp	443.5± 5.7
G-actin + Arp + WAVE2	395.6± 6.4
G-actin + Arp + WAVE2 + GST	399.4± 4.5
G-actin + Arp + WAVE2 + GST-ABI-WT	329.7± 4.8
G-actin + Arp + WAVE2 + GST-ABI-S88/296E	381.9± 10.0

C

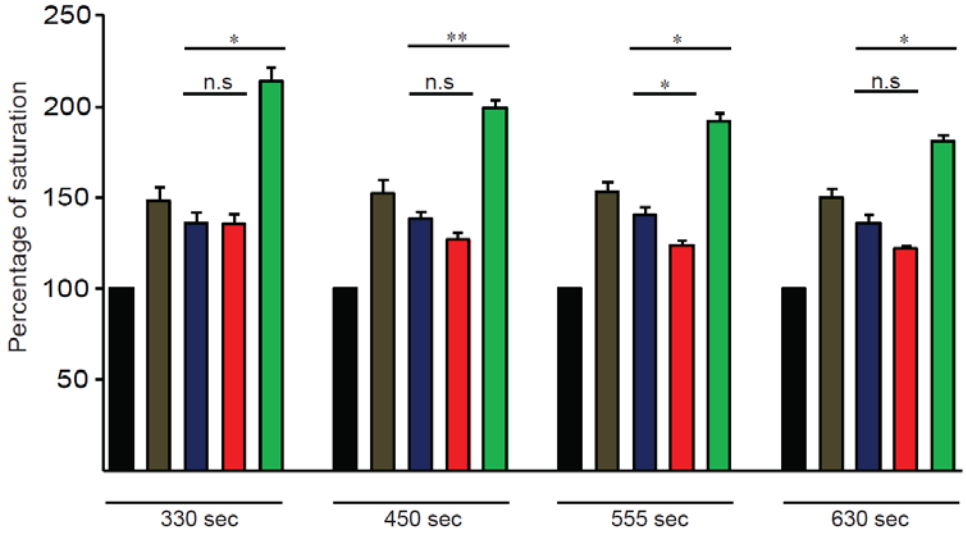

Figure 16: Non modified form of ABI1, (ABI1-WT) in the presence of WAVE2-WT synergistically accelerated Arp-complex-driven actin polymerization as compared to GFP-ABI1-S$^{88/296}$E. (A and B) *Actin polymerization assays were performed with purified proteins as explained in materials and methods. To quantify changes in polymerization, curves were fitted with Boltzmann-sigmoidal equations and V50 values (Half-maxima of saturated polymerization) were calculated.* ***(C)*** *ABI1-WT strongly enhanced actin polymerization. Four*

D

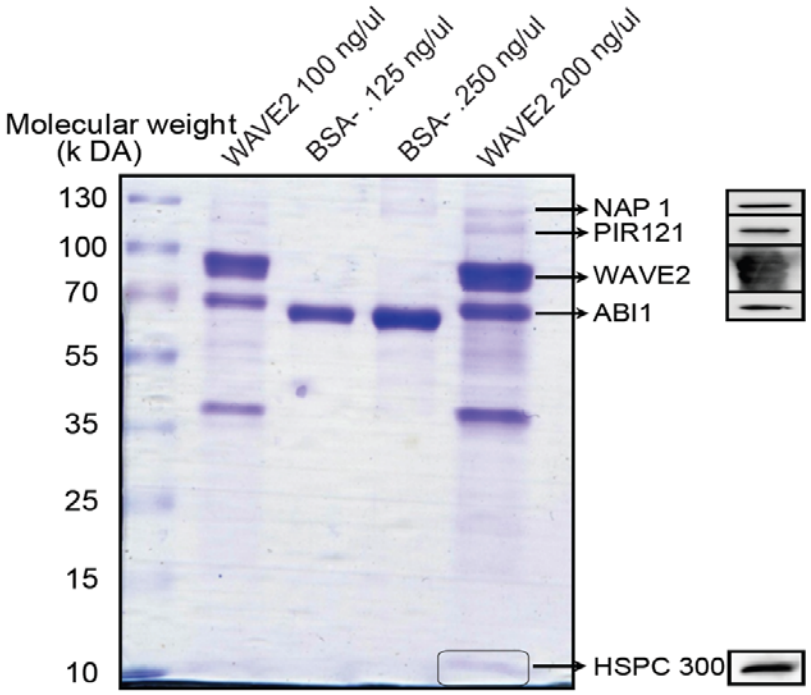

E B

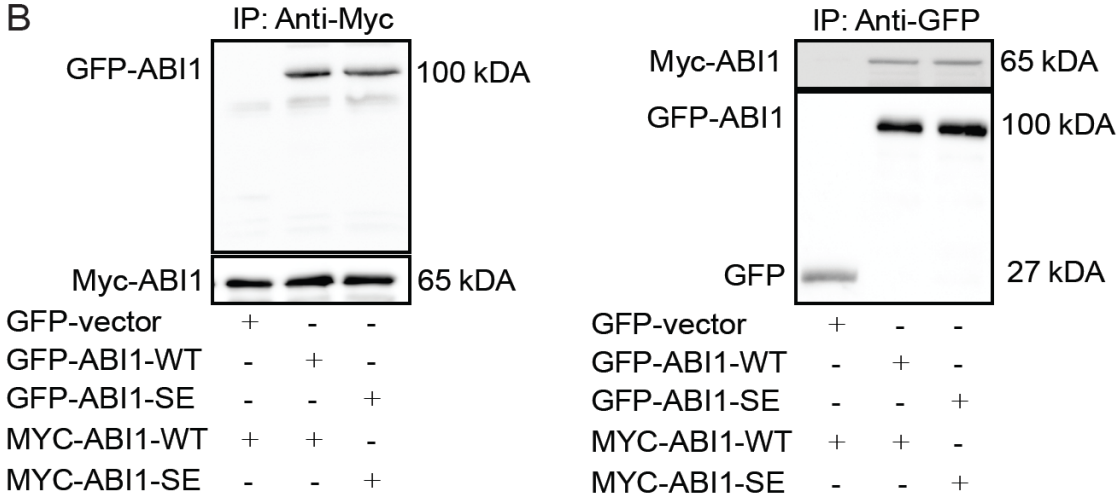

time points in the linear phase of polymerization (330, 450, 555 and 630 sec) were analyzed to quantify extent of individual polymerization reactions. Results shown here are representative of three independent experiments. ***(D)*** *Coomassie-stained gel and western blots confirmed copurification of all the ABI1-WAVE2 complex members in the elution fraction of Flag-WAVE2.* ***(E)*** *Lysates from HEK-293T cells co-expressing GFP-ABI1-WT/ -$S^{88/296}$E, Myc-ABI1-WT/ -$S^{88/296}$E and empty GFP/ yc constructs were immunoprecipitated and immunoblotted with anti-GFP (right panel) and anti-Myc (left panel) antibodies as indicated. (* $p < 0.05$ and ** $p < 0.001$).*

[64]

5.10 ABI1 phosphorylation by PKD2 results in reduced lamellipodia extension in response to heregulin in MCF7 cells

The two basic processes, cell adhesion and motility require the extension of the plasma membrane via the formation of actin rich structures called lamellipodia or fingerlike projections called filopodia (Oster, 1988). During lamellipodia formation WAVE class nucleation promoting factors (NPFs) such as WAVE2, are major activators of the Arp complex at the edge of protruding lamellipodia. Our experiments suggest that phosphorylation of ABI1 by PKD2 destabilizes the interaction between ABI1 and WAVE2 and negatively regulates actin polymerization. To examine a potential effect of ABI1 phosphorylation also on lamellipodia extension and cell motility, we monitored lamellipodia extension. MCF7 cells co-transfected with GFP-ABI1-WT, -$S^{88/296}$E or -$S^{88/296}$A constructs together with Flag-WAVE2-WT were treated with heregulin, a potent stimulus of actin polymerization and lamellipodia extension (Nagata-Ohashi et al., 2004). Cells were then fixed, permeabilized, stained and observed using a fluorescence microscope. A minimum of 125 cells per condition (both GFP- and WAVE2-positive cells) were examined and categorized into three groups of lamellipodial extension as described earlier (Steffen et al., 2004): Lamellipodia present (large continuous sheet of extension), lamellipodia ambiguous (extension as occasional patches) and lamellipodia absent (no extension at all). Cell numbers from three independent experiments were calculated as percentage of entire cell population visualized. MCF7 cells expressing the ABI1-$S^{88/296}$A mutant exhibited well extended lamellipodia as compared to cells expressing the phosphomimetic ABI1 mutant that revealed poor lamellipodia extension. Lamellipodia extension in the ABI1-WT expressing MCF7 cells was in between that observed in GFP-ABI1-$S^{88/296}$E and GFP-ABI1-$S^{88/296}$A expressing cells (Figure 17A). Upon heregulin stimulation, co-localization of ABI1 and WAVE2-WT was far more prominent at leading edge structures of the plasma membrane of cells expressing GFP-ABI1-$S^{88/296}$A and Flag-WAVE2-WT compared to cells expressing GFP-ABI1-WT or GFP-ABI1-$S^{88/296}$E and WAVE2. The proteins also overlapped considerably within the cytoplasm in the perinuclear region following stimulation with Heregulin. As evidenced by phalloidin staining, cells expressing ABI1 $S^{88/296}$A and WAVE2 were characterized by

lamellipodial extensions rich in F-actin as compared to GFP-ABI1-WT and GFP-ABI1-$S^{88/296}$E expressing cells (Figure 17B). To further analyze these differences, cells were categorized into three groups according to their lamellipodia extension as described previously (Steffen et al., 2004): lamellipodia extension present (a large continuous sheet of extension), ambiguous (extension as occasional patches) and absent (no extension at all) (Figure 17C). This analysis indicated that lamellipodia extension was present in the majority of cells expressing GFP-ABI1-$S^{88/296}$A and Flag-WAVE2-WT whereas lamellipodia extension was absent in the majority of cells expressing GFP-ABI1-$S^{88/296}$E and Flag-WAVE2-WT (Figure. 17D). In line with our observations from actin polymerization assays, cells expressing ABI1 $S^{88/296}$E failed to efficiently extend lamellipodia.

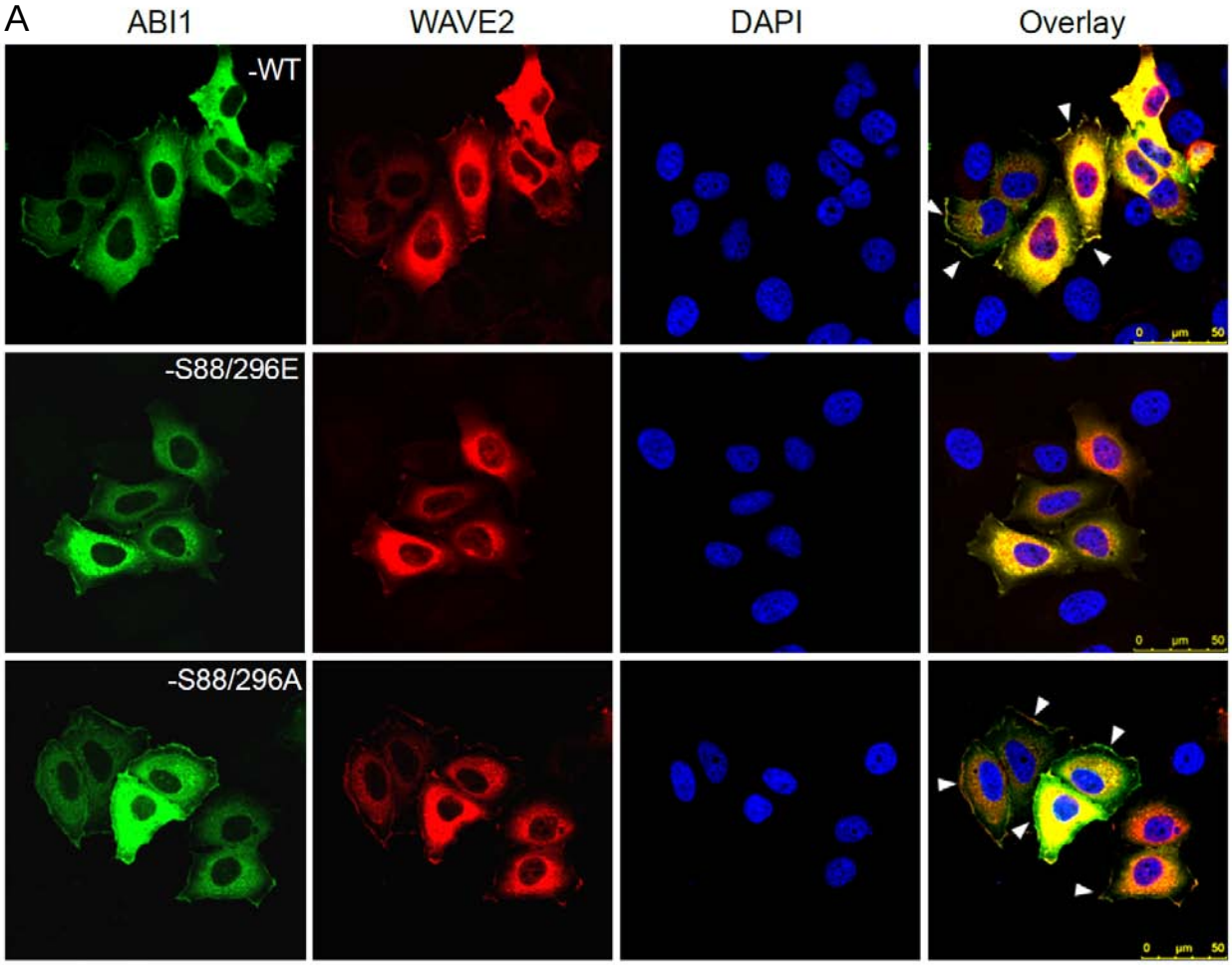

B

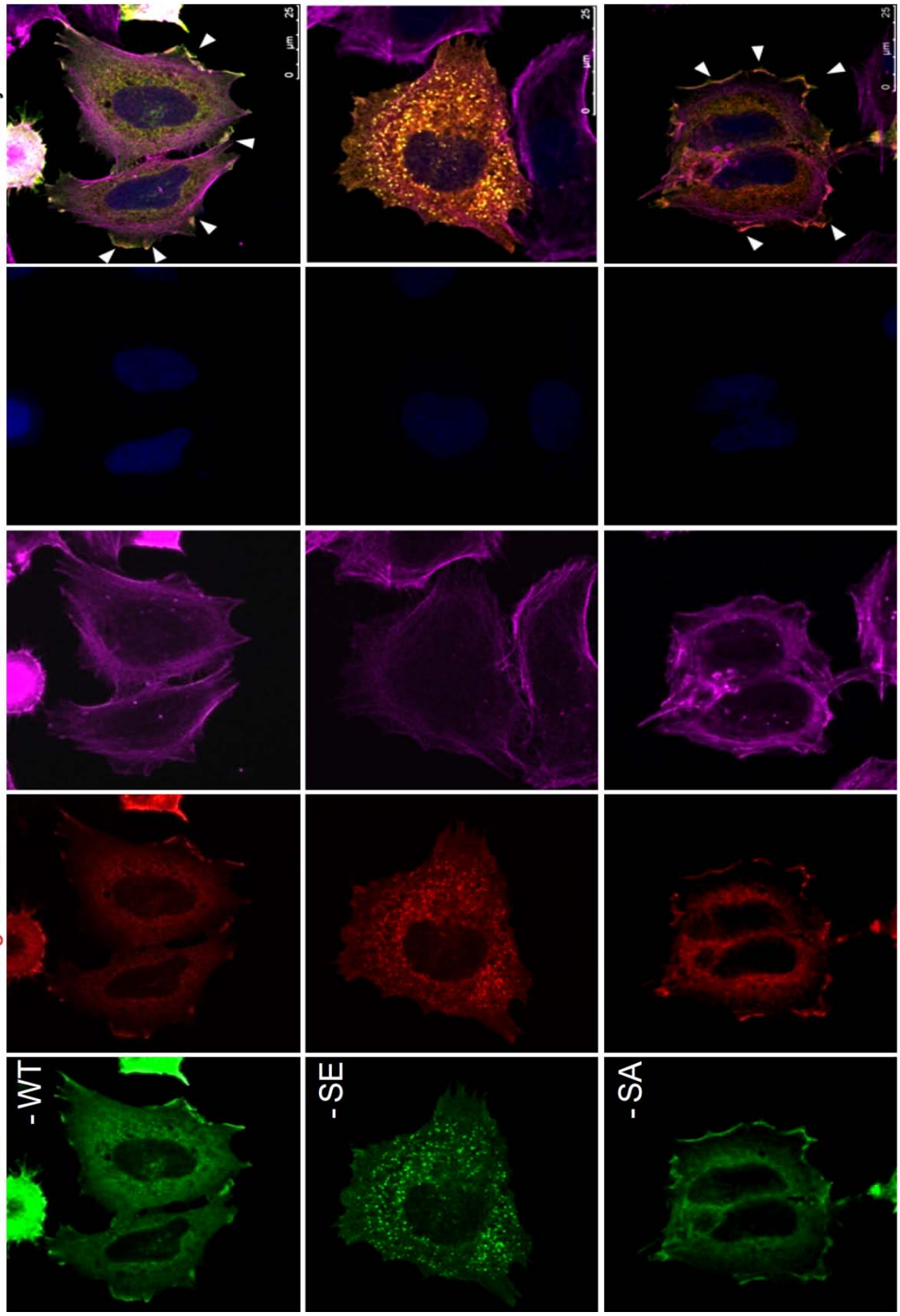

[67]

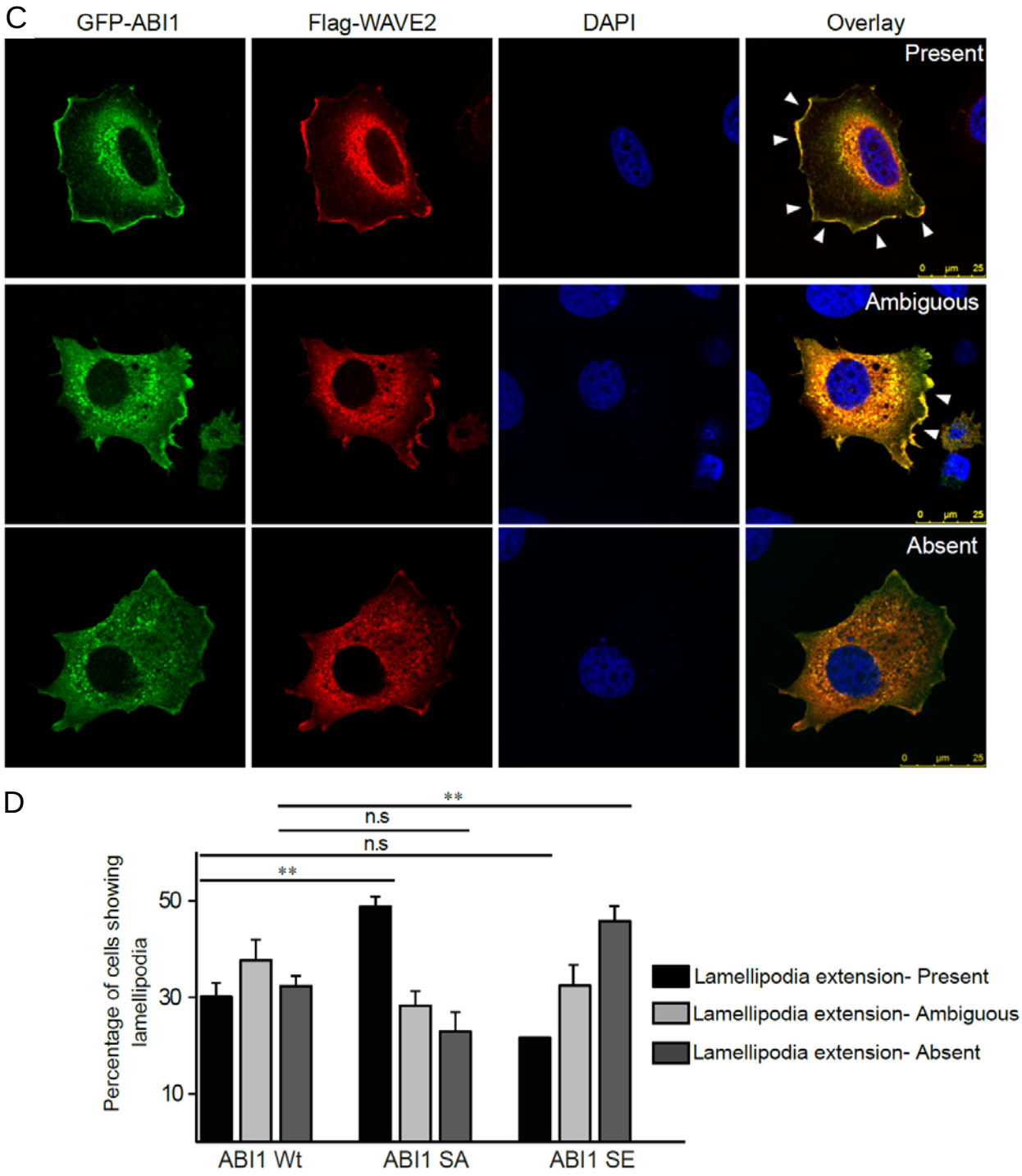

Figure 17: PKD2 mediated phosphorylation of ABI1 hinders lamellipodia extension. (A and B) *MCF7 cells co-expressing GFP-ABI1-WT/ -$S^{88/296}$A / -$S^{88/296}$E and WAVE2-WT were serum starved, heregulin treated, fixed and immunostained with anti-WAVE2/ Alexa 647*

antibodies/ DAPI/ phalloidin and analyzed for any changes in localization and lamellipodia extension. MCF7 cells expressing ABI1S$^{88/296}$A and WAVE2 exhibited a prominent colocalization at the leading edge of the cell. These cells also showed large continuous wavy structures (lamellipodia). The results are also substantiated by actin staining (TRITC-phalloidin) to outline the actin cytoskeleton and mark cell boundaries. ***(C)*** *Representative images for each of the conditions were shown. Scale bar 50 μm.* ***(D)*** *Quantification of lamellipodia extension. Images of cells (n>125, both GFP and WAVE2 positive) were classified into three groups based on extent of lamellipodia extension as explained in materials and methods. Scale bar 25 μm. Means of cell numbers obtained from three independent experiments are presented (in percentage) with standard error. ** p<0.001.*

5.11 Destabilizing the ABI1-WAVE2 interaction by PKD2-induced ABI1 phosphorylation inhibits cancer cell motility

Next we were interested whether the effect of PKD2-induced ABI1 phosphorylation on F actin polymerization and lamellipodia extension would affect tumor cell motility. To test this, we have performed migration assays, random migration and transwell migration assays using HeLa and Panc1 cells respectively. Random migration assays were performed using HeLa cells transfected with GFP vector, GFP-ABI1-WT, -S$^{88/296}$E or -S$^{88/296}$A constructs, respectively. We chose HeLa cells as model, as these cells have been widely used to study cell migration. Fibronectin coated glass bottom disks served as substratum as well as a migration stimulus. Cells expressing the non-phosphorylatable GFP-ABI1-S$^{88/296}$A mutant exhibited significantly enhanced random cell motility as compared to cells transfected with the control vector, ABI1-WT or the phosphomimetic GFP-ABI1-S$^{88/296}$E mutant (Figure 18A). To examine whether PKD2 mediated phosphorylation of ABI1 would also affect directed migration towards a chemotactic gradient we performed transwell migration assays using Panc 1 cells, a pancreatic cancer cell line expressing PKD2 and ABI1 endogenously (Figure 11A). Panc 1 cells were transiently transfected with GFP vector, GFP-ABI1-WT, -S$^{88/296}$E, or -S$^{88/296}$A and seeded onto 8 µm transwell inserts. 10% FCS was used as chemoattractant. Expression of the non phosphorylatable GFP-ABI1-S$^{88/296}$A resulted in

significantly increased directed migration compared to cells expressing ABI1-WT or the phosphomimetic GFP-ABI1-$S^{88/296}$E mutant (Figure 18B). Interestingly, cells expressing ABI1-WT also exhibited decreased cell migration in either migration assay which is most likely due to the fact that ectopically expressed ABI1-WT shows some basal phosphorylation as demonstrated by anti-pMOTIF western blotting (Figures 10, 11B and C). These data imply that PKD2-induced phosphorylation of ABI1-WT indeed inhibits random as well as directed tumor cell motility.

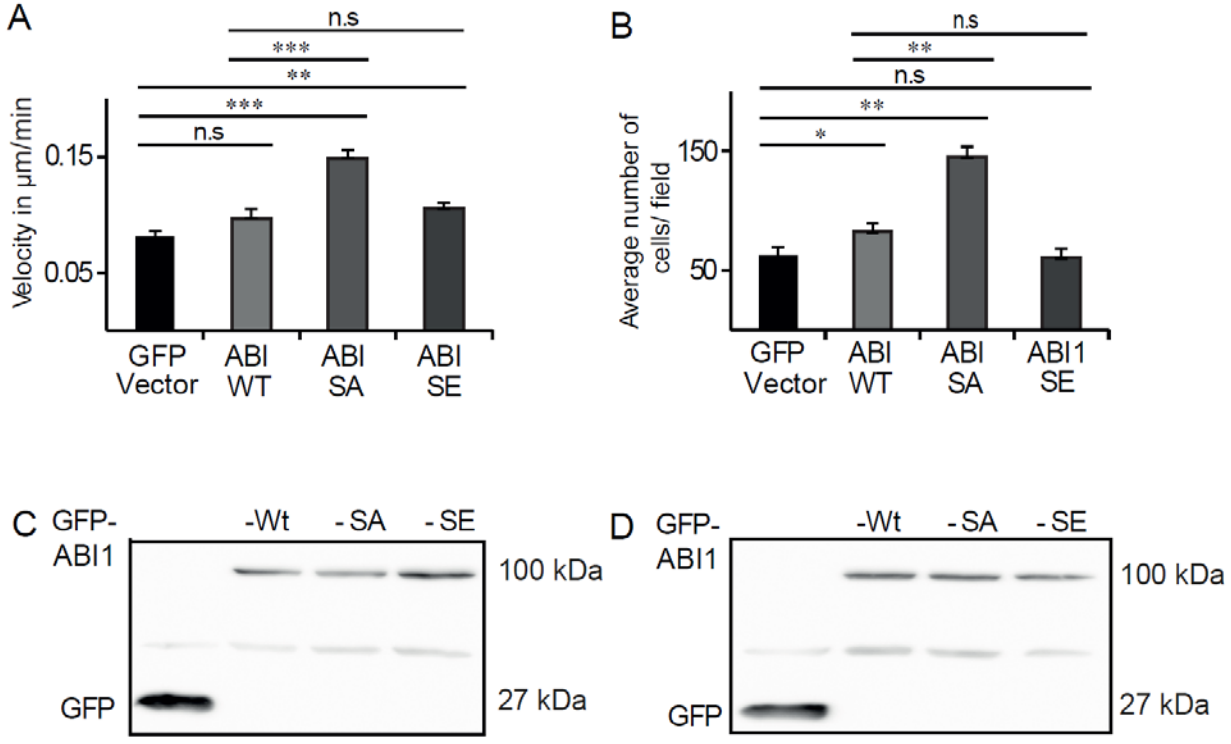

Figure 18: PKD2-induced phosphorylation of ABI1-WT indeed modulates tumor cell motility. (A) *Random migration assay: HeLa cells were transfected with empty GFP-vector/ GFP-ABI1-WT/ -$S^{88/296}$A / -$S^{88/296}$E constructs. Migration of cells (GFP positive) was monitored using time lapse video microscopy (time lapse of 10 min for at least 10 h). Columns represent means of migration velocity (in µm/sec) with standard error of at least 75 cells per condition.* ***(B)*** *Transwell migration assay: Panc 1 cells were transfected with GFP vector/ GFP-ABI1-WT/ -$S^{88/296}$A / -$S^{88/296}$E constructs as indicated. Cells were serum starved for 3 h and allowed to migrate towards a serum gradient for 36 h. Cells migrated through the porous membrane were*

stained with DAPI and visualized by wide field fluorescence microscopy at 20x magnification. Columns represent average number of cells per field with standard error; at least 10 such fields were analyzed. (p<0.05, ** p<0.001 and *** p<0.0001).* ***(C and D)*** *Immunoblotting of lysates using GFP specific antibody confirmed a uniform expression of constructs used in either of the assays*

Taken together, our data suggest that phosphorylation of ABI1 by PKD2 destabilizes the ABI1-WAVE2 interaction and thereby negatively affects actin polymerization, lamellipodia extension and tumor cell motility.

6. Discussion

6.1 Identification of PKD2 substrates: ProtoArray Human Protein Microarray

Our kinase substrate screen yielded several potential substrates including Abelson interactor 1 (ABI1). We focused on the further characterization of this protein, for several reasons. This protein localizes to the leading edge of lamellipodia and filopodia (Stradal et al., 2001), promotes lamellipodia formation (Steffen et al., 2004), actin cytoskeleton reorganization through the regulation of Rho family members (Stovold et al., 2005; Stradal and Scita, 2006) and formation and activation of the WAVE2 signaling complex (Innocenti et al., 2004). Indeed, ABI1 is required for the integrity and the stability of this complex (Dubielecka et al., 2011). It is a key regulator of actin polymerization/ depolymerization and involved in the development of abnormal cytoskeletal functions of cancer cells. ABI1 has been shown to regulate migration, invasion and invadopodia formation and MMP-9 expression in breast cancer cells (Sun et al., 2009; Wang et al., 2007). Taken together there is a functional overlap between PKDs and ABI1 with respect to the regulation of cell motility but also a spatial overlap within the cell: PKDs co-localize at leading edge structures of the plasma membrane with F-actin, Arp2/3 and cortactin (Eiseler et al., 2007). ABI1 localizes to the tips of lamellipodia and filopodia (Echarri et al., 2004; Stradal et al., 2001). This prompted us to further investigate a potential role of ABI1 as substrate of PKDs.

6.2 ABI1 is novel substrate of PKD2

Our results show that PKD2 does phosphorylate ABI1. Using Scansite search (Criteria: individual motif-PKCmu; motif group- basophilic serine/threonine kinase group, stringency level-medium), twelve potential phosphorylation sites in ABI1 were identified. Two of these sites closely resembled the typical PKD substrate phosphorylation motif, S88 and S296. Substitution of these serine residues with alanine confirmed Ser 88 and 296 as PKD2 phosphorylation sites. Further, using an antibody that specifically detects the PKD phosphorylation motif we could identify Ser88 and Ser296 as the relevant PKD2 phosphorylation sites in ABI1 both under overexpressed and endogenous

conditions. The observation that knockdown of all three PKD's abolished phosphorylation of ABI1 in the presence of PMA confirms that these sites are phosphorylated predominantly by the PKD family of protein kinases.

6.3 PKD2 interacts with ABI1 *in vitro* and *in vivo* via second cysteine rich domain (C1b)

PKDs, in particular PKD2, are highly expressed in tumor cells, can localize to the leading edge of cells and play a role in cell motility (Eiseler et al., 2007). ABI1 was also known to localize these areas (Stradal et al., 2001). This prompted us to further examine a potential interaction between ABI1 and PKD2. We found that PKD2 and ABI1 physically interact *in vitro* and *in vivo* and that the interaction is mediated by the second cysteine rich domain of PKD2 (c1b).

Localization studies revealed that PKD2 and ABI1colocalize at leading edge structures like lamellipodia. Phosphorylation of ABI1 by PKDs releases ABI1 from the interaction with the kinase and relocates ABI1 translocates from lamellipodia to the perinuclear region of the cell. Various reports indicate that ABI1 only regulates cell motility when it is localized at the protruding end of the cell, an active site for actin dynamics (Campa et al., 2006; Kheir et al., 2005; Leng et al., 2005; Stradal et al., 2001). Thus we reasoned that the PKD2-induced phosphorylation of ABI1 and consequently the change in its subcellular localization might have an effect on its biological activity.

6.4 PKD2 mediated phosphorylation on ABI1 destabilized ABI1-WAVE2 interaction

ABI1 and WAVE2 proteins interact via the Wave homology domain of WAVE2 and the coiled coil domain of ABI1 (Kheir et al., 2005). ABI1 and WAVE2 are primarily cytosolic in resting conditions. Upon growth factor or integrin stimulation they translocate from the cytosol to the leading edge of the cell where they colocalize with actin with concomitant activation of WAVE2 and actin polymerization (Miki et al., 2000). Disruption of this interaction resulted in a loss of membrane localization and inactivation of WAVE2 (Leng et al., 2005; Stradal et al., 2001). Our data show that phosphorylation

of ABI1 by PKD2 leads to a reduced interaction between ABI1 and WAVE2 and consequently to the relocalization of WAVE2 from leading edge structures to the cytosol. In contrast, cells expressing a non phosphorylatable form of ABI1 and WAVE2 showed a marked co-localization of ABI1 and WAVE2 at the plasma membrane. This data collectively support the conclusion that PKD2-induced ABI1 phosphorylation disrupts the ABI1-WAVE2 interaction and prevents localization of the complex at the plasma membrane.

6.5 Destabilization of the ABI1-WAVE2 interaction negatively regulates actin polymerization and lamellipodia extension

ABI1 supports the assembly and activation of a macromolecular complex containing WAVE2-ABI1-Nap1-PIR121. The ABI1-WAVE2 sub-complex is also active and can stimulate Arp2/3-dependent actin nucleation activity (Innocenti et al., 2004). Our data suggest that phosphorylation of ABI1 by PKD2 destabilizes the ABI1-WAVE2 interaction. Indeed, actin polymerization was markedly reduced in the presence of the phosphomimetic ABI1 mutant, as compared to polymerization rate of ABI1-WT. It was illustrated that ABI1-WAVE2 sub-complex is constitutively active toward Arp2/3 complex while the complete complex is not (Ismail et al., 2009; Lebensohn et al., 2009; Chen et al., 2010). This inactive complex however can be activated by Rac in a nucleotide-dependent fashion. Our observation that the other members of the WAVE regulatory complex (ABI1, HSPC300, NAP1 and SRA1) were also present in the WAVE2 fraction purified from HEK293 cells indicate that the ABI1 $S^{88/296}E$ mutation was able to decelerate the actin polymerization rates almost comparable to that of spontaneous polymerization.

Impaired lamellipodia extension can be the consequence of reduced actin turnover at the plasma membrane. Therefore we monitored lamellipodia extension in response to heregulin, an established stimulus for actin polymerization and lamellipodial extension in MCF7 cells (Nagata-Ohashi et al., 2004) upon expression of ABI1 or its mutants. MCF7 cells expressing the phosphomimetic mutant of ABI1 exhibited a reduced lamellipodial extension. In line with our pyrene labeled actin polymerization

assays, these cells were also characterized by poor staining of F-actin, thus underscoring reduced F-actin turnover as a responsible factor for the observed poor extension of lamellipodia. In contrast, MCF7 cells expressing the non phosphorylatable ABI1 mutant exhibited large protruding lamellipodia.

6.6 PKD2-induced ABI1 phosphorylation inhibits cancer cell motility

Since both PKD2 and ABI1 play a role in the regulation of cell migration (Eiseler et al., 2009a; Eiseler et al., 2009b; Eiseler et al., 2010), we PKD2 mediated phosphorylation of ABI1 would affect migration. Efficient actin polymerization and lamellipodia extension is a prerequisite for cell migration (Lin et al., 2005). Factors that inhibit F-actin turnover and lamellipodia extension will negatively impact motility. Our data show that random cell motility on fibronectin as well as directed migration towards a chemotactic gradient were significantly increased when cells expressed the non-phosphorylatable ABI1 mutant compared to cells expressing ABI1-WT or the phospho-mimetic mutant. These data indicate a role of ABI1 as a mediator of cell migration at the cell periphery.

Integrating the data from our investigation, we propose a model to explain how PKD2 regulates tumor cell motility via ABI1 (Figure 19). PKD2 constitutively interacts with ABI1 via its second cysteine rich domain and phosphorylates ABI1 at Ser88 and Ser296. Under non stimulated conditions, PKD2 constitutively interacts with ABI1. Activation of PKD2 and subsequent phosphorylation of ABI1 by the kinase leads to the disruption of the ABI1-PKD2 and subsequently ABI1-WAVE2 interaction with a subsequent relocation of the proteins from the plasma membrane to the cytoplasm and a decreased WAVE2 activity at the plasma membrane. As a consequence, F-actin polymerization, lamellipodia extension and random and directed tumor cell motility are markedly reduced (Figure 19).

In conclusion our data identify ABI1 as a novel mediator of PKD-induced inhibition of cell migration by affecting actin polymerization and lamellipodia extension.

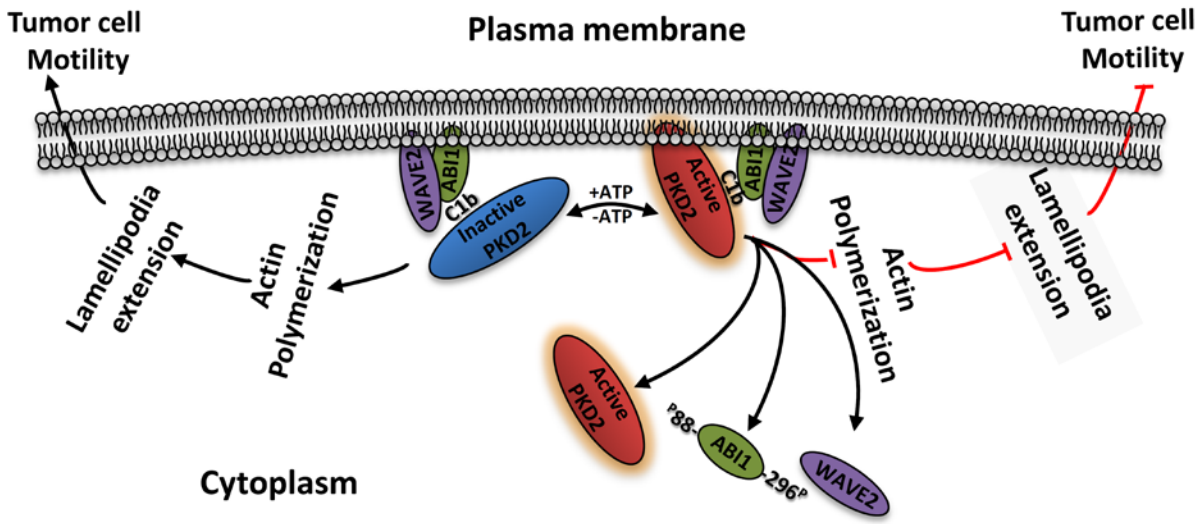

Figure 19: PKD2 regulates the ABI1-WAVE2 interaction, thus the activity of WAVE2 regulatory complex. *PKD2, ABI1 and WAVE2 form a constitutive protein complex in tumor cells. When localized at the plasma membrane, the ABI1- WAVE2 interaction supports efficient actin polymerization, lamellipodia extension and cell motility. Upon activation of PKD2, the kinase phosphorylates ABI1 at Ser88 and Ser296. This leads to the dissociation of the ABI1-PKD2 complex, and also terminates the interaction between ABI1 and WAVE2. The proteins translocate from the plasma membrane to the cytoplasm and the dissolution of the ABI1-WAVE2 interaction results in impaired actin polymerization, decreased lamellipodia extension and reduced tumor cell motility. PKD2 therefore acts as a molecular switch that when turned on dissolves the ABI1-WAVE2 interaction at the plasma membrane.*

7. Summary and future work

The serine/ threonine kinases of the protein kinase D family (PKCmu/ PKD1, PKD2, PKCnu/ PKD3), a subfamily of the calcium/calmodulin-dependent serine protein kinase (CAMK) superfamily, have been implicated in regulation of multiple biological processes including proliferation, survival, apoptosis, angiogenesis and motility. The precise context by which the three PKDs modulate these processes is incompletely understood and requires a better knowledge of their interactors and substrates.

Here we performed a substrate screen using the ProtoArray Human Protein Microarray v4.0 (Invitrogen) with the specific aim to identify potential PKD downstream targets that could have an effect on cell motility. We identify Abelson Interactor 1 (ABI1) as a novel substrate of PKD2. ABI1 was first identified as a downstream target of the Abl tyrosine kinase and is an adaptor protein involved in actin reorganization and lamellipodia formation along with WAVE2.

In the present study we illustrate that PKD2 phosphorylates ABI1 in vitro and in vivo at two serine residues, 88 and 296. ABI1 constitutively interacts with the kinase and its interaction site with PKD2 was mapped to the second cysteine rich domain (C1b). PKD2 and ABI1 colocalize at lamellipodia. Interestingly, we found that upon phosphorylation by PKD2, ABI1 is released from its interaction with the kinase leading to a change in the intracellular distribution of the ABI1 protein: phosphorylated ABI1 translocates from the lamellipodia to the perinuclear region of the cell.

Our data also show that phosphorylation of ABI1 by PKD2 leads to a reduced interaction between ABI1 and WAVE2 and consequently to a relocalization of WAVE2 from leading edge structures to the cytosol. This destabilization of ABI1-WAVE2 sub-complex might negatively impact WAVE2 driven Arp2/3 dependent actin polymerization, as it is known that an intact ABI1-WAVE2 sub-complex is a pre-requisite in stimulating Arp2/3-dependent actin nucleation activity (Innocenti et al., 2004).

In line with co-immunoprecipitation and co-localization studies pyrene-labeled actin polymerization assays also suggested that F-actin turnover was markedly reduced in the presence of the phosphomimetic ABI1 mutant. Supporting these findings, MCF7 cells expressing this mutant exhibited poor extension of lamellipodia

in response to heregulin. Furthermore, our data show that random cell motility on fibronectin as well as directed migration towards a chemotactic gradient was significantly reduced when cells expressed the phospho-mimetic mutant.

Taken together, the sequence of events presented herein , the observation that PKD localizes to the leading edge of the cell (Eiseler et al., 2007) and findings from other laboratories provide a mechanistic understanding of the role of PKD as a negative regulator of cell migration affecting actin polymerization at different levels (Eiseler et al., 2009b; Eiseler et al., 2010). Further work should therefore unravel the molecular details and physiological role of the PKD mediated cytoskeleton regulation that controls fundamental processes such as cell migration and tissue formation.

Furthermore, in breast cancer cells PKD was shown to down-regulate the expression of a number of matrix metalloproteases, which are key factors for cancer cell invasiveness (Eiseler et al., 2009a). ABI1 was also reported in the regulation of invadopodia formation and Src-inhibitor of differentiation protein 1 (Id1)-matrix metalloproteinase (MMP-9) pathway in MDA-MB-231 human breast cancer cells. Thus, a potentially important role of PKD in controlling cancer progression and metastasis via ABI1 can be postulated.

8. German Summary and future work (Deutsche Zusammenfassung und Ausblick)

Die Familie der Protein Kinase D Isoenzyme (PKCmu/PKD1, PKD2, PKD3), welche zu einer Untergruppe der Calcium/Calmodulin-abhängigen Kinasen (CAMK) gehört, ist an der Regulation einer Vielzahl von biologischen Prozessen wie Proliferation, Apoptosis, Angiogenese und Zell-Migration beteiligt. Allerdings ist für ein besseres Verständnis der ablaufenden Prozesse ein tiefergreifendes Wissen über Interaktions-Partner und Substrate notwendig.

In dieser Arbeit haben wir daher mit Hilfe eines humanen ProtoArray Protein Microarray v4.0 einen Screen zur Identifizierung von potentiellen PKD Substraten durchgeführt, welche an der Regulation der Zellmigration beteiligt sein könnten. Dabei wurde Abelson Interactor 1 (ABI1) als neues PKD2 Substrat identifiziert. ABI1 ist ursprünglich als Effektor der Abl Tyrosin Kinase charakterisiert. Es übernimmt zusammen mit WAVE2 wichtige Funktionen bei der Reorganisation des Aktin Zytoskelettes und bei der Ausbildung von Lamellipodien während der Zellmigration. In der hier durchgeführten Arbeit konnten wir aufzeigen, dass PKD2 ABI1 *in vitro* und *in vivo* an den Serinen 88 und 296 phosphoryliert. ABI1 interagiert konstitutiv mit PKD2 und die Interaktionsdomäne konnte für PKD2 auf die zweite Cystein-reiche Sequenz (C1b) eingegrenzt werden. Zudem ko-lokalisieren beide Proteine in Lamellipodien. Nach seiner Phosphorylierung wird ABI1 von PKD2 freigesetzt und dies führt zu einer Veränderung der intrazellulären Lokalisation hin und zu einer verstärkten perinukleären Verteilung. Eine Phosphorylierung von ABI durch PKD2 hat außerdem eine verminderte Interaktion von ABI1 mit WAVE2 zur Folge und führt zu einer Relokalisation von WAVE2 weg from "leading edge" der Zelle in das Zytoplasma. Eine Destabilisierung des ABI-WAVE2 Sub-Komplexes könnte daher die WAVE2-abhängige Arp2/3-Komplex gesteuerte Aktin Polymerisation beeinflussen, wie dies bereits durch Innocenti et al. 2004 gezeigt wurde. Pyrene-Aktin Polymerisations-Studien zeigten dann auch, dass eine phospho-mimetische Mutante von ABI1 die Aktin Polymerisation inhibiert. Darüber hinaus vermindert eine solche Mutante die Ausbildung von Lamellipodien in MCF-7 Zellen, welche durch eine Stimulation mit Heregulin induziert wurden. Es wurde zudem die ungerichtete und gerichtete Zellmigration (Chemotaxis) durch phospho-mimetisches ABI1 inhibiert.

Im Kontext bisher publizierter Arbeiten zeigt sich somit eine Lokalisation von PKD an das "leading edge" der Zelle (Eiseler et al. 2007) und eine Regulation der Aktin Organisation, Polymerisation, sowie Zellmigration auf unterschiedlichen Ebenen (Eiseler et al. 2009b, 2010). Weitere Arbeiten könnten daher zu einem besseren Verständnis der Funktion von PKD bei der Kontrolle der Aktin Regulation und Zellmigration, sowie Gewebe Morphogenese führen. PKD1 spielt zudem bei der Regulation von Matrix-Metalloproteasen in Brustkrebszellen eine wichtige Rolle, welche an der Regulation der Krebszellinvasion beteiligt sind (Eiseler et al. 2009a). Für ABI1 wird ebenfalls eine Funktion während der Krebsinvasion durch eine Regulation der Invadopodien Ausbilung über das "Src-Inhibitor of differentiation Protein 1" (Id1) und Matrix-Metalloprotease 9 (MMP9) in humanen MDA-MB-231 Brustkrebszellen postuliert. Daher könnten weiterführende Untersuchungen eine mögliche wichtige Funktion von PKD bei der Kontrolle der Krebsprogression und Metastasierung aufdecken.

9. Bibilography

Abercrombie, M. (1980). The Croonian Lecture, 1978: The Crawling Movement of Metazoan Cells. **207**, 129-147.

Abramoff, M. D., Magalhaes, P.J., Ram, S.J. (2004). Image Processing with ImageJ. *Biophotonics International* **11**, 36-42.

Altschul, S. F., Gish, W., Miller, W., Myers, E. W. and Lipman, D. J. (1990). Basic local alignment search tool. *J Mol Biol* **215**, 403-10.

Auer, A., von Blume, J., Sturany, S., von Wichert, G., Van Lint, J., Vandenheede, J., Adler, G. and Seufferlein, T. (2005). Role of the regulatory domain of protein kinase D2 in phorbol ester binding, catalytic activity, and nucleocytoplasmic shuttling. *Mol Biol Cell* **16**, 4375-85.

Avkiran, M., Rowland, A. J., Cuello, F. and Haworth, R. S. (2008). Protein kinase d in the cardiovascular system: emerging roles in health and disease. *Circ Res* **102**, 157-63.

Azoitei, N., Pusapati, G. V., Kleger, A., Moller, P., Kufer, R., Genze, F., Wagner, M., van Lint, J., Carmeliet, P., Adler, G. et al. (2010). Protein kinase D2 is a crucial regulator of tumour cell-endothelial cell communication in gastrointestinal tumours. *Gut* **59**, 1316-30.

Bamburg, J. R., McGough, A. and Ono, S. (1999). Putting a new twist on actin: ADF/cofilins modulate actin dynamics. *Trends Cell Biol* **9**, 364-70.

Bard, F. and Malhotra, V. (2006). The formation of TGN-to-plasma-membrane transport carriers. *Annu Rev Cell Dev Biol* **22**, 439-55.

Baron, C. L. and Malhotra, V. (2002). Role of diacylglycerol in PKD recruitment to the TGN and protein transport to the plasma membrane. *Science* **295**, 325-8.

Betz, T., Lim, D. and Kas, J. A. (2006). Neuronal growth: a bistable stochastic process. *Phys Rev Lett* **96**, 098103.

Bi, E. and Zigmond, S. H. (1999). Actin polymerization: Where the WASP stings. *Curr Biol* **9**, R160-3.

Biesova, Z., Piccoli, C. and Wong, W. T. (1997). Isolation and characterization of e3B1, an eps8 binding protein that regulates cell growth. *Oncogene* **14**, 233-41.

Bruce Alberts, A. J., Julian Lewis, Martin Raff, Keith Roberts, and Peter Walter. (2002). Molecular Biology of the Cell. .

Campa, F., Machuy, N., Klein, A. and Rudel, T. (2006). A new interaction between Abi-1 and betaPIX involved in PDGF-activated actin cytoskeleton reorganisation. *Cell Res* **16**, 759-70.

Carlier, M. F., Ressad, F. and Pantaloni, D. (1999). Control of actin dynamics in cell motility. Role of ADF/cofilin. *J Biol Chem* **274**, 33827-30.

Chen, Z., Borek, D., Padrick, S. B., Gomez, T. S., Metlagel, Z., Ismail, A. M., Umetani, J., Billadeau, D. D., Otwinowski, Z. and Rosen, M. K. (2010). Structure and control of the actin regulatory WAVE complex. *Nature* **468**, 533-8.

Chen, H., Wu, X., Pan, Z. K. and Huang, S. (2010). Integrity of SOS1/EPS8/ABI1 tri-complex determines ovarian cancer metastasis. *Cancer Res* **70**, 9979-90.

Chhabra, E. S. and Higgs, H. N. (2007). The many faces of actin: matching assembly factors with cellular structures. *Nat Cell Biol* **9**, 1110-21.

Cowell, C. F., Doppler, H., Yan, I. K., Hausser, A., Umezawa, Y. and Storz, P. (2009). Mitochondrial diacylglycerol initiates protein-kinase D1-mediated ROS signaling. *J Cell Sci* **122**, 919-28.

Cozier, G. E., Carlton, J., Bouyoucef, D. and Cullen, P. J. (2004). Membrane targeting by pleckstrin homology domains. *Curr Top Microbiol Immunol* **282**, 49-88.

Cui, M., Yu, W., Dong, J., Chen, J., Zhang, X. and Liu, Y. (2010). Downregulation of ABI1 expression affects the progression and prognosis of human gastric carcinoma. *Med Oncol* **27**, 632-9.

Dai, Z. and Pendergast, A. M. (1995). Abi-2, a novel SH3-containing protein interacts with the c-Abl tyrosine kinase and modulates c-Abl transforming activity. *Genes Dev* **9**, 2569-82.

De Kimpe, L., Janssens, K., Derua, R., Armacki, M., Goicoechea, S., Otey, C., Waelkens, E., Vandoninck, S., Vandenheede, J. R., Seufferlein, T. et al. (2009). Characterization of cortactin as an in vivo protein kinase D substrate: interdependence of sites and potentiation by Src. *Cell Signal* **21**, 253-63.

Dequiedt, F., Van Lint, J., Lecomte, E., Van Duppen, V., Seufferlein, T., Vandenheede, J. R., Wattiez, R. and Kettmann, R. (2005). Phosphorylation of histone deacetylase 7 by protein kinase D mediates T cell receptor-induced Nur77 expression and apoptosis. *J Exp Med* **201**, 793-804.

Doppler, H., Storz, P., Li, J., Comb, M. J. and Toker, A. (2005). A phosphorylation state-specific antibody recognizes Hsp27, a novel substrate of protein kinase D. *J Biol Chem* **280**, 15013-9.

Du, C., Zhang, C., Hassan, S., Biswas, M. H. and Balaji, K. C. (2010). Protein kinase D1 suppresses epithelial-to-mesenchymal transition through phosphorylation of snail. *Cancer Res* **70**, 7810-9.

Duan, Z., Lamendola, D. E., Duan, Y., Yusuf, R. Z. and Seiden, M. V. (2005). Description of paclitaxel resistance-associated genes in ovarian and breast cancer cell lines. *Cancer Chemother Pharmacol* **55**, 277-85.

Dubielecka, P. M., Ladwein, K. I., Xiong, X., Migeotte, I., Chorzalska, A., Anderson, K. V., Sawicki, J. A., Rottner, K., Stradal, T. E. and Kotula, L. (2011). Essential role for Abi1 in embryonic survival and WAVE2 complex integrity. *Proc Natl Acad Sci U S A* **108**, 7022-7.

Echarri, A., Lai, M. J., Robinson, M. R. and Pendergast, A. M. (2004). Abl interactor 1 (Abi-1) wave-binding and SNARE domains regulate its nucleocytoplasmic shuttling, lamellipodium localization, and wave-1 levels. *Mol Cell Biol* **24**, 4979-93.

Eiseler, T., Doppler, H., Yan, I. K., Goodison, S. and Storz, P. (2009a). Protein kinase D1 regulates matrix metalloproteinase expression and inhibits breast cancer cell invasion. *Breast Cancer Res* **11**, R13.

Eiseler, T., Doppler, H., Yan, I. K., Kitatani, K., Mizuno, K. and Storz, P. (2009b). Protein kinase D1 regulates cofilin-mediated F-actin reorganization and cell motility through slingshot. *Nat Cell Biol* **11**, 545-56.

Eiseler, T., Hausser, A., De Kimpe, L., Van Lint, J. and Pfizenmaier, K. (2010). Protein kinase D controls actin polymerization and cell motility through phosphorylation of cortactin. *J Biol Chem* **285**, 18672-83.

Eiseler, T., Schmid, M. A., Topbas, F., Pfizenmaier, K. and Hausser, A. (2007). PKD is recruited to sites of actin remodelling at the leading edge and negatively regulates cell migration. *FEBS Lett* **581**, 4279-87.

Ernest Dodd, M., Ristich, V. L., Ray, S., Lober, R. M. and Bollag, W. B. (2005). Regulation of protein kinase D during differentiation and proliferation of primary mouse keratinocytes. *J Invest Dermatol* **125**, 294-306.

Eto, K., Nishikii, H., Ogaeri, T., Suetsugu, S., Kamiya, A., Kobayashi, T., Yamazaki, D., Oda, A., Takenawa, T. and Nakauchi, H. (2007). The WAVE2/Abi1 complex differentially regulates megakaryocyte development and spreading: implications for platelet biogenesis and spreading machinery. *Blood* **110**, 3637-47.

Fan, P. D. and Goff, S. P. (2000). Abl interactor 1 binds to sos and inhibits epidermal growth factor- and v-Abl-induced activation of extracellular signal-regulated kinases. *Mol Cell Biol* **20**, 7591-601.

Fazioli, F., Minichiello, L., Matoska, V., Castagnino, P., Miki, T., Wong, W. T. and Di Fiore, P. P. (1993). Eps8, a substrate for the epidermal growth factor receptor kinase, enhances EGF-dependent mitogenic signals. *EMBO J* **12**, 3799-808.

Feilner, T., Hultschig, C., Lee, J., Meyer, S., Immink, R. G., Koenig, A., Possling, A., Seitz, H., Beveridge, A., Scheel, D. et al. (2005). High throughput identification of potential Arabidopsis mitogen-activated protein kinases substrates. *Mol Cell Proteomics* **4**, 1558-68.

Frame, M. C., Fincham, V. J., Carragher, N. O. and Wyke, J. A. (2002). v-Src's hold over actin and cell adhesions. *Nat Rev Mol Cell Biol* **3**, 233-45.

Fu, Y. and Rubin, C. S. (2011). Protein kinase D: coupling extracellular stimuli to the regulation of cell physiology. *EMBO Rep* **12**, 785-96.

Fugmann, T., Hausser, A., Schoffler, P., Schmid, S., Pfizenmaier, K. and Olayioye, M. A. (2007). Regulation of secretory transport by protein kinase D-mediated phosphorylation of the ceramide transfer protein. *J Cell Biol* **178**, 15-22.

Gasteiger, E., Gattiker, A., Hoogland, C., Ivanyi, I., Appel, R. D. and Bairoch, A. (2003). ExPASy: The proteomics server for in-depth protein knowledge and analysis. *Nucleic Acids Res* **31**, 3784-8.

Gautreau, A., Ho, H. Y., Li, J., Steen, H., Gygi, S. P. and Kirschner, M. W. (2004). Purification and architecture of the ubiquitous Wave complex. *Proc Natl Acad Sci U S A* **101**, 4379-83.

Gimona, M., Buccione, R., Courtneidge, S. A. and Linder, S. (2008). Assembly and biological role of podosomes and invadopodia. *Curr Opin Cell Biol* **20**, 235-41.

Goff, S. P., Gilboa, E., Witte, O. N. and Baltimore, D. (1980). Structure of the Abelson murine leukemia virus genome and the homologous cellular gene: studies with cloned viral DNA. *Cell* **22**, 777-85.

Graham, T. R. and Burd, C. G. (2011). Coordination of Golgi functions by phosphatidylinositol 4-kinases. *Trends Cell Biol* **21**, 113-21.

Ha, C. H., Jhun, B. S., Kao, H. Y. and Jin, Z. G. (2008). VEGF stimulates HDAC7 phosphorylation and cytoplasmic accumulation modulating matrix metalloproteinase expression and angiogenesis. *Arterioscler Thromb Vasc Biol* **28**, 1782-8.

Hao, Q., Wang, L., Zhao, Z. J. and Tang, H. (2009). Identification of protein kinase D2 as a pivotal regulator of endothelial cell proliferation, migration, and angiogenesis. *J Biol Chem* **284**, 799-806.

Hausser, A., Link, G., Hoene, M., Russo, C., Selchow, O. and Pfizenmaier, K. (2006). Phospho-specific binding of 14-3-3 proteins to phosphatidylinositol 4-kinase III beta protects from dephosphorylation and stabilizes lipid kinase activity. *J Cell Sci* **119**, 3613-21.

Hausser, A., Storz, P., Martens, S., Link, G., Toker, A. and Pfizenmaier, K. (2005). Protein kinase D regulates vesicular transport by phosphorylating and activating phosphatidylinositol-4 kinase IIIbeta at the Golgi complex. *Nat Cell Biol* **7**, 880-6.

Haworth, R. S., Cuello, F., Herron, T. J., Franzen, G., Kentish, J. C., Gautel, M. and Avkiran, M. (2004). Protein kinase D is a novel mediator of cardiac troponin I phosphorylation and regulates myofilament function. *Circ Res* **95**, 1091-9.

Hofman, P., d'Andrea, L., Guzman, E., Selva, E., Le Negrate, G., Far, D. F., Lemichez, E., Boquet, P. and Rossi, B. (1999). Neutrophil F-actin and myosin but not

microtubules functionally regulate transepithelial migration induced by interleukin 8 across a cultured intestinal epithelial monolayer. *Eur Cytokine Netw* **10**, 227-36.

Hu, H., Bliss, J. M., Wang, Y. and Colicelli, J. (2005). RIN1 is an ABL tyrosine kinase activator and a regulator of epithelial-cell adhesion and migration. *Curr Biol* **15**, 815-23.

Hurd, C., Waldron, R. T. and Rozengurt, E. (2002). Protein kinase D complexes with C-Jun N-terminal kinase via activation loop phosphorylation and phosphorylates the C-Jun N-terminus. *Oncogene* **21**, 2154-60.

Iglesias, T., Cabrera-Poch, N., Mitchell, M. P., Naven, T. J., Rozengurt, E. and Schiavo, G. (2000). Identification and cloning of Kidins220, a novel neuronal substrate of protein kinase D. *J Biol Chem* **275**, 40048-56.

Iglesias, T., Matthews, S. and Rozengurt, E. (1998a). Dissimilar phorbol ester binding properties of the individual cysteine-rich motifs of protein kinase D. *FEBS Lett* **437**, 19-23.

Iglesias, T. and Rozengurt, E. (1998). Protein kinase D activation by mutations within its pleckstrin homology domain. *J Biol Chem* **273**, 410-6.

Iglesias, T. and Rozengurt, E. (1999). Protein kinase D activation by deletion of its cysteine-rich motifs. *FEBS Lett* **454**, 53-6.

Iglesias, T., Waldron, R. T. and Rozengurt, E. (1998b). Identification of in vivo phosphorylation sites required for protein kinase D activation. *J Biol Chem* **273**, 27662-7.

Innocenti, M., Frittoli, E., Ponzanelli, I., Falck, J. R., Brachmann, S. M., Di Fiore, P. P. and Scita, G. (2003). Phosphoinositide 3-kinase activates Rac by entering in a complex with Eps8, Abi1, and Sos-1. *J Cell Biol* **160**, 17-23.

Innocenti, M., Gerboth, S., Rottner, K., Lai, F. P., Hertzog, M., Stradal, T. E., Frittoli, E., Didry, D., Polo, S., Disanza, A. et al. (2005). Abi1 regulates the activity of N-WASP and WAVE in distinct actin-based processes. *Nat Cell Biol* **7**, 969-76.

Innocenti, M., Tenca, P., Frittoli, E., Faretta, M., Tocchetti, A., Di Fiore, P. P. and Scita, G. (2002). Mechanisms through which Sos-1 coordinates the activation of Ras and Rac. *J Cell Biol* **156**, 125-36.

Innocenti, M., Zucconi, A., Disanza, A., Frittoli, E., Areces, L. B., Steffen, A., Stradal, T. E., Di Fiore, P. P., Carlier, M. F. and Scita, G. (2004). Abi1 is essential for the formation and activation of a WAVE2 signalling complex. *Nat Cell Biol* **6**, 319-27.

Ismail, A. M., Padrick, S. B., Chen, B., Umetani, J. and Rosen, M. K. (2009). The WAVE regulatory complex is inhibited. *Nat Struct Mol Biol* **16**, 561-3.

Jaggi, M., Rao, P. S., Smith, D. J., Wheelock, M. J., Johnson, K. R., Hemstreet, G. P. and Balaji, K. C. (2005). E-cadherin phosphorylation by protein kinase D1/protein kinase C{mu} is associated with altered cellular aggregation and motility in prostate cancer. *Cancer Res* **65**, 483-92.

Jamora, C., Yamanouye, N., Van Lint, J., Laudenslager, J., Vandenheede, J. R., Faulkner, D. J. and Malhotra, V. (1999). Gbetagamma-mediated regulation of Golgi organization is through the direct activation of protein kinase D. *Cell* **98**, 59-68.

Janssens, K., De Kimpe, L., Balsamo, M., Vandoninck, S., Vandenheede, J. R., Gertler, F. and Van Lint, J. (2009). Characterization of EVL-I as a protein kinase D substrate. *Cell Signal* **21**, 282-92.

Jensen, E. D., Gopalakrishnan, R. and Westendorf, J. J. (2009). Bone morphogenic protein 2 activates protein kinase D to regulate histone deacetylase 7 localization and repression of Runx2. *J Biol Chem* **284**, 2225-34.

Johannes, F. J., Prestle, J., Eis, S., Oberhagemann, P. and Pfizenmaier, K. (1994). PKCu is a novel, atypical member of the protein kinase C family. *J Biol Chem* **269**, 6140-8.

Johannessen, M., Delghandi, M. P., Rykx, A., Dragset, M., Vandenheede, J. R., Van Lint, J. and Moens, U. (2007). Protein kinase D induces transcription through direct phosphorylation of the cAMP-response element-binding protein. *J Biol Chem* **282**, 14777-87.

Just, S., Berger, I. M., Meder, B., Backs, J., Keller, A., Marquart, S., Frese, K., Patzel, E., Rauch, G. J., Katus, H. A. et al. (2011). Protein kinase D2 controls cardiac valve formation in zebrafish by regulating histone deacetylase 5 activity. *Circulation* **124**, 324-34.

Kakiuchi, S., Daigo, Y., Tsunoda, T., Yano, S., Sone, S. and Nakamura, Y. (2003). Genome-wide analysis of organ-preferential metastasis of human small cell lung cancer in mice. *Mol Cancer Res* **1**, 485-99.

Kaverina, I., Krylyshkina, O. and Small, J. V. (2002). Regulation of substrate adhesion dynamics during cell motility. *Int J Biochem Cell Biol* **34**, 746-61.

Kelly, T., Mueller, S. C., Yeh, Y. and Chen, W. T. (1994). Invadopodia promote proteolysis of a wide variety of extracellular matrix proteins. *J Cell Physiol* **158**, 299-308.

Kheir, W. A., Gevrey, J. C., Yamaguchi, H., Isaac, B. and Cox, D. (2005). A WAVE2-Abi1 complex mediates CSF-1-induced F-actin-rich membrane protrusions and migration in macrophages. *J Cell Sci* **118**, 5369-79.

Kim, M. S., Fielitz, J., McAnally, J., Shelton, J. M., Lemon, D. D., McKinsey, T. A., Richardson, J. A., Bassel-Duby, R. and Olson, E. N. (2008). Protein kinase D1 stimulates MEF2 activity in skeletal muscle and enhances muscle performance. *Mol Cell Biol* **28**, 3600-9.

Kleger, A., Loebnitz, C., Pusapati, G. V., Armacki, M., Muller, M., Tumpel, S., Illing, A., Hartmann, D., Brunner, C., Liebau, S. et al. (2011). Protein kinase D2 is an essential regulator of murine myoblast differentiation. *PLoS One* **6**, e14599.

Lebensohn, A. M. and Kirschner, M. W. (2009). Activation of the WAVE complex by coincident signals controls actin assembly. *Mol Cell* **36**, 512-24.

Leng, Y., Zhang, J., Badour, K., Arpaia, E., Freeman, S., Cheung, P., Siu, M. and Siminovitch, K. (2005). Abelson-interactor-1 promotes WAVE2 membrane translocation and Abelson-mediated tyrosine phosphorylation required for WAVE2 activation. *Proc Natl Acad Sci U S A* **102**, 1098-103.

Lin, J., Liu, J., Wang, Y., Zhu, J., Zhou, K., Smith, N. and Zhan, X. (2005). Differential regulation of cortactin and N-WASP-mediated actin polymerization by missing in metastasis (MIM) protein. *Oncogene* **24**, 2059-66.

Machesky, L. M. and Gould, K. L. (1999). The Arp2/3 complex: a multifunctional actin organizer. *Curr Opin Cell Biol* **11**, 117-21.

Machesky, L. M. and Insall, R. H. (1999). Signaling to actin dynamics. *J Cell Biol* **146**, 267-72.

Machuy, N., Campa, F., Thieck, O. and Rudel, T. (2007). c-Abl-binding protein interacts with p21-activated kinase 2 (PAK-2) to regulate PDGF-induced membrane ruffles. *J Mol Biol* **370**, 620-32.

Macoska, J. A., Xu, J., Ziemnicka, D., Schwab, T. S., Rubin, M. A. and Kotula, L. (2001). Loss of expression of human spectrin src homology domain binding protein 1 is associated with 10p loss in human prostatic adenocarcinoma. *Neoplasia* **3**, 99-104.

Maeda, Y., Beznoussenko, G. V., Van Lint, J., Mironov, A. A. and Malhotra, V. (2001). Recruitment of protein kinase D to the trans-Golgi network via the first cysteine-rich domain. *EMBO J* **20**, 5982-90.

Manning, G., Whyte, D. B., Martinez, R., Hunter, T. and Sudarsanam, S. (2002). The protein kinase complement of the human genome. *Science* **298**, 1912-34.

Matthews, S. A., Liu, P., Spitaler, M., Olson, E. N., McKinsey, T. A., Cantrell, D. A. and Scharenberg, A. M. (2006). Essential role for protein kinase D family kinases in the regulation of class II histone deacetylases in B lymphocytes. *Mol Cell Biol* **26**, 1569-77.

Matthews, S. A., Rozengurt, E. and Cantrell, D. (1999). Characterization of serine 916 as an in vivo autophosphorylation site for protein kinase D/Protein kinase Cmu. *J Biol Chem* **274**, 26543-9.

Matthews, S. A., Rozengurt, E. and Cantrell, D. (2000). Protein kinase D. A selective target for antigen receptors and a downstream target for protein kinase C in lymphocytes. *J Exp Med* **191**, 2075-82.

Miki, H., Yamaguchi, H., Suetsugu, S. and Takenawa, T. (2000). IRSp53 is an essential intermediate between Rac and WAVE in the regulation of membrane ruffling. *Nature* **408**, 732-5.

Miyazaki, K., Matsuda, S., Ichigotani, Y., Takenouchi, Y., Hayashi, K., Fukuda, Y., Nimura, Y. and Hamaguchi, M. (2000). Isolation and characterization of a novel human gene (NESH) which encodes a putative signaling molecule similar to e3B1 protein. *Biochim Biophys Acta* **1493**, 237-41.

Mullins, R. D., Heuser, J. A. and Pollard, T. D. (1998). The interaction of Arp2/3 complex with actin: nucleation, high affinity pointed end capping, and formation of branching networks of filaments. *Proc Natl Acad Sci U S A* **95**, 6181-6.

Nagata-Ohashi, K., Ohta, Y., Goto, K., Chiba, S., Mori, R., Nishita, M., Ohashi, K., Kousaka, K., Iwamatsu, A., Niwa, R. et al. (2004). A pathway of neuregulin-induced activation of cofilin-phosphatase Slingshot and cofilin in lamellipodia. *J Cell Biol* **165**, 465-71.

Nishikawa, K., Toker, A., Johannes, F. J., Songyang, Z. and Cantley, L. C. (1997). Determination of the specific substrate sequence motifs of protein kinase C isozymes. *J Biol Chem* **272**, 952-60.

Obenauer, J. C., Cantley, L. C. and Yaffe, M. B. (2003). Scansite 2.0: Proteome-wide prediction of cell signaling interactions using short sequence motifs. *Nucleic Acids Res* **31**, 3635-41.

Oster, G. (1988). Biophysics of the leading lamella. *Cell Motil Cytoskeleton* **10**, 164-71.

Paolucci, L. and Rozengurt, E. (1999). Protein kinase D in small cell lung cancer cells: rapid activation through protein kinase C. *Cancer Res* **59**, 572-7.

Paolucci, L., Sinnett-Smith, J. and Rozengurt, E. (2000). Lysophosphatidic acid rapidly induces protein kinase D activation through a pertussis toxin-sensitive pathway. *Am J Physiol Cell Physiol* **278**, C33-9.

Peterburs, P., Heering, J., Link, G., Pfizenmaier, K., Olayioye, M. A. and Hausser, A. (2009). Protein kinase D regulates cell migration by direct phosphorylation of the cofilin phosphatase slingshot 1 like. *Cancer Res* **69**, 5634-8.

Pollard, T. D., Blanchoin, L. and Mullins, R. D. (2000). Molecular mechanisms controlling actin filament dynamics in nonmuscle cells. *Annu Rev Biophys Biomol Struct* **29**, 545-76.

Preisinger, C. and Barr, F. A. (2005). Kinases regulating Golgi apparatus structure and function. *Biochem Soc Symp*, 15-30.

Prestle, J., Pfizenmaier, K., Brenner, J. and Johannes, F. J. (1996). Protein kinase C mu is located at the Golgi compartment. *J Cell Biol* **134**, 1401-10.

Proepper, C., Johannsen, S., Liebau, S., Dahl, J., Vaida, B., Bockmann, J., Kreutz, M. R., Gundelfinger, E. D. and Boeckers, T. M. (2007). Abelson interacting protein 1 (Abi-1) is essential for dendrite morphogenesis and synapse formation. *EMBO J* **26**, 1397-409.

Ptacek, J., Devgan, G., Michaud, G., Zhu, H., Zhu, X., Fasolo, J., Guo, H., Jona, G., Breitkreutz, A., Sopko, R. et al. (2005). Global analysis of protein phosphorylation in yeast. *Nature* **438**, 679-84.

Pusapati, G. V., Krndija, D., Armacki, M., von Wichert, G., von Blume, J., Malhotra, V., Adler, G. and Seufferlein, T. (2010). Role of the second cysteine-rich domain and Pro275 in protein kinase D2 interaction with ADP-ribosylation factor 1, trans-Golgi network recruitment, and protein transport. *Mol Biol Cell* **21**, 1011-22.

Rasband, W. S. (1997). ImageJ, U. S. National Institutes of Health, Bethesda, Maryland, USA.

Rennecke, J., Rehberger, P. A., Furstenberger, G., Johannes, F. J., Stohr, M., Marks, F. and Richter, K. H. (1999). Protein-kinase-Cmu expression correlates with enhanced keratinocyte proliferation in normal and neoplastic mouse epidermis and in cell culture. *Int J Cancer* **80**, 98-103.

Rey, O., Reeve, J. R., Jr., Zhukova, E., Sinnett-Smith, J. and Rozengurt, E. (2004). G protein-coupled receptor-mediated phosphorylation of the activation loop of protein kinase D: dependence on plasma membrane translocation and protein kinase Cepsilon. *J Biol Chem* **279**, 34361-72.

Rey, O., Sinnett-Smith, J., Zhukova, E. and Rozengurt, E. (2001). Regulated nucleocytoplasmic transport of protein kinase D in response to G protein-coupled receptor activation. *J Biol Chem* **276**, 49228-35.

Rey, O., Yuan, J. and Rozengurt, E. (2003a). Intracellular redistribution of protein kinase D2 in response to G-protein-coupled receptor agonists. *Biochem Biophys Res Commun* **302**, 817-24.

Rey, O., Yuan, J., Young, S. H. and Rozengurt, E. (2003b). Protein kinase C nu/protein kinase D3 nuclear localization, catalytic activation, and intracellular

redistribution in response to G protein-coupled receptor agonists. *J Biol Chem* **278**, 23773-85.

Ridley, A. J. (2001). Rho GTPases and cell migration. *J Cell Sci* **114**, 2713-22.

Ring, C., Ginsberg, M. H., Haling, J. and Pendergast, A. M. (2011). Abl-interactor-1 (Abi1) has a role in cardiovascular and placental development and is a binding partner of the alpha4 integrin. *Proc Natl Acad Sci U S A* **108**, 149-54.

Rogers, S. L., Wiedemann, U., Stuurman, N. and Vale, R. D. (2003). Molecular requirements for actin-based lamella formation in Drosophila S2 cells. *J Cell Biol* **162**, 1079-88.

Rozengurt, E. (2011). Protein kinase D signaling: multiple biological functions in health and disease. *Physiology (Bethesda)* **26**, 23-33.

Rozengurt, E., Rey, O. and Waldron, R. T. (2005). Protein kinase D signaling. *J Biol Chem* **280**, 13205-8.

Rykx, A., De Kimpe, L., Mikhalap, S., Vantus, T., Seufferlein, T., Vandenheede, J. R. and Van Lint, J. (2003). Protein kinase D: a family affair. *FEBS Lett* **546**, 81-6.

Schafer, D. A., Jennings, P. B. and Cooper, J. A. (1996). Dynamics of capping protein and actin assembly in vitro: uncapping barbed ends by polyphosphoinositides. *J Cell Biol* **135**, 169-79.

Schnack, C., Hengerer, B. and Gillardon, F. (2008). Identification of novel substrates for Cdk5 and new targets for Cdk5 inhibitors using high-density protein microarrays. *Proteomics* **8**, 1980-6.

Scita, G., Nordstrom, J., Carbone, R., Tenca, P., Giardina, G., Gutkind, S., Bjarnegard, M., Betsholtz, C. and Di Fiore, P. P. (1999). EPS8 and E3B1 transduce signals from Ras to Rac. *Nature* **401**, 290-3.

Shi, Y., Alin, K. and Goff, S. P. (1995). Abl-interactor-1, a novel SH3 protein binding to the carboxy-terminal portion of the Abl protein, suppresses v-abl transforming activity. *Genes Dev* **9**, 2583-97.

Sinnett-Smith, J., Jacamo, R., Kui, R., Wang, Y. M., Young, S. H., Rey, O., Waldron, R. T. and Rozengurt, E. (2009). Protein kinase D mediates mitogenic

signaling by Gq-coupled receptors through protein kinase C-independent regulation of activation loop Ser744 and Ser748 phosphorylation. *J Biol Chem* **284**, 13434-45.

Sinnett-Smith, J., Zhukova, E., Hsieh, N., Jiang, X. and Rozengurt, E. (2004). Protein kinase D potentiates DNA synthesis induced by Gq-coupled receptors by increasing the duration of ERK signaling in swiss 3T3 cells. *J Biol Chem* **279**, 16883-93.

Sinnett-Smith, J., Zhukova, E., Rey, O. and Rozengurt, E. (2007). Protein kinase D2 potentiates MEK/ERK/RSK signaling, c-Fos accumulation and DNA synthesis induced by bombesin in Swiss 3T3 cells. *J Cell Physiol* **211**, 781-90.

Song, K., Backs, J., McAnally, J., Qi, X., Gerard, R. D., Richardson, J. A., Hill, J. A., Bassel-Duby, R. and Olson, E. N. (2006). The transcriptional coactivator CAMTA2 stimulates cardiac growth by opposing class II histone deacetylases. *Cell* **125**, 453-66.

Spratley, S. J., Bastea, L. I., Doppler, H., Mizuno, K. and Storz, P. (2011). Protein kinase D regulates cofilin activity through P21-activated kinase 4. *J Biol Chem*.

Steffen, A., Rottner, K., Ehinger, J., Innocenti, M., Scita, G., Wehland, J. and Stradal, T. E. (2004). Sra-1 and Nap1 link Rac to actin assembly driving lamellipodia formation. *EMBO J* **23**, 749-59.

Storz, P. (2007). Mitochondrial ROS--radical detoxification, mediated by protein kinase D. *Trends Cell Biol* **17**, 13-8.

Storz, P., Doppler, H., Johannes, F. J. and Toker, A. (2003). Tyrosine phosphorylation of protein kinase D in the pleckstrin homology domain leads to activation. *J Biol Chem* **278**, 17969-76.

Storz, P., Doppler, H. and Toker, A. (2004). Protein kinase Cdelta selectively regulates protein kinase D-dependent activation of NF-kappaB in oxidative stress signaling. *Mol Cell Biol* **24**, 2614-26.

Storz, P., Doppler, H. and Toker, A. (2005). Protein kinase D mediates mitochondrion-to-nucleus signaling and detoxification from mitochondrial reactive oxygen species. *Mol Cell Biol* **25**, 8520-30.

Storz, P., Hausser, A., Link, G., Dedio, J., Ghebrehiwet, B., Pfizenmaier, K. and Johannes, F. J. (2000). Protein kinase C [micro] is regulated by the multifunctional chaperon protein p32. *J Biol Chem* **275**, 24601-7.

Stovold, C. F., Millard, T. H. and Machesky, L. M. (2005). Inclusion of Scar/WAVE3 in a similar complex to Scar/WAVE1 and 2. *BMC Cell Biol* **6**, 11.

Stradal, T., Courtney, K. D., Rottner, K., Hahne, P., Small, J. V. and Pendergast, A. M. (2001). The Abl interactor proteins localize to sites of actin polymerization at the tips of lamellipodia and filopodia. *Curr Biol* **11**, 891-5.

Stradal, T. E. and Scita, G. (2006). Protein complexes regulating Arp2/3-mediated actin assembly. *Curr Opin Cell Biol* **18**, 4-10.

Sturany, S., Van Lint, J., Muller, F., Wilda, M., Hameister, H., Hocker, M., Brey, A., Gern, U., Vandenheede, J., Gress, T. et al. (2001). Molecular cloning and characterization of the human protein kinase D2. A novel member of the protein kinase D family of serine threonine kinases. *J Biol Chem* **276**, 3310-8.

Sun, X., Li, C., Zhuang, C., Gilmore, W. C., Cobos, E., Tao, Y. and Dai, Z. (2009). Abl interactor 1 regulates Src-Id1-matrix metalloproteinase 9 axis and is required for invadopodia formation, extracellular matrix degradation and tumor growth of human breast cancer cells. *Carcinogenesis* **30**, 2109-16.

Tan, M., Hao, F., Xu, X., Chisolm, G. M. and Cui, M. Z. (2009). Lysophosphatidylcholine activates a novel PKD2-mediated signaling pathway that controls monocyte migration. *Arterioscler Thromb Vasc Biol* **29**, 1376-82.

Tan, M., Xu, X., Ohba, M. and Cui, M. Z. (2004). Angiotensin II-induced protein kinase D activation is regulated by protein kinase Cdelta and mediated via the angiotensin II type 1 receptor in vascular smooth muscle cells. *Arterioscler Thromb Vasc Biol* **24**, 2271-6.

Tan, M., Xu, X., Ohba, M., Ogawa, W. and Cui, M. Z. (2003). Thrombin rapidly induces protein kinase D phosphorylation, and protein kinase C delta mediates the activation. *J Biol Chem* **278**, 2824-8.

Tanos, B. E. and Pendergast, A. M. (2007). Abi-1 forms an epidermal growth factor-inducible complex with Cbl: role in receptor endocytosis. *Cell Signal* **19**, 1602-9.

Tilney, L. G., Bonder, E. M., Coluccio, L. M. and Mooseker, M. S. (1983). Actin from Thyone sperm assembles on only one end of an actin filament: a behavior regulated by profilin. *J Cell Biol* **97**, 112-24.

Tilney, L. G., Bonder, E. M. and DeRosier, D. J. (1981). Actin filaments elongate from their membrane-associated ends. *J Cell Biol* **90**, 485-94.

Uhle, S., Medalia, O., Waldron, R., Dumdey, R., Henklein, P., Bech-Otschir, D., Huang, X., Berse, M., Sperling, J., Schade, R. et al. (2003). Protein kinase CK2 and protein kinase D are associated with the COP9 signalosome. *EMBO J* **22**, 1302-12.

Valverde, A. M., Sinnett-Smith, J., Van Lint, J. and Rozengurt, E. (1994). Molecular cloning and characterization of protein kinase D: a target for diacylglycerol and phorbol esters with a distinctive catalytic domain. *Proc Natl Acad Sci U S A* **91**, 8572-6.

Van Lint, J., Rykx, A., Maeda, Y., Vantus, T., Sturany, S., Malhotra, V., Vandenheede, J. R. and Seufferlein, T. (2002). Protein kinase D: an intracellular traffic regulator on the move. *Trends Cell Biol* **12**, 193-200.

Van Lint, J. V., Sinnett-Smith, J. and Rozengurt, E. (1995). Expression and characterization of PKD, a phorbol ester and diacylglycerol-stimulated serine protein kinase. *J Biol Chem* **270**, 1455-61.

Vantus, T., Vertommen, D., Saelens, X., Rykx, A., De Kimpe, L., Vancauwenbergh, S., Mikhalap, S., Waelkens, E., Keri, G., Seufferlein, T. et al. (2004). Doxorubicin-induced activation of protein kinase D1 through caspase-mediated proteolytic cleavage: identification of two cleavage sites by microsequencing. *Cell Signal* **16**, 703-9.

Vega, R. B., Harrison, B. C., Meadows, E., Roberts, C. R., Papst, P. J., Olson, E. N. and McKinsey, T. A. (2004). Protein kinases C and D mediate agonist-dependent cardiac hypertrophy through nuclear export of histone deacetylase 5. *Mol Cell Biol* **24**, 8374-85.

von Blume, J., Knippschild, U., Dequiedt, F., Giamas, G., Beck, A., Auer, A., Van Lint, J., Adler, G. and Seufferlein, T. (2007). Phosphorylation at Ser244 by CK1 determines nuclear localization and substrate targeting of PKD2. *EMBO J* **26**, 4619-33.

Waldron, R. T., Iglesias, T. and Rozengurt, E. (1999). The pleckstrin homology domain of protein kinase D interacts preferentially with the eta isoform of protein kinase C. *J Biol Chem* **274**, 9224-30.

Waldron, R. T. and Rozengurt, E. (2000). Oxidative stress induces protein kinase D activation in intact cells. Involvement of Src and dependence on protein kinase C. *J Biol Chem* **275**, 17114-21.

Waldron, R. T. and Rozengurt, E. (2003). Protein kinase C phosphorylates protein kinase D activation loop Ser744 and Ser748 and releases autoinhibition by the pleckstrin homology domain. *J Biol Chem* **278**, 154-63.

Wang, C., Navab, R., Iakovlev, V., Leng, Y., Zhang, J., Tsao, M. S., Siminovitch, K., McCready, D. R. and Done, S. J. (2007). Abelson interactor protein-1 positively regulates breast cancer cell proliferation, migration, and invasion. *Mol Cancer Res* **5**, 1031-9.

Wang, C., Tran-Thanh, D., Moreno, J. C., Cawthorn, T. R., Jacks, L. M., Wang, D. Y., McCready, D. R. and Done, S. J. (2011). Expression of Abl interactor 1 and its prognostic significance in breast cancer: a tissue-array-based investigation. *Breast Cancer Res Treat* **129**, 373-86.

Wang, Q. J. (2006). PKD at the crossroads of DAG and PKC signaling. *Trends Pharmacol Sci* **27**, 317-23.

Wang, S., Li, X., Parra, M., Verdin, E., Bassel-Duby, R. and Olson, E. N. (2008). Control of endothelial cell proliferation and migration by VEGF signaling to histone deacetylase 7. *Proc Natl Acad Sci U S A* **105**, 7738-43.

Wang, Y., Kedei, N., Wang, M., Wang, Q. J., Huppler, A. R., Toth, A., Tran, R. and Blumberg, P. M. (2004). Interaction between protein kinase Cmu and the vanilloid receptor type 1. *J Biol Chem* **279**, 53674-82.

Wong, C. and Jin, Z. G. (2005). Protein kinase C-dependent protein kinase D activation modulates ERK signal pathway and endothelial cell proliferation by vascular endothelial growth factor. *J Biol Chem* **280**, 33262-9.

Yu, W., Sun, X., Clough, N., Cobos, E., Tao, Y. and Dai, Z. (2008). Abi1 gene silencing by short hairpin RNA impairs Bcr-Abl-induced cell adhesion and migration in vitro and leukemogenesis in vivo. *Carcinogenesis* **29**, 1717-24.

Zemlickova, E., Dubois, T., Kerai, P., Clokie, S., Cronshaw, A. D., Wakefield, R. I., Johannes, F. J. and Aitken, A. (2003). Centaurin-alpha(1) associates with and is phosphorylated by isoforms of protein kinase C. *Biochem Biophys Res Commun* **307**, 459-65.

Zhang, C., Yadava, P. and Hughes, J. (2004). Polyethylenimine strategies for plasmid delivery to brain-derived cells. *Methods* **33**, 144-50.

Zhukova, E., Sinnett-Smith, J. and Rozengurt, E. (2001). Protein kinase D potentiates DNA synthesis and cell proliferation induced by bombesin, vasopressin, or phorbol esters in Swiss 3T3 cells. *J Biol Chem* **276**, 40298-305.

Ziegler, S., Eiseler, T., Scholz, R. P., Beck, A., Link, G. and Hausser, A. (2011). A novel protein kinase D phosphorylation site in the tumor suppressor Rab interactor 1 is critical for coordination of cell migration. *Mol Biol Cell* **22**, 570-80.

Zigmond, S. H. (1993). Recent quantitative studies of actin filament turnover during cell locomotion. *Cell Motil Cytoskeleton* **25**, 309-16.

Zugaza, J. L., Sinnett-Smith, J., Van Lint, J. and Rozengurt, E. (1996). Protein kinase D (PKD) activation in intact cells through a protein kinase C-dependent signal transduction pathway. *EMBO J* **15**, 6220-30.

Zugaza, J. L., Waldron, R. T., Sinnett-Smith, J. and Rozengurt, E. (1997). Bombesin, vasopressin, endothelin, bradykinin, and platelet-derived growth factor rapidly activate protein kinase D through a protein kinase C-dependent signal transduction pathway. *J Biol Chem* **272**, 23952-60.

10. CURRICULUM VITAE

Personal details

Subbaiah Chary Nimmagadda
Date of birth: 30th June 1983
Place of birth: Hyderabad, India
Nationality: Indian
Languages known: English, Hindi and Telugu.

Contact address

Listemann strasse 18, Room 55
Magdeburg 039104, Germany
Email: chary.nimmagadda@student.uni-halle.de

Education and employment

Present position: Postdoctoral research fellow at Prof. Michael Naumann's Laboratory, Universitätsklinikum Magdeburg, Germany from **July 2012 till date**

PhD student at Prof. Thomas Seufferlein's Laboratory, Universitätsklinikum Halle, Halle (Saale), Germany from **July 2008- June 2012**

Research assistant at Dr. Mahalingam's Laboratory of Virology at Center for DNA Fingerprinting and Diagnostics, Hyderabad and Indian Institute of Technology, Madras, India from **January 2007-June 2008**

Master's in Biotechnology, Bharathidasan University, India. Result: First class with distinction-84.95%, **August 2004- May 2006**

Bachelor's in Biotechnology, Osmania University, India, Result: First class with distinction-71.86%, **August 2001- May 2004**

Publications

1. PKD2 mediated phosphorylation on ABI1 negatively affects tumor cell motility via ABI1/WAVE2 sub-complex

Subbaiah Chary Nimmagadda, Tim Eiseler, Peter Storz, Johan Van Lint and Thomas Seufferlein.

Journal of Biological Chemistry: In revision

2. A novel splice variant of Calcium and Integrin Binding Protein 1 mediates protein kinase D2 stimulated tumor growth by regulating angiogenesis

Milena Armacki , Golsa Joodi, Subbaiah Chary Nimmagadda, Line de Kimpe, Ganesh Varma Pusapati, Sandy Vandoninck, Johan Van Lint and Thomas Seufferlein.

Oncogene (Advance online publication): 18th March; doi: 10.1038/onc.2013.43.

3. PKD1 mediates anchorage-dependent and independent growth of tumor cells via snail1.

Tim Eiseler, Subbaiah Chary Nimmagadda[#], Conny Köhler[#], Arsia Jamali, Nancy Funk, Golsa Joodi, Peter Storz, Thomas Seufferlein. [#]Equal contribution

Journal of Biological Chemistry: 2012 Sep 21; 287 (39):32367-80. Epub 2012 Jul 12.

Presentations

1. **Subbaiah Chary Nimmagadda**, Tim Eiseler, Peter Storz and Thomas Seufferlein (2012). *Abelson Interactor 1 is a novel substrate of Protein kinase D2: Potential implications in tumor cell migration.* Poster no. LB- 513 (Section: Tumor biology) at American Association for Cancer Research 2012 meeting, Chicago, USA. Cancer Research, 2012 April; Volume 72, Issue 8, Supplement 1.

2. **Subbaiah Chary Nimmagadda,** Peter Storz, Thomas Seufferlein (2010). *Identification and characterization of ABI1, as a novel substrate of PKD2.* Poster no. 2071, 50th annual meeting of American Society for Cell Biology, Philadelphia, USA.

3. **Subbaiah Chary Nimmagadda,** Tim Eiseler, Peter Storz, Thomas Seufferlein (2011). *PKD2 mediated phosphorylation on ABI1 negatively regulates tumor cell motility.* Poster no. 071, 66th Gastroenterologie Viszeralmedizin meeting Leipzig, Germany.

11. Declaration/ Erklärung

Declaration

This thesis is a presentation of my original research work. Wherever contributions of others are involved, every effort is made to indicate this clearly, with due reference to the literature, and acknowledgement of collaborative research and discussions.

Erklärung

Ich erkläre hiermit, dass ich mich mit der vorliegenden wissenschaftlichen Arbeit erstmals um die Erlangung des Doktorgrades bewerbe. Ich erkläre, die Arbeit selbstständig verfasst und keine anderen als die angegebenen Quellen und Hilfsmittel benutzt und die den benutzten Werken wörtlichen oder inhaltlich entnommenen Stellen als solche kenntlich gemacht habe.

Subbaiah Chary Nimmagadda
Halle, August 2012

12. Acknowledgements

One of the joys of completion is to look over the journey, and remember all my friends and family who have been instrumental throughout this long yet fulfilling road. Many people have contributed either directly or indirectly to this investigation. It is a pleasure to thank all those who made this thesis possible. Above all, I would like my parents for their unequivocal support throughout as always, for which my mere expression of thanks does not suffice. I heartily thank God, for giving me the strength, perseverance, intelligence, and patience to accomplish all that I have, to this point.

With an immense pleasure and profound sense of gratitude, I take this privilege to express heart-felt and sincere thanks to my supervisor, Prof. Thomas Seufferlein, Director, Internal medicine 1, Universitätsklinikum Halle for his constant help, support and patience. His timely and most importantly critical comments always quoted with a realistic example, constituted the driving force of this doctoral thesis.

I would also like to extend thanks to my second supervisor, Prof. Dr. Sven Erik Behrens, Institute for Biochemistry and Biotechnology, Martin-Luther-Universität Halle-Wittenberg, who has been invaluable on both an academic and a personal front. I gratefully acknowledge the funding sources that made my Ph.D. work possible. The project was funded in part by the German Federal Ministry of Education and Research (BMBF). In addition, would like to acknowledge GRK 1591 for providing me the required financial assistance, to present part of my work at American Society for Cell Biology 50th annual meeting, Philadelphia USA.

This work would have not been possible without the generosity of investigators who shared their reagents with us. Dr. Johan Van Lint (University of Leuven, Belgium) for providing pEGFP-ABI1 construct, Dr. Tadaomi Takenawa (Kobe University, Japan) for the Flag-WAVE2 construct and Dr. Peter Storz (Clinic Cancer Center, Jacksonville, USA) for the pMOTIF antibody.

I especially thank, Dr. Stefan Hüttelmaier, Dr. Andreas Simm and their group members for allowing and helping me to carry out some of the experiments in their labs. I also would like to acknowledge the financial, academic and technical support by the Universitätsklinikum Halle. The library and computer facilities of the University, as well as the clinic computer service center, have been indispensable.

I am thankful to all current and former members of my lab for their support and creating an enjoyable working atmosphere, especially Milena, Tim, Rashi, Silvia, Marc, Caludia, Nancy, Holger, Ganesh, Claudia Ruhland, Ninel and others.

I thank all my previous scientific mentors back at home, who are largely responsible for helping my unrealistic dream come true: Dr. Kaiser Jamil, Bhagwan Mahaveer Medical Research Center, Dr. Satti Vishnupriya, Osmania University, Dr. Kalluri Subba Rao, University of Hyderabad, and Dr. Sundarasamy Mahalingam Center for DNA printing and Diagnostics, Hyderabad, India.

My friends and group members have made my stay in Halle enjoyable rather memorable and have became an integral part of my daily life. I am grateful for the time spent with my first friends in Halle Deepak, Ashwin, Sudheer, Lakshmi kanth, Harish and Joby, my group members Anita, Rashi, Gaurav, Snigdha, Shilpa, Anshu, Dinesh and members of Halle Cricket Club (HCC). Special thanks to Pushpa Raj Joshi, for helping me with administrative procedures, german tranlations and most importantly VISA extensions. You have been my 24X7 help line buddy :)

Rashi and Ashwin's support during the final and probably the toughest phase of my Ph.D. deserves a special mention in this section. You guys are amazing; my ride wouldn't have been so smooth without you people. Thank you once again for constantly supporting and guarding me through tough times. Last, but by no means least, I thank Dr. Anandita Singh and my friends in India for their love, support and encouragement throughout.